2018-06-28

The Role of Eukaryotic ABC-Transporters in Eliciting Neutrophil infiltration during Streptococcus pneumoniae infection

Andrew Zukauskas
University of Massachusetts Medical School

The Role of Eukaryotic ABC-Transporters in Eliciting Neutrophil infiltration during *Streptococcus pneumoniae* infection

A Dissertation Presented

By

Andrew Zukauskas

Submitted to the Faculty of the

University of Massachusetts Graduate School of Biomedical Sciences, Worcester

In partial fulfillment of the requirements for the degree of

DOCTOR OF PHILOSOPHY

June 28th, 2018

Molecular Genetics and Microbiology Program

Table of Contents

Page

List of Figures

Figure **Page**

Figure **Page**

Acknowledgements

As with any scientific exploration, I have stood on the shoulders of giants. I must thank Dr. Michael Pazos and Dr. Terence Agbor, who laid much of the foundation of this work before I began it. Dr. John Leong and Dr. Rudra Bhowmick were instrumental in helping guide this work. In later years, two other members of Dr. Leong's lab, Dr. Elsa Bou-Ghanem and Dr. Walter Adams also provided a number of important observations. Many hands have helped in the technical aspects of this work and must be acknowledged: Zach Demma, Christopher Louissaint, and Christine Tuohy all were diligent and supremely helpful lab mates who assisted in any way they could, and I thank them for their generosity.

Past and present lab members have felt more like extended family and I would like to thank, in no particular order: Dr. Ana-Luisa Maldonado-Contreras, Dr. Regino Mercado-Lubo, Dr. Rose Szabady, Dr. Erik Boll, Dr. Kelly Hallstrom, Samir Patel, and Sage Foley.

Dr. Beth McCormick requires her own acknowledgement section in the completion of this work and words cannot convey the support and guidance, both professionally and personally, I have experienced over the years.

Lastly, I must thank my family. My mother and parents-in-law have always been so incredibly supportive throughout the years. Many thanks to my children, Selah and Zoe. And lastly, to my wife, my biggest cheerleader, my partner throughout the years. This would not be possible without Becky Zukauskas.

Abstract

Streptococcus pneumoniae (*S. pneumoniae*) is a Gram-positive, encapsulated bacterium capable of causing significant morbidity and mortality throughout the world. A hallmark of *S. pneumoniae* infection is infiltration of neutrophils (PMNs) that assist in controlling the spread infection but may also contribute to pathology. Paradoxically, studies have shown that limiting PMN infiltration into the lumen of the lung during infection actually betters clinical outcome in experimental *S. pneumoniae* infection. The final step in PMN luminal trafficking is a Hepoxilin A_3 (HXA_3)-dependent migration across the pulmonary epithelium. HXA_3 is a PMN chemoattractant that forms gradients along the polarized epithelial face, drawing PMNs from the basolateral to the apical surface during proinflammatory responses. HXA_3 requires assistance of an integral-membrane protein transporter to escape the cell and form the gradient. The pulmonary HXA_3 transporter is currently unidentified.

In this work, we identify the pulmonary HXA_3 transporter as the ATP-Binding Cassette Transporter (ABC transporter) Multi-drug Resistance Associated Protein 2 (ABCC2, MRP2). We demonstrate that MRP1 and MRP2 are divergent ABC-transporters that control transepithelial PMN migration through efflux of a distinct anti-inflammatory substance and the pro-inflammatory HXA_3 in the context of *Streptococcus pneumoniae* infection. Enrichment of MRP2 on the plasma membrane requires detection of the bacterial virulence factors pneumolysin (PLY) and hydrogen peroxide. PLY and hydrogen peroxide not only coordinate MRP2 apical membrane enrichment but also influence HXA_3-dependent PMN transepithelial migration. They influence migration

through stimulation of epithelial intracellular calcium increases that are crucial for HXA_3 production as well as MRP2 translocation to the plasma membrane. PLY and hydrogen peroxide are not sufficient in their signaling alone, however, and require at least one additional bacterial signal to induce HXA_3/MRP2 proinflammatory activities.

Chapter I

Introduction

1.1 Infection and neutrophil infiltration

The microbiome is a critical component of healthy intestinal and immune systems. The symbiotic microbes provide training for our immature immune system at early ages, provide metabolites from different biochemical processes, and form physical barriers preventing pathogenic bacteria from gaining a foothold in our mucosal systems.

When pathogens do break through, they initiate host immune responses that combat infection through a variety of methods. The innate immune neutrophils (PMNs), granulocytes, macrophages, and dendritic cells (DCs) are the cellular components that immediately attempt to control the infection through relatively non-specific means. In particular, PMNs are the most abundant and effective innate immune cells that respond to bacterial invasion of the host. To enter the infected site, PMNs are recruited from the vasculature, through the endo- and epithelial cell layers, and are finally able to combat the bacterial challenge in the lumen of the organ. While much is known about transendothelial recruitment of PMNs, such as the need for NF-κB and attachment molecule expression (1), less is known about transepithelial movement. Classically, PMNs are activated through a combination of chemoattractants released into the blood stream in close proximity to the site of infection. These chemoattractants assist in activating selectin tethering molecules in both the endothelium and the PMNs to induce a process of “rolling”. As the PMNs adhere to the endothelium, they are further activated

by heparan sulfate proteoglycans (2). PMNs release metalloproteases and other degradation molecules to degrade the extracellular matrix as they transcytose both para- and trans-cellularly through the endothelium.

To progress from the endo- to epithelial cell layer, IL-8 and other NF-κB-dependent cytokines draw PMNs from the circulation towards the basolateral portion of the epithelium (3) while lipid Hepoxilin A_3 (HXA_3) draws PMNs from the basolateral surface to the apical surface (4). Basolateral docking of the PMN to the epithelium appears to be the initial stage by which epithelium tight-junction disintegration occurs (5). Once in the lumen, PMNs act by phagocytosing bacteria and then using oxidative burst, proteases, and Neutrophil Extracellular Traps (NETs**)** to eliminate bacterial invaders. PMNs also use secreted reactive oxygen metabolites that both injure bacteria and tissue in the surrounding area. Some predominant proteases released and activated during PMN excitation are elastases, proteinase 3, and capthepsin G that assist in degradation of extracellular membrane components and intracellular digestion of phagocytosed bacteria (6). One of the most critical molecules in charge of drawing PMNs to the site of infection is the epithelial-cell derived chemoattractant HXA_3.

1.2 HXA_3-mediated PMN migration

HXA_3 was originally identified as an arachidonic acid metabolite that influences insulin release in pancreatic islets of Langerhans (7). It has been identified to have roles in liver (8), neuronal biology (9), an activator of calcium mobilization, and activation in PMNs (10). Originally identified as PEEC, McCormick et al. described a bioactive lipid

mediator of PMN migration elicited from epithelial cells during infection with *Salmonella* enterica Typhimurium, later identified to be HXA_3. In the years since, HXA_3-dependent PMN migration has been observed during intestinal infection with *Shigella flexneri* (11), *E. coli* (12), and as a component of PMN infiltration during active inflammation in Inflammatory Bowel Disease (IBD) (13).

With the identification of this process being widespread in different intestinal infections, additional research inquired as to the HXA_3 dependency during PMN infiltration at other mucosal sites. The ocular, pulmonary, and urogenital tract all require similar epithelial cell layers to segregate exposure to the outside world from the relatively sterile internal system of the host. To that end, we examined whether the HXA_3 pathway is conserved in the pulmonary system, which is subject to dysbiosis similar to the intestine in the form of bacterial infection, Chronic Obstructive Pulmonary Disease (COPD), and Acute Respiratory Distress Syndrome (ARDS), to name a few.

The upper respiratory system, which includes the nasopharynx and entry to the trachea, has its own natural microbiota and commensal bacteria. These bacteria tend to be both harmless, resident bacteria as well as opportunistic bacteria such as *Haemophilus influenzae* and *Streptococcus pneumoniae*. Respiratory pathology due to these opportunistic bacteria classically begins with invasion of the lower respiratory system. Macroscopically, there are two distinct regions of the lower respiratory system: the bronchus/trachea and alveolar-containing region of the lung. Each region has a distinct distribution of specialized epithelium. For instance, the bronchus region contains ciliated epithelium, secretory clara, goblet cells, and basal cells. As the pulmonary system

narrows towards the alveolar spaces, there is a trend toward fewer secretory cells and an increase in the alveolar type I and type II epithelium.

The epithelium forms a physical barrier between the pulmonary lumen and the endo-/epithelial basement membrane. Epithelial cells are held together by a variety of connections, including gap junctions, desmosomes, adherence junctions, and tight junctions. The Claudin family of proteins reinforces many of these connections. The tight junctions allow for the classic delineation between the lumen-facing apical portion of the epithelium, and the basolateral surface. During inflammation, there are a number of cytokines, such as IL-4 and IL-13 that reduce tight junction integrity and increase permeability (14). As in the intestine, PMNs exit the vasculature and migrate into the pulmonary lumen in a HXA_3-dependent manner. The activity of IL-8 appears distinct from HXA_3, as IL-8 is critical during the inflammatory process to draw PMNs to the basolateral surface of the epithelium but does not appear to influence the transepithelial migration from basolateral-to-apical surface (3).

Hepoxilin synthesis begins with the activation of Protein Kinase C (PKC) and Phospholipase A_2 (PLA_2), stimulating release of arachidonic acid from the membranes of the epithelium into the cytoplasm (11, 15-17). 12/15-lipoxygenase converts the arachidonic acid to Hepoxilin A_3, which is effluxed to the apical surface of the epithelium and creates a chemotactic gradient through the epithelial cell layer to attract PMNs through the tight junctions (Figure 1.1). Hurley et al. found that *Pseudomonas aeruginosa* induces HXA_3-dependent PMN migration during infection of lung cells *in vitro*, much like bacterial infection of the intestine (18). Likewise, Bhowmick et al. reported that *S.*

pneumoniae is able to elicit PMN migration from infected epithelium, and that this effect is curtailed by ablating *Lox15*, the 12/15-Lipoxygenase gene from mice (19). Such studies illuminate several specifics of the HXA_3 cascade and signaling process: first, this appears to be a conserved process across different mucosal surfaces, as similar effects occur in both the lung and intestine; second, HXA_3-dependent PMN migration is not isolated to Gram-negative bacteria because it occurs with the Gram-positive *S. pneumoniae*; third, HXA_3 is induced by both intracellular and extracellular pathogens, Despite these observations, there have been few reports of individual virulence factors that influence the production and release of HXA_3 from infected epithelial cells. *Salmonella* Typhimurium requires expression of genes from pathogenicity island 1 (SPI-1) for both epithelial invasion as well as infection-driven HXA_3 efflux. The SPI-1 virulence factor SipA is one of specific factors required for HXA_3-induced PMN migration (20). With exception to this report, the mechanism of HXA3 induction by bacterial pathogens is not known.

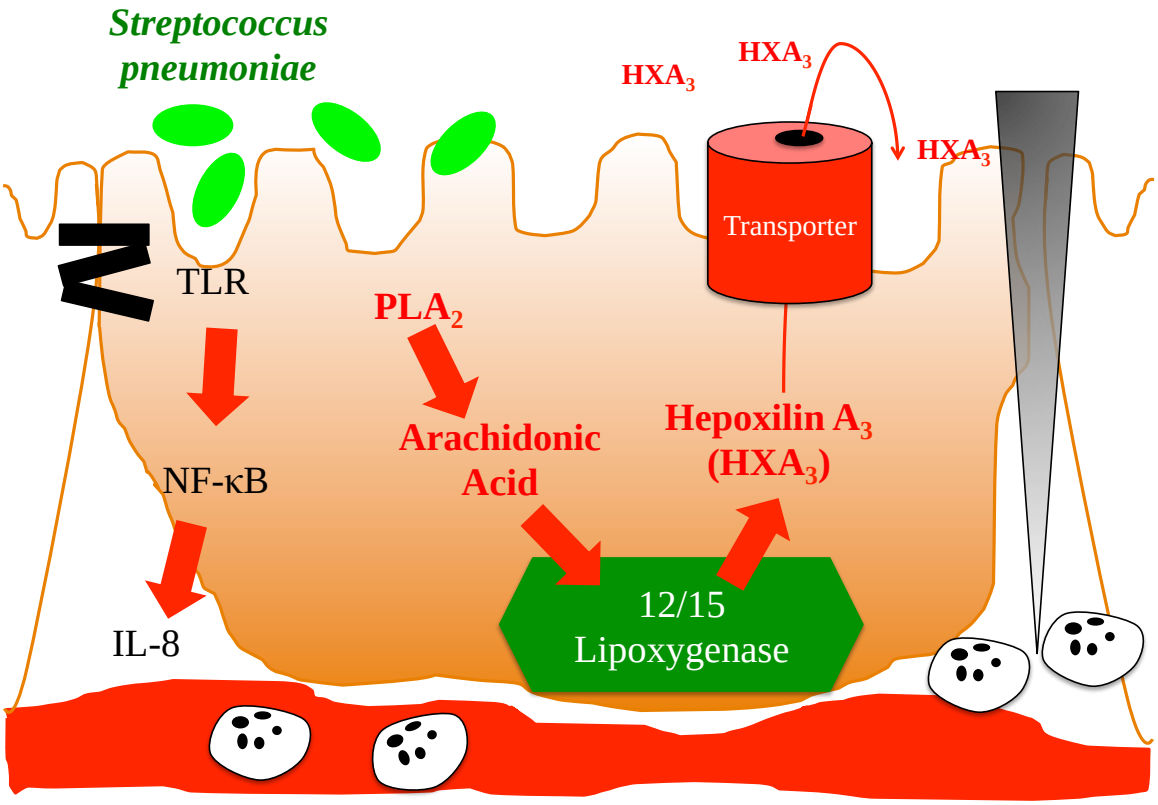

Figure 1.1 Model of HXA_3 induction

During infection, bacteria, such as *Streptococcus pneumoniae*, encounter the apical surface of the epithelium that is held together with a variety of junction proteins. Bacterial components engage TLR receptors and induce NF-κB signaling which produces IL-8 in addition to a number of other pro-inflammatory signals. These signals initiate PMN escape from the vasculature to the basolateral surface of the epithelium. In a separate set of events, PLA_2 activates and releases arachidonic acid. This is converted to HXA_3 and effluxed to the apical surface of the epithelium, forming a chemotactic gradient that attracts PMNs to the lumen of the organ.

1.3 ABC-transporters

In both the intestine and the lung, the upstream epithelial machinery controlling the synthesis of HXA_3 is similar. PKC and PLA_2 are needed to release arachidonic acid and produce HXA_3 via 12/15-lipoxygenase activity, regardless of the epithelial cell origin. One critical aspect of HXA_3 release is that it does not passively transverse the plasma membrane but is pumped by a specific efflux transporter. Using both inhibitor studies and siRNA, the intestinal HXA_3 transporter was identified as the Multi-Drug Resistance associated Protein 2 (MRP2, or ABCC2) (13).

MRP2 belongs to a family of transmembrane ATP-Binding Cassette Transporters (ABC-Transporters) that hydrolyze ATP into ADP and expel or import payload across a membrane bilayer. Naming of the ABC-transporters usually employs the “Multi-Drug-Resistance Protein” (MDR) or “Multidrug-Resistance-associated Protein” (MRP) nomenclature. These molecules are highly conserved throughout bacteria and eukaryotes, though the ligand interactions are both diverse and promiscuous. While bacterial transporters tend to be exclusively found on the exterior membrane, eukaryotes have transporters embedded on vesicles or internal organelles, as well as the exterior membrane bilayer.

Normally, ABC-transporters primarily function to efflux xenobiotics that enter the cells. Cells most likely to encounter toxins and xenobiotics are those mucosal surfaces that frequently come in contact with substances from the surrounding environment: the intestine, lung, and urogenital tract, among others. ABC-transporters are detected in many other tissues, including the blood-brain-barrier, adrenals, heart, kidney, liver,

ovaries, pancreas, placenta, prostrate, skin, spleen, and testes (21). Subcellularly, ABC-transporters have been found on both the apical and basolateral portions of the epithelium as well as the plasma, peroxisomal, endosomal, lamellar body, and lysosomal membranes (22). ABC-transporters tend to localize to specific faces of polarized cellular barriers: MRP2, for instance, is almost exclusively found on the apical surface of the epithelium, whether in the liver, lung, or intestine. In contrast, MRP3 in the intestine is almost exclusively on the basolateral surface of the epithelium (Figure 1.2).

Structurally, ABC-transporters contain three domains: transmembrane, linker, and nucleotide-binding (NTB) domains. The transmembrane domains make up the body of the protein pump and the recognition sites for ligands while the NTB domains provide pockets for ATP and ADP binding. Linker regions are physical connections that join different transmembrane or NTB domains to one another. ABC-transporters tend to be either of the shorter variety (12-to-14-transmembrane domain long), or longer (17-transmembrane domains). Shorter pumps have cytosolic amino terminals while longer pumps have extracellular amino terminals (23). During activation, a ligand encounters the active pocket of the transporter, usually at the cytosolic face, and then allows ATP to bind the NTB site. ATP hydrolysis induces a conformational change in the transmembrane domain, forcing the ligand to the extracellular face of the transporter. The ADP interaction with the NTB domain reduces the binding affinity for the ligand and it is released, allowing the ABC-transporter to reset and repeat. ABC-transporters are able to undergo post-translational modifications, including glycosylation (24), SUMOylation (25), and phosphorylation (26).

Fig. 1.2

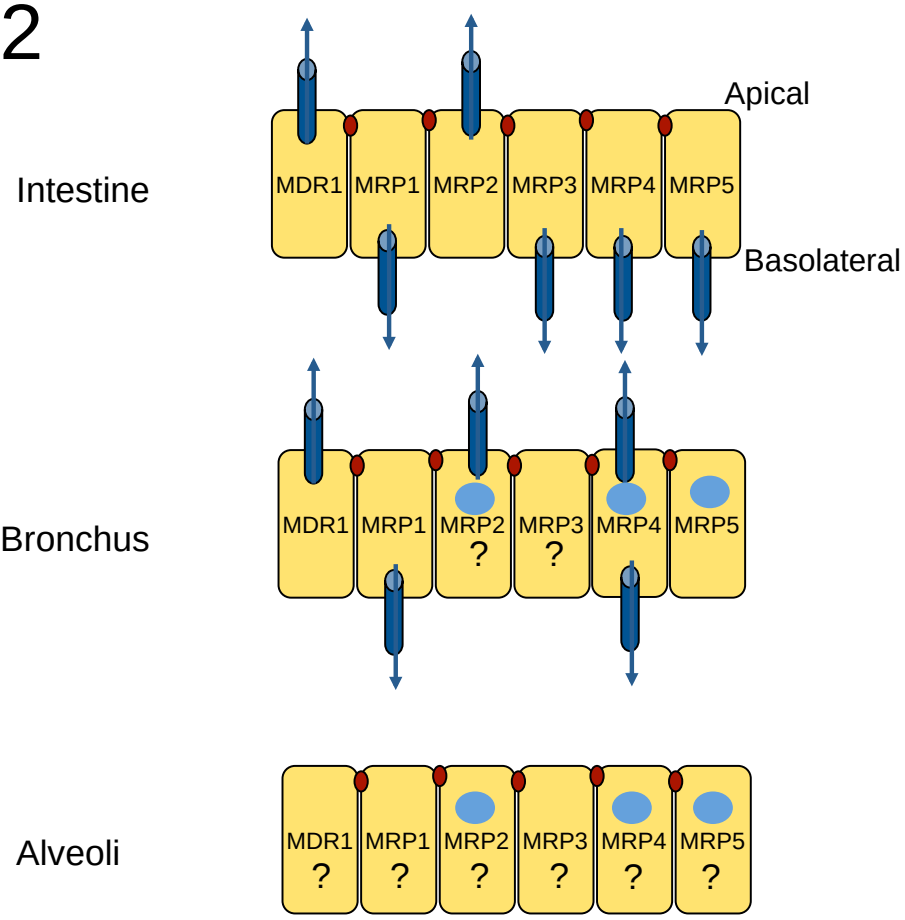

Figure 1.2 Schematic of ABC-transporter location on polarized epithelial

ABC-transporters tend to locate to specific faces on polarized epithelium. MDR1 (P-gp), for instance, localizes almost exclusively to the apical surface of polarized intestinal epithelium. Conversely, MRP1 is almost exclusively basolateral in the intestine. Less is know about the location of the ABC-transporters in the lung. Arrows indicate the face the transporter is normally located in the given organ. Circles indicate that the transporter is found in intracellular vesicles. "?" denotes conflicts in the literature. Bronchus and Alveolar localization modified from van der Deen 2005 (27).

Due to its propensity to efflux toxins and xenobiotics, ABC-transporters are most known for conferring multi-drug resistance to chemotherapeutic agents. There are many studies indicating a correlation between ABC-transporter expression and worsening chemotherapeutic resistance in a variety of cancers (28). While ABC-transporters have a somewhat promiscuous nature, not all transporters are able to efflux the same ligands. P-glycoprotein (P-gp), for instance, is able to efflux hydrophobic molecules as well as vinblastine (27). MRP4 effluxes nucleoside analogs and organic anions (29). Likewise, there are specific inhibitors that target one ABC-transporter but not the others. There are entire studies focused specifically on eliminating targeted MRPs or MDR proteins in unique chemotherapeutic-resistant carcinomas, and there is a wealth of knowledge on inhibition and ABC-transporter activity in the context of cancer chemotherapeutics. In contrast, there is a dearth of knowledge on the endogenous activity of these transporters.

1.3 Efflux Transporters and their contribution to inflammation

The majority of ABC-transporter research outside the context of cancer chemotherapy has focused on the intestine. This focus was stimulated by the observation that mice deficient in the efflux pump P-gp develop spontaneous colitis (30). P-gp knockout mice now serve as model for Inflammatory Bowel Disease (IBD).

P-gp is a smaller, 12-pass transmembrane efflux pumps localized to the apical surface of the intestine. It transports hydrophobic, positive-, or neutral-charge compounds. Elimination of this gene leads to a hyper-inflammatory phenotype, supporting the supposition that P-gp suppresses basal inflammation and assists in

microbiome equilibrium. P-gp is not only found on the epithelium but also on leukocytes. One study in 1999 examined P-gp expression on different leukocyte subtypes and noted decreases in P-gp activity in ulcerative colitis (UC) patients compared control subjects (31). In addition, a 2006 meta-analysis revealed that certain P-gp alleles are associated with severe UC (32, 33). Independent of IBD-associated diseases, P-gp is also known to be targeted by bacteria during infection; studies have shown that the *Salmonella* secreted protein SipA cleaves P-gp and may play a central role in bacterial attachment (34).

Another ABC-transporter that has associations with inflammation is Multidrug Resistance- associated Protein 1 (MRP1 or ABCC1). MRP1 is a 17-transmembrane-domain protein that localizes to the basolateral portion of the intestinal epithelium. The substrate specificity of MRP1 encompasses glutathione-, glucuronide-, and sulfate-conjugated organic anions; drugs vincristine, daunorubicin, and methotrexate; and Leukotriene (LTC_4), as well as glutathione disulfide. Studies indicate that MRP1 may be increased during episodes of IBD (35), which could lead to increased secretion of the pro-inflammatory mediator LTC_4. LTC_4 is an eicosanoid that increases mucus secretions and can cause vasoconstriction and vasodilation, but can also induce leukocyte rolling via P-selectin induction. Another leukotriene, LTB_4, primarily assists in leukocyte extravasation activation. Studies conducted by Tessa Tan Hove also suggest that LTB_4 and LTC_4 are increased during TNBS-induced colitis. In the same study, MRP1 knockout mice had less inflammation and less cellular damage as compared to wild-type mice during times of TNBS-induced intestinal inflammation, but were more susceptible to ethanol- or Dextran sulfate sodium (DSS)-induced damage than wild-type mice (36).

DSS-induced colitis was substantially worse in *Mrp1-/-* mice compared to their wild-type counter-parts, causing both severe pathology and decreased survival. During this time period, there was an observed increase in LTB_4. Because LTB_4 and LTC_4 both share a common precursor, it was postulated that a decrease in MRP1 could lead to a decrease in LTC_4 and, therefore, an increase in LTB_4 as more LTA_4 is sequestered to that pathway. Application of an LTB_4 inhibitor did not improve outcomes, suggesting that LTB_4 increases due to MRP1 elimination may not be the only contributing factor in this particular model (36). The study did not include an examination on the possible effects of exogenous LTC_4 application, so it remains to be seen whether LTC_4 could relieve the increased DSS-sensitivity, though addition of a pro-inflammatory agent to relieve inflammation seems paradoxical. The MRP1 increase during IBD seen in patients could be compensatory.

Other aspects of MRP1 expression that point to a protective role are the effects of Tissue Necrosis Factor–α (TNF-α). Overexpression of MRP1 has been shown to protect cells during exposure to TNF-α or FAS-ligand (35). Studies in glial cells showed that MRP1 might be upregulated during exposure to TNF-α in a JNK-dependent manner (37). Additionally, Blokzijl et al. detected MRP1 overexpression during cytokine- and FAS-induced apoptosis and noted that epithelial cells that overexpress MRP1 showed lower levels of apoptosis compared to wildtype controls (35). Epithelial cell death is a hallmark of DSS-induced colitis and thought to be an initiating step that degrades barrier integrity and allows the microbiota to induce inflammation. Increase of MRP1 would reduce cell death and stabilize barrier integrity, thereby reducing the permeability of the epithelial-

wall structure. Oxidative stress, too, has been implicated in exacerbation of damage in IBD while glutathione, a known ligand of MRP1 (38), is known to quench oxidative stress. Increasing MRP1 may quench oxidative stress during times of intestinal inflammation via GSH excretion. An MRP1 increase would neutralize oxidative stress. Without this increase, epithelial damage in models of IBD would be exacerbated.

When inspecting specific leukocytes, expression of MRP1 has been shown to increase on the surface of macrophages during exposure to lipopolysaccharide (LPS), though there has been no extensive work examining the endogenous actions of MRP1 on these cells (39). While no specific studies have linked MRP1 and DC activation to IBD or other inflammatory conditions, MRP1 is critical for DC maturation, and this could also impact TNF-α expression and leukocyte migration to the site of inflammation (40).

P-gp and MRP1 have implied anti-inflammatory effects that appear to protect the epithelium from excess inflammatory stress. MRP2, unlike P-gp and MRP1, has exhibited very clear pro-inflammatory activity. Several substrates overlap between MRP2 and MRP1, though the localization of MRP2 is typically apical in contrast to the basolateral localization of MRP1. MRP2 substrates include amphiphilic anions, bilirubin, glucuronosides, LTC_4, and the aforementioned HXA_3. MRP2 is highly expressed in the intestine, kidneys and liver of mammals. While elimination of MRP2 leads to Dubin-Johnson syndrome, highlighted by a state of hyperbilirubinemia, there is sparse information about the role of MRP2 in IBD and related diseases. In studies conducted in rats, basal MRP2 protein and mRNA expression decreased descending from the

proximal-to-distal intestine, meaning that the highest expression was in the small intestine and decreased descending towards the colon (41).

During *Salmonella* infection of mice, Pazos et. al reported that MRP2 increased, presumably to release HXA_3 (13). In this same study, mice underwent T-cell transfer and were treated with a lipoxygenase inhibitor, which alleviated much of the inflammation observed in mock-treated animals. In addition to examination in mice, intestinal sections of patients suffering from IBD also exhibited increased MRP2 signaling via immunofluorescence (13). MRP2 increase could promote PMN influx during the onset of IBD, creating a pro-inflammatory condition. While influx would not be seen as aberrant during a bacterial infection, an uncontrolled response by PMNs without exposure to a stimulus could lead to host-tissue damage. HXA_3 secretion by MRP2 could lead to PMN transmigration, activation, and subsequent epithelial damage as seen in IBD; it is therefore possible that targeting MRP2, and the subsequent inhibition of HXA_3, may be therapeutic.

It is known that *E. coli* that express Shiga-toxin II (Enterohemorrhagic *Escherichia coli*, or EHEC) reduce expression of both P-gp and MRP2 in the kidneys and livers of patients (42), whereas *E. coli* without Shiga-toxin, a strain of Enteroaggregative *E. coli*, upregulate MRP2 expression in the gut and assists in PMN migration (12). Similarly, *Shigella flexneri* also upregulates MRP2 during infection, implying that Gram-negative intestinal pathogens may cause MRP2 increases during infection by some common mechanism and that it is Shiga-toxin independent.

In contrast to findings with MRP1, it has been shown in rat hepatocytes that TNF-α may reduce the expression of MRP2 (42). Additionally, it has been shown that liver cells exposed to LPS from Gram-negative bacteria may also reduce MRP2 protein (43). In contrast, bacterial infection increases MRP2 protein in intestinal infections, emphasizing tropism differences in eukaryotic cells. There is no report of MRP2 expression in leukocytes during resting states or infection, indicating epithelial cells are the most likely to be impacted by varying MRP2 expression.

One transporter that has been studied but not shown to have many critical activities in the context of bacterial inflammation is Multi-drug-Resistance-associated-Protein 4 (MRP4). MRP4 effluxes nucleoside agents, Prostaglandins 1 and 2, organic anions, bile acids, and folic acid. It is purported to localize on both the apical and basolateral surface of intestinal epithelial cells. Prior reports have shown that MRP4 is important in its interactions with chemicals commonly used to treat IBD, specifically thiopurines (44). Japanese patients with a allelic mutation of *MRP4*, G2269A, showed increased sensitivity to thiopurines because MRP4 is incapable of pumping it out of myeloid cells. These patients also showed lower white-blood-cell counts than wild-type allelic control patients with IBD, though there does not appear to be any direct correlation between this and any reduction in auto-immune diseases (44). Additionally, a recent publication examined a downregulation of MRP4 during IBD in the context of bile-acid reabsorption perturbations (45). Copies of *MRP4* mRNA were reduced in endoscopy tissue isolated from older IBD patients as compared to healthy colons. In recent years, there has also been emerging information on MRP4 efflux of LTC_4 (46).

MRP4 was previously reported to be critical during DC migration, however van der Deen and colleagues noted that murine DC movement had no dependency on MRP4 (40). In the same study, inhibition of dendritic-expressed human MRP4 led to a reduction in migrating DCs in skin explants and *in vitro*-derived Langerhan cells. Any links between MRP4, dendritic cells, and IBD must take into account differences between murine and human data.

1.4 ABC Transporters in the Lung

While research into the activity of ABC-transporters in the intestine has illuminated roles for this family of proteins, the digestive tract is only one particular mucosal surface. Recently, details have emerged as to the activities and expression patterns of ABC-transporters elsewhere, especially the lung. As this field is still evolving, there remains controversy about expression and localization of the various pulmonary transporters. For instance, a review by Margaretha van der Deen indicates that conflicts about localization of the MRPs in Type I epithelial cells exist for MRP1, MRP2, MRP3, MRP4, MRP5, P-gp, and CFTR (27). Much of this divergence centers on the low expression of these proteins in the lung at basal level and how expression can subtly change depending on the method of examination and how the lung is processed.

There are observations that appear to be consistent between studies. P-gp has a relatively low expression in the lung; it is thought to be present in the bronchus and trachea but absent as the airway constricts. Although the role of P-gp in the lung remains unknown, it has been shown that P-gp expression is increased in smokers as compared to

non-smokers. In *in vitro* lung cell lines, while Calu-3 and A549 cell lines express P-gp, it appears absent in H292 cells (Figure 1.2).

MRP1 is mRNA and protein is detectable in pulmonary tissue (27), though it is unclear whether MRP1 is expressed consistently on the apical surface of epithelial cells or strictly on the basolateral surface. Although there have been reports of no change in mRNA levels of *MRP1* during COPD and smoking studies, there have been separate observations of MRP1 protein level reductions in COPD patients (47). There are also indications that MRP1 could be protective during inflammation caused by COPD (47). *Mycobacterium tuberculosis*-infected mice deficient in *Mrp1* have higher bacterial burdens as compared to wild-type mice, though there is no difference in survival between the two groups (48). There has also been investigation involving *M*rp1-knockout mice in *Streptococcus pneumoniae* infection in which *Mrp1*-knockout mice showed increased survival as compared to infected wild-type mice (49). This work is discussed later in Chapters 2 and 4. MRP1 is known to efflux LTC_4 and may influence LTB_4 release from cells, a fact that was reported in the context of PMN infiltration during *S. pneumoniae* infection (49). Expression of MRP1 is one of the many proteins controlled by the transcription factor NRF2. *Nrf2*-knockout mice developed earlier and more severe emphysema during smoking studies with more leukocyte, especially macrophage, infiltration (50).

There is little known about the role of MRP2 in the lung and there are debates as to where and in what contexts MRP2 is expressed in lung tissue (27, 51). In most studies, it is almost undetectable in the absence of inflammation and is much more studied in the

context of lung carcinomas than at basal, non-pathogenic states. Likewise, MRP3 appears almost undetectable in pulmonary tissue, although it is highly expressed in the liver, adrenal glands, pancreas, kidney, intestine, and gall bladder (27). Increases in MRP3 in the human lung are more often associated with tumor development. The activity of MRP3 in non-tumor pulmonary tissue is still unknown. MRP5 has been confirmed to be expressed in pulmonary tissue but the activity and localization is still undetermined (27).

MRP4 has similar activity in the lung and other tissues, such as brain and skeletal muscle. It is known to efflux PGE1 and PGE2 that assist in modulating the immune system (52). In light of that, however, a number of studies have concluded MRP4 does not act in a variety of immune stimuli. For instance, a 2013 study reported no differences in PMN or eosinophil recruitment in the lung during LPS, allergen, or cigarette smoke challenges (53). To that end, while it is known that the lung expresses MRP4, it remains to be seen how dramatically it is able to impact endogenous pulmonary immune function.

It would be imprudent not to recognize another major ABC-transporter in the lung, Cystic Fibrosis Transmembrane Conductance Regulator (CFTR). Though CFTR does not behave as the other ABC-transporters on this list, it is significant in pulmonary physiology. While the MRPs pump a variety of drugs and are widely known for conferring chemotherapeutic resistance, CFTR is a chloride channel that opens and closes during respiration. Cystic Fibrosis is a disease that occurs when a *CFTR* mutation leads to chloride retention in the epithelium, resulting in a buildup of mucus in the pulmonary tract. This leads to obstruction of the air way and results in frequent bacterial infections. CFTR does not directly result in the modulation of the immune system but certainly

modifies the microenvironment, providing a niche for bacteria such as *Pseudomonas aeruginosa*.

1.5 *Streptococcus pneumoniae*

S. pneumoniae (pneumococcus) is a Gram-positive, encapsulated bacterium that normally colonizes the human nasopharynx asymptomatically. Although pneumococcus is permissible to other organisms, such as rodents or other mammals, the natural reservoir seems to be *Homo sapiens*. Depending on given locations and regions of habitation, up to 90% of human population will, at one time, have *S. pneumoniae* inhabiting their respiratory system.

There are currently two available pneumococcal vaccines that are administered to children before two years of age. These vaccines target serotypes of *S. pneumoniae,* as identified by the glycan composition of the pneumococcal capsule. The vaccines target 13- and 23-polyvalent capsular serotypes, which encompass many of the clinically relevant pneumococcal strains. Problematic to the healthcare sector, the capsule is highly divergent and there are over 100 capsule isolates, meaning there are some serotypes that are not protected by the current vaccine regimen. In addition, *S. pneumoniae* goes through certain phase transitions during infection where the acapsular bacteria are predominant in specific regions of the respiratory system (54).

Although pneumococcus can inhabit the nasopharynx asymptomatically, problems arise when bacteria enter the lower respiratory system. Initially, infection can lead to inflammation, presenting clinically as pneumonia. Pathology can progress from

lung infection and enter the blood stream leading to the development of bacteremia and sepsis. *S. pneumoniae* can also cross the blood-brain-barrier and cause meningitis. Prior to introduction of the polyvalent pneumococcal vaccine, invasive disease rates for children under the age of 5 approached 100 cases per 100,000 as reported by the CDC (55). This dropped sharply by approximately 60% after introduction of the pneumococcal vaccine and is currently ~10 per 100,000 in the United States (55). This means, though, that almost 400,000 cases of pneumococcal pneumonia are reported annually to the Centers for Disease Control (56). It is reported that 25-30% of these pneumonia patients develop pneumococcal bacteremia, a condition that has a case-fatality rate of 20% (though, this is closer to 60% in elderly individuals) (56). Complications from infection can also lead to brain injury, amputations, and multi-organ dysfunction.

A number of virulence factors assist in asymptomatic colonization and persistence of *S. pneumoniae*. More information about specific pneumococcal virulence factors and the interactions with the host epithelium as well as other resident bacteria can be found in two extensive reviews: the first in 2008 by Aras Kadioglu (57) and the second from Mook-Kanamori in 2011 (58). It is important to note that normal transmission of *S. pneumoniae* is not contingent on diseased state: *S. pneumoniae* can equally be transmitted by asymptomatic carriers as well as actively diseased individuals. Many of the virulence factors that mediate pathology are originally utilized to assist in asymptomatic carriage. It is widely accepted that a number of bacterial factors, such as pneumococcal phosphorylcholine and Choline-binding Protein A, are able to bind specific receptors on the surface of the epithelium and assist in adherence or internalization of the bacterium

(59-61). Hyaluronate lyase released by *S. pneumoniae* is able to degrade extracellular matrix components (62). Still others, like Pneumococcal Adherence and Virulence factor A and α-Enolase bind fibronectin and plasminogen, respectively (63, 64). Pneumococcal neuraminidase A cleaves terminal sugars, which may reveal adherence molecules, provide carbon sources for energy generation, or assist in biofilm formation. Neuraminidases also cleave mucin, which may reduce mucin density and allow the bacteria to form a niche for growth much easier.

One of the most widely-studied virulence factors, the cholesterol-dependent-cytolysin pneumolysin (PLY), has many effects, including disrupting ciliary beating to allow bacteria to form a static niche within the mucosal surface. To combat secreted host-defenses, Pneumococcal Surface Protein A prevents complement C3 deposition and lysis of the bacteria while pneumococcal IgA cleaves resident IgA1 that might affect the bacteria.

S. pneumoniae not only faces pressure from the host but also from other resident bacteria. To defend itself from other bacteria, *S. pneumoniae* produces bacteriocin, an antimicrobial molecule that targets other species and even other strains of *Streptococcus* (65). One of the more unique virulence factors is pneumococcal hydrogen peroxide. Most bacteria harbor catalase to neutralize hydrogen peroxide, but because *S. pneumoniae* does not have an endogenous catalase, hydrogen peroxide builds up to (potentially) hazardous levels for surrounding bacteria. *Haemophilus influenzae*, for example, is unable to grow *in vitro* in the presence of pneumococcus unless an exogenous catalase is present during growth stages (66). Unique to *S. pneumoniae* in the context of this study is that, unlike

many of the other Gram-negative bacteria mentioned previously, *S. pneumoniae* doesn't have a classic secretion system. To release soluble virulence factors, it is presumed that the bacteria must self-lyse. In a coordinated but not altogether understood process, LytA, a lytic-initializing gene activates and causes the bacteria to lyse (57). In the case of PLY, it is thought that autolysis assists in releasing PLY to the extracellular milieu, though this is contentious as certain serotypes do not appear to need autolysis to release PLY (67). Autolysis would also release intracellular hydrogen peroxide that accumulates during normal metabolism.

S. pneumoniae also needs to defend itself from innate host defenses. Although pathology is not normally observed in nasopharyngeal carriage, resident leukocytes still respond by attempting to engulf bacteria. During carriage, other bacterial species may also try to form niches in the nasal passage. This highlights the two-front arms race that *S. pneumoniae* enters when colonizing. To neutralize the eukaryotic defenses, pneumococcus has an immunogenic capsule that prevents mucus entrapment and opsonization from white blood cells (68). Somewhat ironically *S. pneumoniae* employs a number of different mechanisms to avoid killing by PMNs, rendering the overall PMN response necessary in the early stages but also highly inefficient. *S. pneumoniae* is primarily killed via elastase and cathepsin G (69), though van der Windt and colleagues recently determined that acapsular pneumococcus are more resistant than their encapsuled counterparts (70). EndA, an endonuclease, is also thought to provide protect from PMN NETs as it degrades DNA. D-analynation of lipoteichoic acid (modifying

lipoteichoic acid with D-alanine) also confers some resistance to NETs via electrostatic repulsion of the anti-microbial peptides contained there within (71).

PMN activity is necessary to contain the initial pneumococcal infection and combat the infection through a variety of non-specific ways, such as release of granules, ROS, anti-microbials, and activation of humoral cytokines. The tradeoff of this activity is that it causes potential damage to both the bacteria and the surrounding healthy pulmonary tissue. There is a growing body of literature to suggest that either PMN activity or epithelial transcytosis itself could cause gaps in the paracellular junctions, permitting bacteria to reach the underlying basement membrane and then travel through the endothelium to the blood stream, causing bacteremia (Discussed in greater detail Chapter II). Blood infection is also e pre-requisite for bacteria to cross the blood-brain-barrier and cause meningitis. One viewpoint supports that by limiting entry of the PMNs in the lumen of the lung, without eliminating PMNs entirely, the host might be able to control the infection without subjecting the pulmonary tissue to collateral damage. Numerous reports have shown that if PMN infiltration is suppressed, murine infections fail to progress as quickly to bacteremia, if at all (19, 72, 73). Given that HXA_3 is critical in lumenal PMN migration, one desire of our studies was to identify potential targets involved in HXA_3-mediated transepithelial migration and to assay whether inhibition of these new targets would recapitulate the previously observed reduction in bacteremia.

1.6 Thesis summary: How is HXA_3 effluxed during pulmonary infections and what virulence factors impact this/these efflux transporter(s)?

The foundational work that influenced this particular thesis project described *S. pneumoniae*-induced PMN migration as HXA_3-dependent (19). The second identified MRP2 as the HXA_3 efflux transporter in the intestine (13). In comparing and contrasting the HXA_3 effects in the lung and the intestine, studies show that all of the bacterial species investigated initiate the release of arachidonic acid via PLA_2 and that arachidonic acid is processed by 12/15-lipoxygenase. It is currently unknown, however, how the HXA_3 is effluxed from the pulmonary epithelium, whether by MRP2 or another, similar, transporter. As stated in section 1.4 and 1.5, there are a number of possible ABC-transporters that could be contributing to immune modulation in the lung during *S. pneumoniae* infection.

The identification of the HXA_3 efflux transporter is critical for future therapeutic and intellectual endeavors focusing on PMN inflammation. Bhowmick et al. describes not only that HXA_3 is critical for PMN infiltration during *S. pneumoniae* infection but also bolsters previous findings that there is a correlation between dissemination of *S. pneumoniae* and PMN infiltration. However, targeting HXA_3 and its synthesis gene, 12/15-Lipoxygenase, is challenging, as these are intracellular processes that could have multiple off target effects. Efflux transporters, on the other hand, are surface-exposed targets that have relatively localized expression patterns. In addition, there are multiple drugs approved for human use targeting these efflux transporters, making it a strong drug-repurposing candidate. If the efflux transporter is the same as in the intestine,

MRP2, it points to the conserved nature of systemic mucosal immunity. If it is different, it emphasizes that tropic uniqueness could be key to targeting specific therapies for localized inflammation/anti-inflammation interventions. Either answer would yield a wealth of information with which one may move forward examining how PMNs infiltrate the mucosal lumen during inflammatory events.

Likewise, identifying the virulence factors that affect this/these transporters(s) is critical to establish how conserved the HXA_3 pathway and efflux activity is across a variety of mucosal surfaces. By identifying those *S. pneumoniae* virulence factors that are critical for HXA_3 and PMN transepithelial migration, additional eukaryotic targets critical to transepithelial PMN migration might be identified. By identifying common pathways between *S. pneumoniae* infection and the prior identified intestinal inflammatory events, universal pro-inflammatory pathways could come to light.

To investigate the pulmonary HXA_3 transporter and *S. pneumoniae* virulence factors that influence PMN transepithelial migration, the specific aims that we will be examining are the following:

1) What efflux transporters are modulated during *S. pneumoniae* infection?

a. Is MRP2 the efflux transporter in pulmonary infections or is it a different transporter?

b. Are there other transporters involved in the process?

c. Will manipulation of the efflux transporter yield similar phenotypes as the blockade of HXA_3 expression in *in vitro* and *in vivo* experiments?

2) What virulence factors might be influencing the efflux transporter?

a. Can we identify the specific players that are critical for PMN migration?

b. Is there a common thread between the *S. pneumoniae* virulence factors and other bacterial virulence factors that are important for HXA_3?

c. What upstream eukaryotic pathways or secondary signals might be triggered by these virulence factors to influence the HXA_3 transporter/PMN migration?

We set out to initially to identify the efflux transporter assisting in the generation of HXA_3 gradients during *S. pneumoniae* infection. We took a semi-biased screening approach to examine the pulmonary Multi-drug-Resistance associated Proteins that are modulated during infection with *S. pneumoniae.* We then assessed the likely role of each MRP that changed during the infection. We discovered that during infection with *S. pneumoniae*, apical MRP1 is reduced while MRP2 increases its presence on the plasma membrane apical surface. After identifying MRP1 and MRP2 as proteins of interest, we examined the likely role they played in infection. We specifically focused on suppressing the PMN infiltration through inhibition of MRP2 and tracked any changes in disease progression in mice infected with *S. pneumoniae*.

To elucidate how *S. pneumoniae* influences the MRPs on the surface of the epithelium, we then examined the virulence factors that influence HXA_3-dependent PMN transmigration. Our observations highlighted that virulence factors influencing transepithelial PMN migration in general also appear to influence MRP2 translocation, such that there appears to be a direct correlation between MRP2 increase on the apical

surface of the epithelium and PMN migration. There are likely a number of virulence factors that induce MPR2 translocation and HXA_3 production. We identified that PMN migration and MRP2 increases are dependent on at least PLY presence and hydrogen peroxide production. There is at least a third factor produced by live bacteria that induces this effect, as purified PLY and hydrogen peroxide, alone or together, were insufficient to induce PMN migration in our model. These virulence factors appear to signal through calcium influx and only certain types of intracellular calcium increases facilitate PMN migration and MRP2 apical localization.

Preface to Chapter II

Data and text from this Chapter appears in publication through the publisher mSphere in Volume 3, Issue 4, 2018 titled

Transporters MRP1 and MRP2 regulate opposing inflammatory signals to control transepithelial neutrophil migration during *Streptococcus pneumoniae* lung infection

Manuscript was prepared with assistance from the following authors:

Randall J. Mrsny (University of Bath), Paula Cortés Barrantes (Brigham and Women's Hospital), Jerrold R. Turner (Brigham and Women's Hospital), John M. Leong (Tufts University), and Beth A. McCormick (UMASS Medical School)

All experiments and figures completed by Andrew Zukauskas

Pathology scoring (Figure 2.12) completed by Paula Cortés Barrantes and Jerrold R. Turner

Intellectual input and editing completed by Andrew Zukauskas, Randall J. Mrsny, John M. Leong, and Beth A. McCormick

Chapter II

Transporters MRP1 and MRP2 regulate opposing inflammatory signals to control transepithelial neutrophil migration during *Streptococcus pneumoniae* lung infection

2.1 Introduction

Despite the availability of vaccines, antibiotics, and improved hygienic advancements, bacterial pneumonia remains a demanding worldwide medical challenge. The Centers for Disease Control and Prevention (CDC) estimate that *Streptococcus pneumoniae* (pneumococcus, *S. pneumoniae*), the most common bacteria associated with community-acquired pneumonia, causes ~400,000 pneumonia cases in the United States, and leads to ~35,000 deaths annually. 30% of those presenting with pneumococcal pneumonia develop bacteremia, a condition with mortality rates close to 20% (56, 74).

A hallmark of pneumonia pathophysiology is the recruitment of polymorphonuclear cells (PMNs, or neutrophils) to the pulmonary lumen via extravasation and trans-epithelial transcytosis. Although PMN recruitment serves initially to clear invading bacteria, it also contributes directly to lung injury and pulmonary dysfunction (75-77). Studies have indicated that transepithelial PMN migration can actually mediate bacterial blood infiltration (19, 72, 73, 78, 79).

To better understand mechanisms regulating PMN influx during pneumococcal infection, we previously examined host mediators of *S. pneumoniae*-induced PMN migration. Transepithelial leukocyte migration during pneumococcal infection required the lipid chemoattractant hepoxilin A_3 (HXA_3), an eicosanoid synthesized from arachidonic acid via 12-lipoxygenase (LOX) and secreted by lung epithelial cells (19).

Pharmacologic inhibition or genetic ablation of 12-LOX profoundly decreased PMN influx into the lungs of *S. pneumoniae*–infected mice and resulted in both uniform survival and reduced bacteremia during an otherwise lethal pulmonary challenge (19). Thus, 12-LOX-dependent production of HXA_3 and subsequent PMN transepithelial migration appears to be required for high-level bacteremia.

Most information regarding HXA_3-induced PMN emigration is derived from studies involving intestinal Gram-negative bacterial infection (4, 11, 12, 80). At the intestinal surface, HXA_3 apical epithelial secretion requires the ATP-Binding Cassette (ABC) Transporter multi-drug resistance associated protein 2 (MRP2; also known as ABCC2 or c-MOAT) to establish a chemotactic gradient targeting PMNs to sites of inflammation (4, 13). Although ABC transporters were originally identified as contributors to multi-drug resistance due to their capacity to extrude cytotoxic drugs, emerging reports suggest that they play roles in host defense and immune regulation (27, 31, 35, 52, 81-83). To date, few studies have identified ABC transporters that mediate proinflammatory activity in the lung during bacterial infection.

Herein, we demonstrate that ABC transporters MRP1 and MRP2 are diametrically expressed at the apical epithelial surface and actively efflux substrates that control PMN migration. Characterizing this relationship, MRP1 effluxes substrates that suppress PMN transmigration; MRP1 apical expression greatly diminishes upon *S. pneumoniae* infection. In contrast, MRP2 becomes highly enriched on the epithelial apical surface during pneumococcal infection and promotes PMN migration. Overall, these findings reveal a paradigm that epithelial cells at the lung mucosal surface act as critical sensors

that can determine when to initiate PMN transmigration in response to a pro-inflammatory stimulus such as *S. pneumoniae*, and when to maintain a non-inflammatory state.

2.2 Results

Survey of MRP expression patterns during *S. pneumoniae* infection

To study inflammatory responses during infection with *S. pneumonia*e we have established an *in vitro* model of PMN migration using polarized monolayers of NCI-H292 cells (H292) (84-86). We used this model to examine the profiles of MRPs that differ in mRNA or protein expression during *S. pneumoniae* infection. Whether analyzing whole cell protein or mRNA (Figure 2.1), little change was observed. Of note, MRP1 decreased slightly during infection at both the mRNA and protein level. No other values reached 10% difference among MRP2, MRP4, or MRP5. MRP3 and P-glycoprotein were undetectable at basal state and during infection at the protein or mRNA level (data not shown).

MRP1 and MRP2 show inverse patterns of expression during *Streptococcus pneumoniae* infection

Though there were few changes observed in mRNA and protein levels, it is documented that MRPs undergo critical post-translational modification that affect their subcellular localization (26, 87). HXA_3 efflux draws PMNs to the site of infection, in this case to the epithelial cell apical surface. To that end, we sought to specifically examine

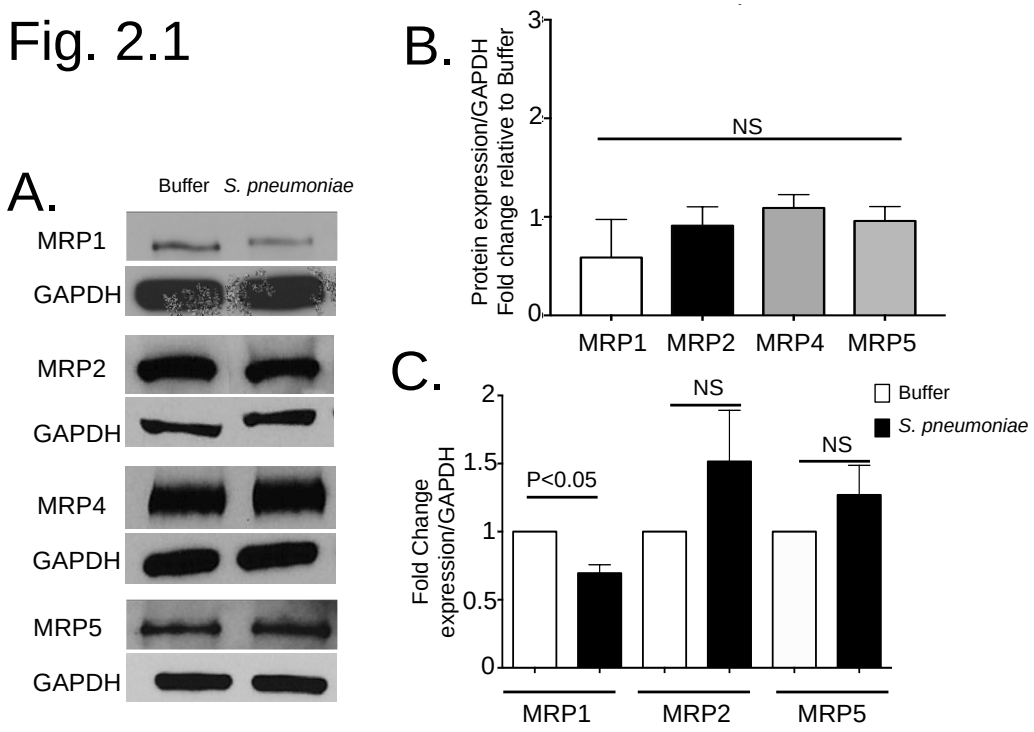

Figure 2.1. MRP inquiry during infection

NCI-H292 cells were infected with *Streptococcus pneumoniae* and MRP profiles were initially generated by 2 different techniques: protein western blots and mRNA RT-PCR quantification. **(A)** MRP1, 2, 3, 4, 5, and P-gp were investigated for possible changes upon infection with *Streptococcus pneumoniae* via western blot which showed slight reduction in MRP1 but no other strong changes. Shown is a representative blot from 3 separate experiments **(B)** Densitometry of western blots of n=3. Protein of interest was normalized to loading control (GAPDH) and fold changes comparing the infected samples to uninfected buffer samples were calculated. **(C)** RT-PCR revealed a slight reduction in MRP1 and slight increases in MRP2 and MRP5 during pneumococcal infection. P-gp and MRP3 were not detectable by any of these methods.

changes in apical localization of our chosen proteins. We, therefore, selectively labeled the apical surface of infected epithelial surfaces with biotin and compared labeled proteins in infected and uninfected surfaces.

Biotinylated apical MRP1 drastically decreased after infection with *S. pneumoniae*, while apical MRP2 increased (Fig. 2.2 A and B). In comparison, surface-expressed MRP4 and MRP5 did not change (Fig. 2.2 A and B). Using immunofluorescence microscopy, we confirmed that pneumococcal infection induced localized decreases in MRP1 and reciprocal increases in MRP2 (Fig. 2.2 C and D). Importantly, we observed no change in MRP4 or MRP5 surface localization via immunofluorescence following pneumococcal infection. Based on these data, we focused our studies on potential modulation of MRP1 and MRP2.

To examine whether *in vitro* observations correlated to changes in *in vivo* MRP localization, C57BL/6J mice were infected with $2.5x10^5$ CFU of *S. pneumoniae* or mock-infected with PBS alone. Two days post-infection, mice were sacrificed. Lungs were excised, sectioned, and probed to detect MRP1, MRP2, MRP4, and MRP5 via immunofluorescence (Fig. 2.3). Similar to our *in vitro* data, we saw decreases in the MRP1 signal and increases in MRP2 during pneumococcal infection. No such changes were observed with MRP4 or MRP5, pointing to a consistency in MRP modulation in both cell lines and the mouse (Fig. 2.3 A and B).

Fig. 2.2

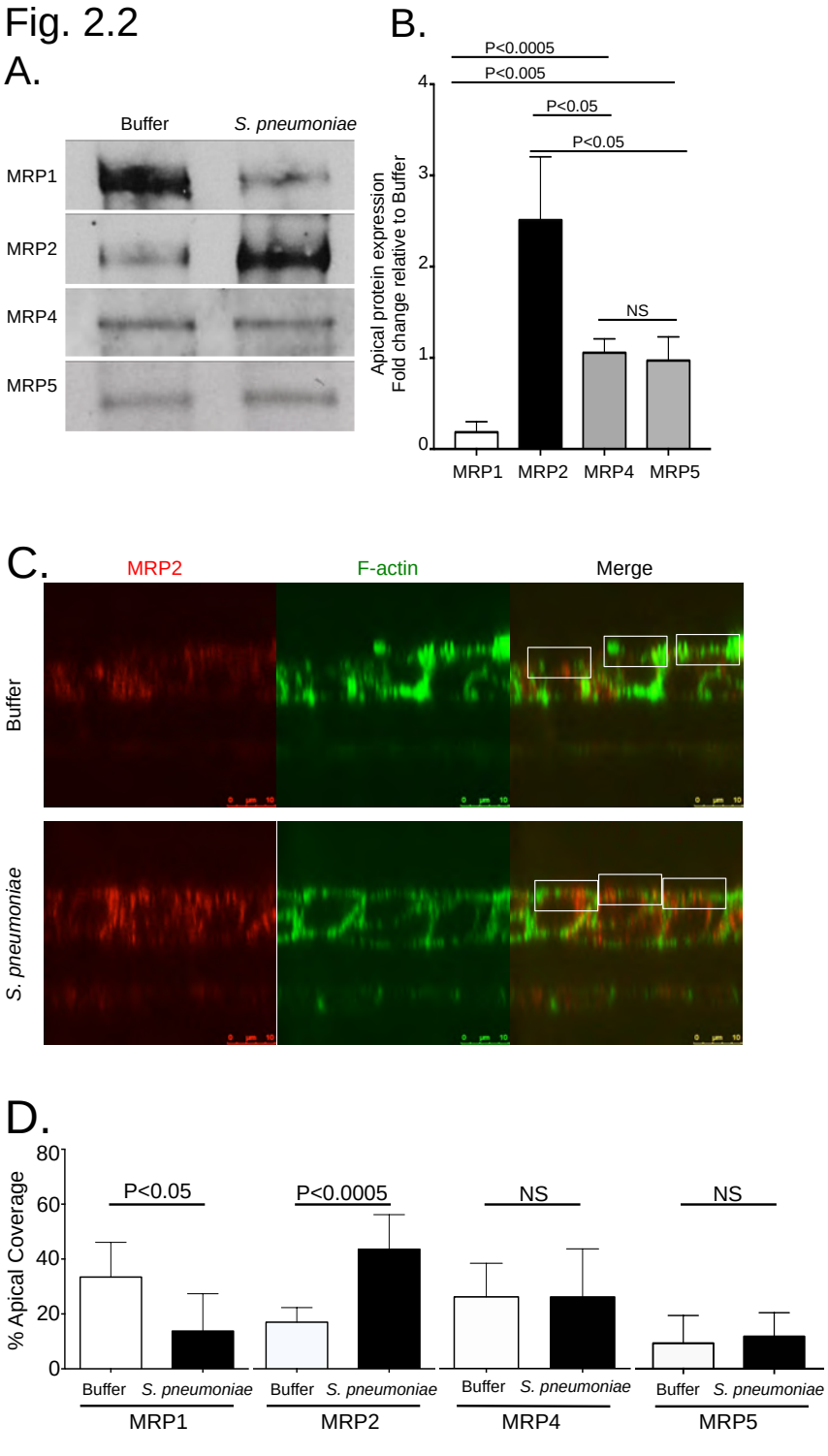
A.
Buffer
S. pneumoniae
MRP1
MRP2
MRP4
MRP5
B.
P<0.0005
P<0.005
P<0.05
P<0.05
NS
Apical protein expression
Fold change relative to Buffer
0
1
2
3
4
MRP1
MRP2
MRP4
MRP5
C.
MRP2
F-actin
Merge
Buffer
S. pneumoniae
D.
% Apical Coverage
0
20
40
60
80
P<0.05
P<0.0005
NS
NS
Buffer
S. pneumoniae
MRP1
MRP2
MRP4
MRP5

Figure 2.2. MRP1 protein on the apical surface reduces during infection with *Streptococcus pneumoniae* while MRP2 increases

The apical surface examination of mock-infected (Buffer) or TIGR4-infected (*S. pneumoniae*) polarized H292 cells. Cells were treated with HBSS (Buffer) or infected (*S. pneumoniae*), washed, and allowed to rest at 37 degrees for 1 hour post-infection. **(A)** Apical surfaces were then labeled with biotin and lysed. Samples were normalized to protein content against a BSA standard, exposed to streptavidin beads, and subjected to an SDS-PAGE gel. Blots were probed with primary antibodies for the selected proteins. Shown is a representative western blot of apical biotinylation probing MRP expression. **(B)** Densitometry of summated western blot samples, across multiple experiments. Statistics calculated using student's T-test as compared with MRP4 or MRP5, n=3. **(C)** Buffer treated or infected cells were fixed and stained for MRP2 and F-actin. Immunofluorescence cross-section Z-stack images of F-actin were utilized to identify cellular borders and apical surface (green). The corresponding region of MRP2-stained Z-stack (red) was marked for the particular region of interest (white boxes) and calculated for the total apical coverage using ImageJ. **(D)** The calculated percentage of the area taken up by the indicated MRPs in (C) via calculations completed in ImageJ (see Materials and Methods). P-value calculated using student t-test comparing uninfected and infected percentages for the given protein (n=8). Quantification samples for biotinylation and immunofluorescence were taken from at least 2 separate infections with similar results.

Fig. 2.3 A.

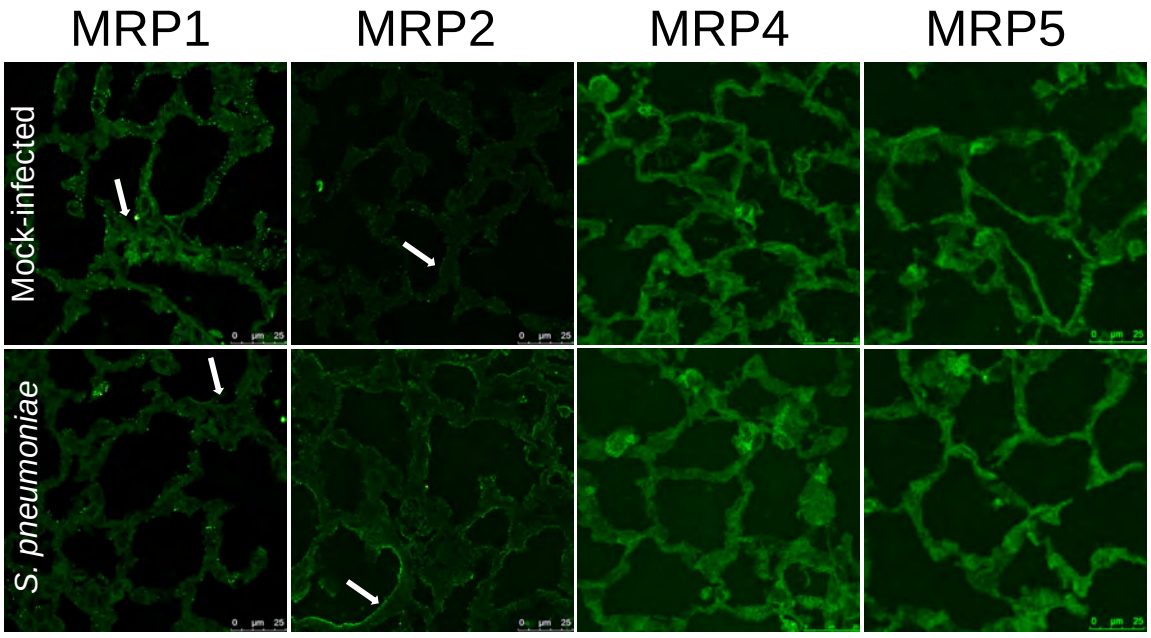
MRP1
MRP2
MRP4
MRP5
Mock-infected
S. pneumoniae

B.

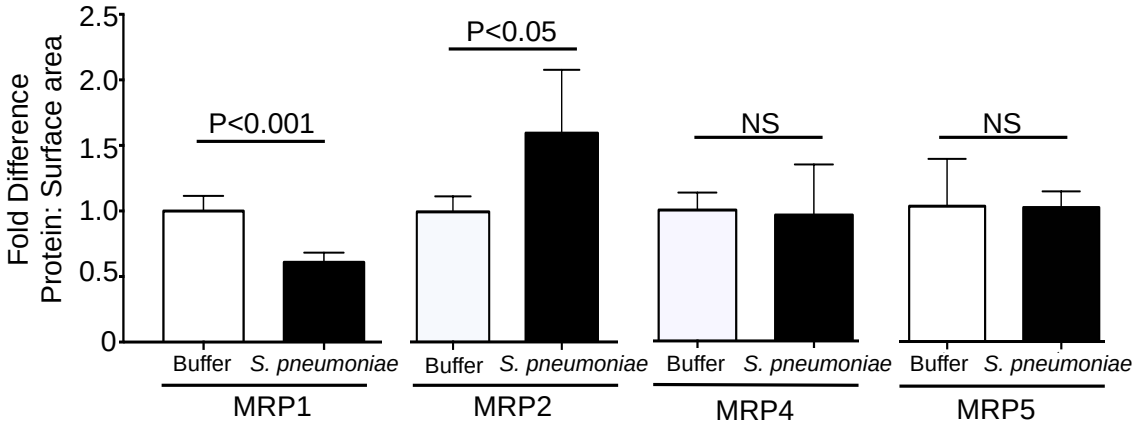
Fold Difference
Protein: Surface area
2.5
2.0
1.5
1.0
0.5
0
P<0.001
P<0.05
NS
NS
Buffer
S. pneumoniae
MRP1
MRP2
MRP4
MRP5

Figure 2.3. *S. pneumoniae* infection reduces MRP1 and increases MRP2 upon pulmonary infection in mice

Mice were infected via an intratracheal route with *S. pneumoniae* and sacrificed 2 days post-infection. Lungs were excised, re-inflated, sectioned, and stained for MRP1, MRP2, MRP4, or MRP5. **(A)** Shown are representative images from 3 different experiments. Arrows indicate points of interest. In particular, areas of similar density in MRP1-stained lungs appear to have reduced expression in infected lungs as compared to uninfected lungs (arrow). MRP2 staining appears to increase significantly on the cell periphery during infection as compared to mock-infected lungs (arrow). No such increases or decreases are observed in MRP4 and MRP5. **(B)** Quantification of staining. Antibody staining was quantified and normalized to surface area (measured by F-actin, not shown). Shown are the fold differences of signal: surface area for each given antibody comparing infected (*S. pneumoniae*) to uninfected (Buffer) animals. Values are expressed as fold increase or decrease to uninfected samples.

MRP2 controls PMN transepithelial migration

Given that MRP2 controls aspects of PMN transcytosis in intestinal epithelium (13), we sought to examine MRP2s ability to drive pro-inflammatory events in the context of *S. pneumoniae* infection. We previously showed that PMN transmigration into lung airways during pneumococcal infection required HXA_3 (19). We also demonstrated that MRP2 upregulates during intestinal inflammation and that inhibition of MRP2 function suppresses PMN migration (13). It has not been shown, however, that MRP2 location or activity is affected by infection by Gram-positive bacteria, such as *S. pneumoniae*. Based upon these previous findings, we examined whether pharmacological inhibition of MRP2 suppresses PMN transepithelial migration across pulmonary epithelium during pneumococcal infection.

To inhibit MRP2, cells were treated with Probenecid, a MRP2 inhibitor (13, 88-90). *In vivo* Probenecid is relatively well tolerated with death occurring in mice that received 1600 mg/kg (91). It is possible for Probenecid to affect other transporters, but more often these transporters need higher concentrations than that which is efficient to inhibit MRP2 (29, 81, 92, 93). In addition, Probenecid has been shown to have some effects in inhibiting MRP1 (94); however, biotinylation data in Fig. 1 and 2 would indicate that MRP1 is already reduced during infection. Any effects inhibiting MRP1 would likely exacerbate, rather than curtail, PMN recruitment during infection. This idea will also be explored in more detail later in the manuscript.

Cells were treated 1 hour pre-infection with Probenecid and then subjected to infection and a PMN-migration assay. Probenecid treatment had no effect on the basal

PMN migration across uninfected cells but suppressed PMN transmigration across infected H292 monolayers by ~3-fold ($p<0.05$) compared to mock-treated controls (Fig. 2.4A). However, when we used a different PMN chemoattractant that acts independently of the HXA_3 pathway, formyl-methionyl-leucyl-phenylalanine (fMLP) (95, 96), we failed to observe any Probenecid-related reduction in PMN migration (Fig. 2.4B).To ensure the PMN transmigration was not due to pneumococcal-mediated epithelial cell apoptosis, we performed Annexin V staining (Fig. 2.4C) and found no significant increase in apoptosis during infection, consistent with previous reports (97).

MRP2 inhibition mitigates pulmonary PMN infiltration and bacteremia following lung challenge with *S. pneumoniae.*

S. pneumoniae intratracheal infection of C57BL/6J mice initially causes pneumonia, leads to bacteremia, and, ultimately, septicemia that causes death (98). As shown previously, reduced PMN migration can diminish bacteremia and improve survivability of pneumococcal-infected mice (19, 72, 73). With the knowledge that MRP2 inhibition diminishes PMN migration *in vitro*, we sought to test whether MRP2 function had subsequent impact on disease in our murine infection model, especially in the context of PMN transmigration.

Four sets of experiments were conducted: all involved mice that were pre-treated with either PBS or Probenecid at 1mg/kg delivered via the trachea to inhibit MRP2 function. Previous studies in this specific model have indicated that maximal PMN recruitment occurs between 18- and 24-hours post-infection (73); therefore, two sets of

mice were sacrificed at either 24- or 48-hours post infection to examine the leukocytes entering the lung via Bronchial-Alveolar Lavage (BAL) collection (see Materials and Methods). The third set was sacrificed 2 days post-infection to test for bacteremia, and total lung burden. The fourth set was monitored for morbidity that would require sacrifice as dictated by our SOP (see Materials and Methods).

Upon examining the contents of BAL fluid, we noted that Probenecid treatment consistently reduced the number of neutrophils on the first day post-infection by ~35% (Fig. 2.5A). This trend continued through 48-hours post-infection and the combined values of 24- and 48-hour PMN infiltration showed significant differences as calculated using two-way ANOVA. When measuring expression of pro- and anti-inflammatory cytokines from the BAL, we noted that there appeared to be no substantial differences between probenecid-treated and mock-treated animals in any of the measured inflammatory cytokines at the times mentioned, with exception to a reduction in IL-10 in probenecid treated mice at 24-hours post-infection (Fig. 2.6). We don't believe that this is a substantial physiological difference as reductions or eliminations of IL-10 in *S. pneumoniae* infected mice generally lead to a larger infiltration of PMNs, not fewer ((99)). No other significant differences in T-cells, macrophages, or dendritic cells were observed (Fig. 2.7). Despite the reduction in PMNs, no differences were observed in pulmonary bacterial burden 48-hours post-infection (sacrificed whether exhibiting morbidity or active and healthy, Fig. 2.5 B) or upon death during survival experiments (Fig. 2.7D).

Fig 2.4 A.

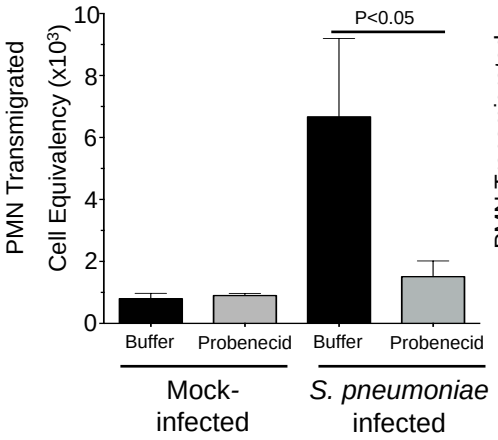
PMN Transmigrated
Cell Equivalency (x10³)
10
8
6
4
2
0
P<0.05
Buffer
Probenecid
Buffer
Probenecid
Mock-infected
S. pneumoniae infected

B.

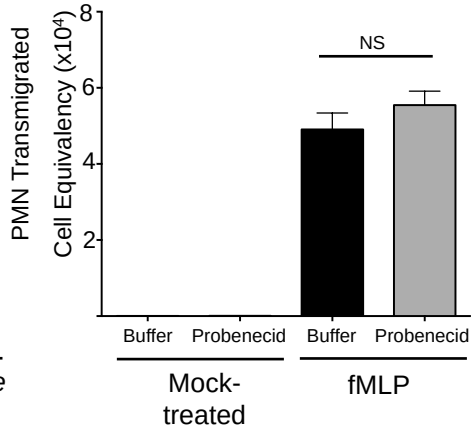
PMN Transmigrated
Cell Equivalency (x10⁴)
8
6
4
2
NS
Buffer
Probenecid
Buffer
Probenecid
Mock-treated
fMLP

C.

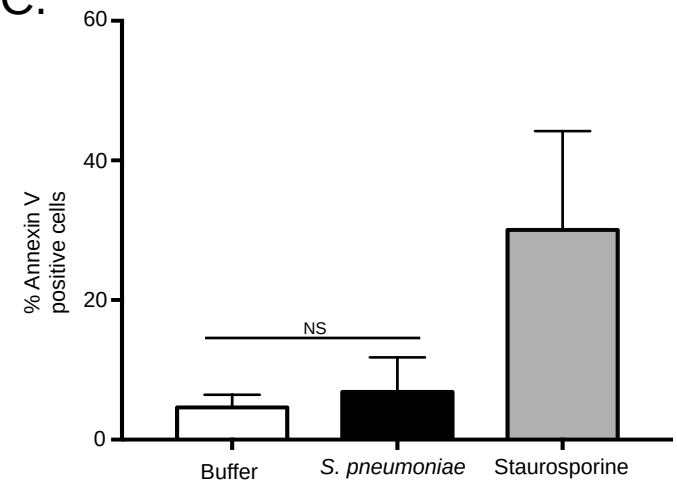
% Annexin V positive cells
60
40
20
0
NS
Buffer
S. pneumoniae
Staurosporine

Figure 2.4. MRP2 inhibition via probenecid reduces PMN migration across polarized pulmonary epithelial cells which is not dependent on apoptosis

Polarized NCI-H292 cells on filter membranes were incubated with 100μM of the MRP2 inhibitor Probenecid or mock-treated for 1 hour with PBS before **(A)** apical infection with *S. pneumoniae* at 10 MOI or **(B)** the HXA_3-independent bacterial product formyl-methionyl-leucyl-phenylalanine (fMLP). For both (A) and (B), mock-infected/treated cells were exposed to HBSS for the treatment time- period and basolateral-to-apical migration of PMNs was quantified with a myeloperoxidase assay against a standard number of PMNs (see Materials and Methods). Shown is one representative experiment from at least 3 experiments performed. Statistics completed using students T-test. **(C)** H292 cells were treated with HBSS, wild-type TIGR4 *S. pneumoniae*, or the cytotoxic compound staurosporine at 1 μM. There was no significant increase in Annexin V staining in infected cells (black) when compared to uninfected buffer control cells (white).

In line with previously mentioned data supporting that reduction of infiltrating PMNs reduces bacteremia, probenecid treated animals showed fewer mice exhibiting bacteremia and ~10-fold lower CFU in the blood during the first 24-hours as compared to PBS-treated mice (Fig. 2.5 C). This trend continued in the 48-hour time-point though did not reach statistical significance. The resulting survival curves showed probenecid treatment improved survival by 30-40% consistently (Fig. 2.5 D). Therefore, MRP2 inhibition via Probenecid treatments was found to be effective at limiting PMN infiltration to the lung 24 h post-infection, corresponding to a reduction in bacteremia and increased survival. This is not to say, however, that we seek to use Probenecid as a treatment for *S. pneumoniae* infection or that it should be given prophylactically. We merely are using Probenecid to highlight that MRP2 is an interesting molecule for further research/therapeutic targeting.

MRP2 and MRP1 promote the secretion of proinflammatory and anti-inflammatory lipids, respectively.

To better understand how MRP1 or MRP2 function could impact pneumococcal-induced PMNs, we generated H292 cell lines constitutively expressing shRNAs targeting MRP1 or MRP2 expression (Fig. 2.8). Because it is known that MRP2 is able to efflux the pro-inflammatory molecule HXA_3 in the intestines (13), we hypothesized limiting MRP2 expression would reduce the amount of HXA_3 effluxed during pneumococcal infection. As HXA_3 is an eicosanoid, we began by assessing the properties of hydrophobic material(s) enriched from apical secretions of *S. pneumoniae*-infected

Fig. 2.5

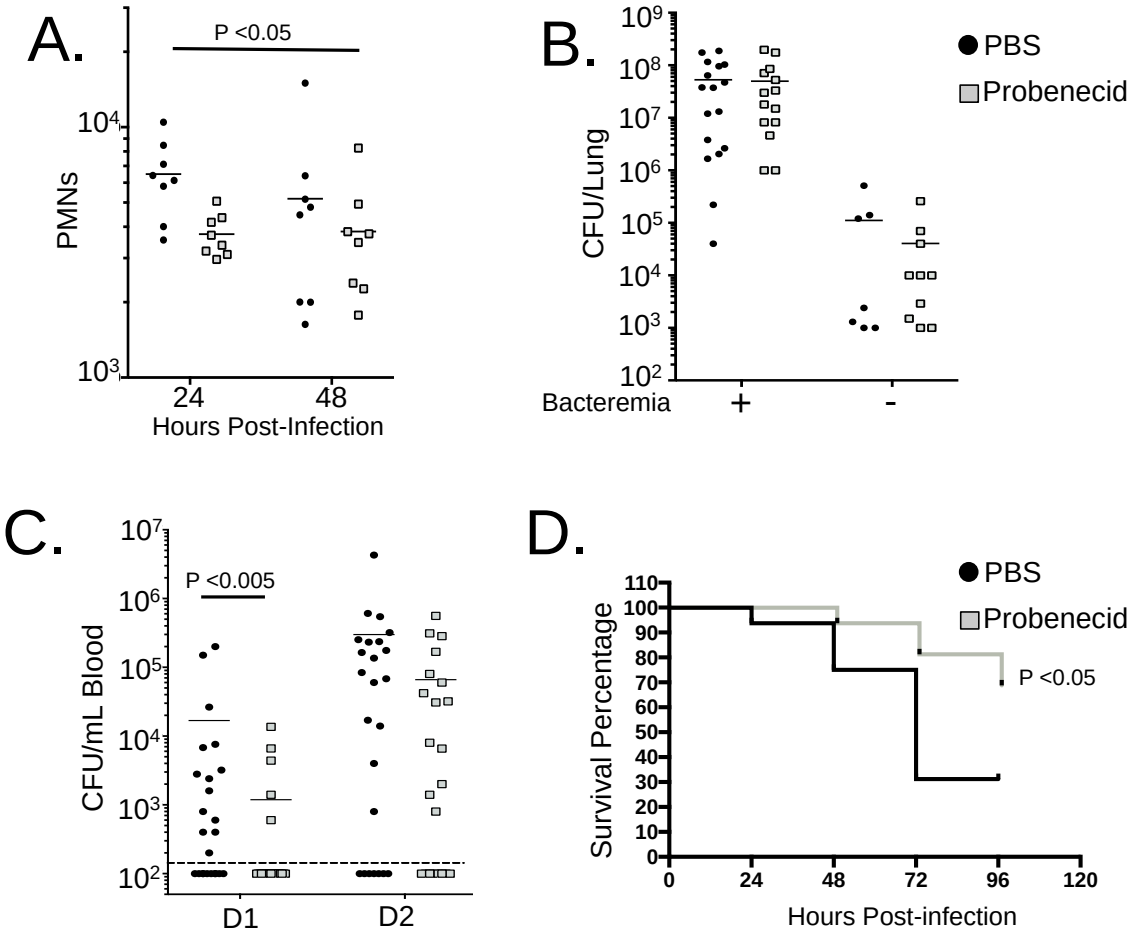
A.
P <0.05
PMNs
10^4
10^3
24
48
Hours Post-Infection
B.
CFU/Lung
10^9
10^8
10^7
10^6
10^5
10^4
10^3
10^2
Bacteremia
+
-
PBS
Probenecid
C.
CFU/mL Blood
10^7
10^6
10^5
10^4
10^3
10^2
P <0.005
D1
D2
D.
Survival Percentage
110
100
90
80
70
60
50
40
30
20
10
0
0
24
48
72
96
120
Hours Post-infection
PBS
Probenecid
P <0.05

Figure 2.5. MRP2 inhibition mitigates pulmonary burden and bacteremia following lung challenge with *S. pneumoniae*

Using an *in vivo* model of PMN migration, we examined the results of MRP2 inhibition. C57/Bl6 mice were treated with either PBS or Probenecid 3 hours prior to- and 3 hours post-intratracheal application of $2.5x10^5$ *S. pneumoniae*. Four sets of mice were infected in this way **(A)** Comparing the number of PMNs found in the lumen after isolating BAL after 24- and 48-hours post-infection. PMNs, identified as Ly6g-positive cells were quantified by flow cytometry (n=8). **(B)** Overall lung burden from mice sacrificed on day 2. Mice were sacrificed, lungs were excised, homogenized, and total burden was calculated using serial dilutions (n=24 each condition). (+) Bacteremia indicates that mice had detectable levels of bacteria in the blood 48-hours post-infection. (-) Bacteremia indicates no bacteria were detectable in the blood during tail-vein bleeds **(C)** Bacteremia, as measured by tail vein bleeds, from cohort from (B) (see Materials and Methods). Shown are detectable events of colony formation on D1 and D2 (n=24). The dotted line represents the limit of detection and, as such, mice without visible bacteremia were represented as "100 CFU/mL", just below this level of detection. B and C statistical significance was calculated using Mann-Whitney test. **(D)** Presented is the 4^{th} set of mice, a survival experiment. n= 16 mice per condition, statistics were calculated using Mantel-Cox test and Gehan-Breslow-Wilcoxon test. Probenecid-treatment consistently increased survival by approximately 30-40% during survival experiments and often delayed symptoms, such as lethargy. Mouse experiments were repeated and observed to have similar results in at least 2 different experiments.

Fig. 2.6

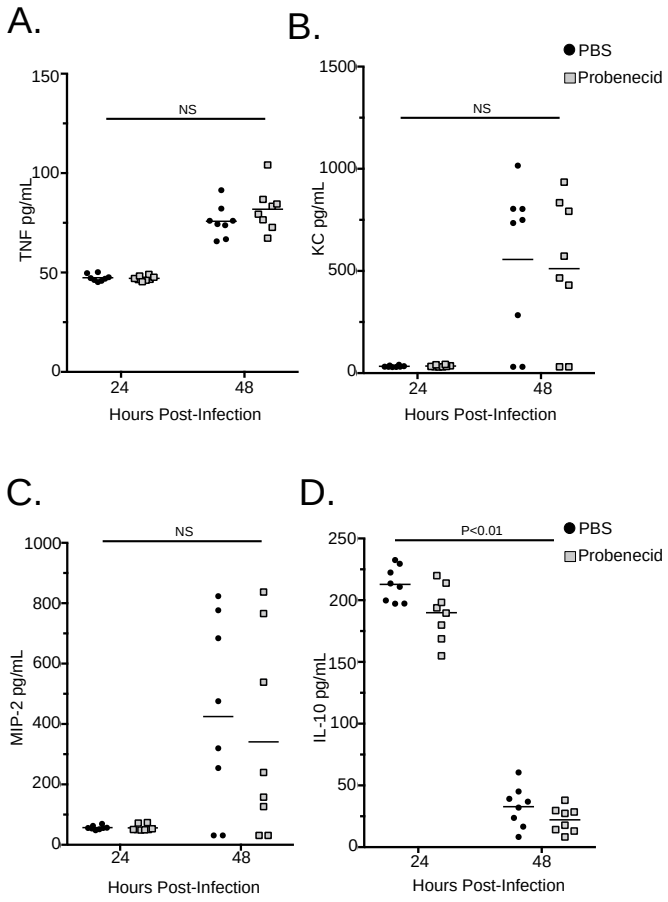

Figure 2.6. ELISA data shows no significant pro-inflammatory differences

3 mL BAL samples from infected mice in Figure 4A (and Supplemental Figure 4 B, C, and D – all samples are from the same 8 mice). Both PBS mock-treated and Probenecid-treated mice were infected and BAL was tested for TNF **(A)**, KC **(B)**, the murine equivalent to IL-8), MIP2 **(C)**, and IL-10 **(D)**. No significant differences were observed except for IL-10, as calculated by 2-way ANOVA. Values were slightly lower than expected due to the elution of BAL fluid in 3mL instead of the classic 800 µL-1mL.

Fig. 2.7

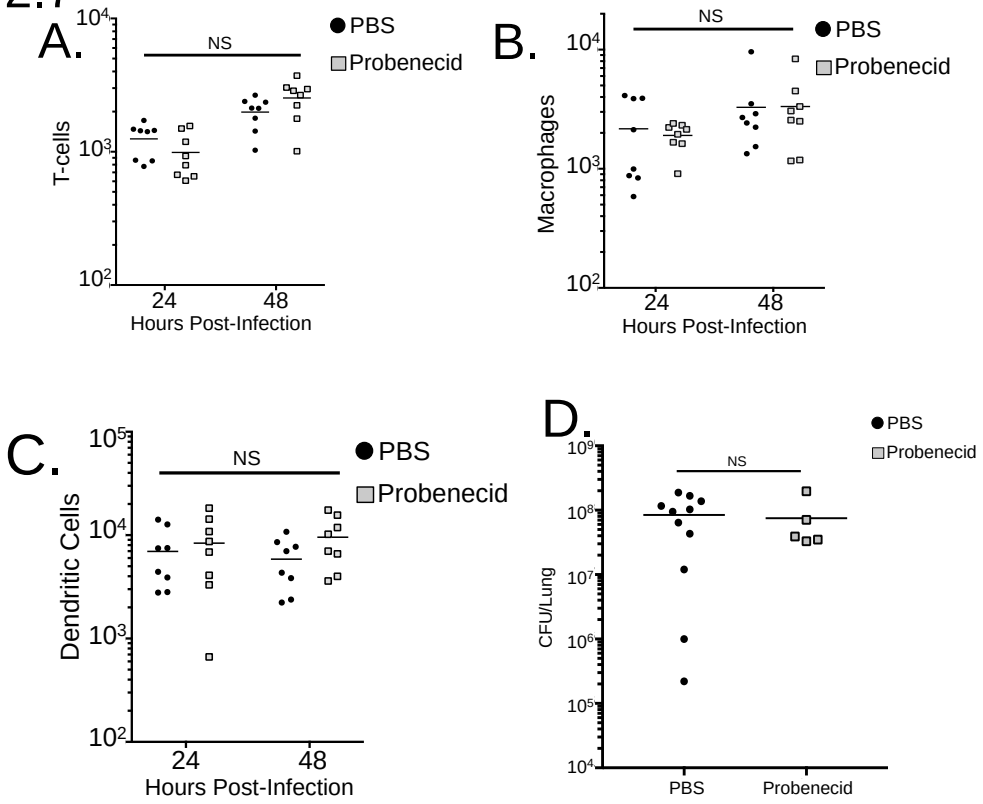

Figure 2.7. Pulmonary burden during survival experiments and *in vivo* granulocyte enumeration

(A, B, C) Additional leukocytes identified in the BAL quantified by flow cytometry. These include T-cells (B, Cd3+ cells), Macrophages (C, Cd11b+/Cd45+/Ly6g- cells), and Dendritic cells (D, Cd11c+/Cd11b-/Ly6g- cells). Samples are from the same sample set as Figure 2.5A. **(D)** Pulmonary burden calculated using serial-dilution of lung homogenates during survival experiments in Figure 2.5, taken from mice that died. No difference in bacterial burden was observed at the end-point of survival examinations. All statistical significances were calculated using Mann-Whitney test (for individual time-points) as well as 2-way ANOVA (combined time-points).

Fig. 2.8

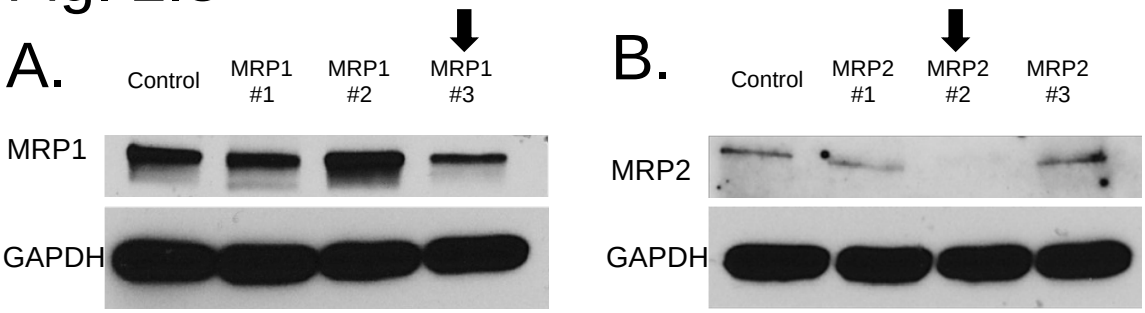

Figure 2.8. shRNA constructs result in knockdown of MRP1 and MRP2 expression

H292 cells were transfected with a control shRNA plasmid containing a scrambled construct, 1 of 3 MRP1 shRNA constructs, or 1 of 3 shRNA MRP2 constructs. Cells were selected under puromycin antibiotic selection and assessed via western blot. Shown is a representative western blot of 3 lysis events. Cultures with arrows indicate the shRNA pool selected for MRP1/MRP2 knockdown experiments.

polarized H292 cell monolayers. We used a previously described method (13) utilizing methanol elution of a C18 column to enrich bioactive lipid(s) following application of a pathogen to the apical surface of epithelial monolayer (Fig. 2.9A). To reconstitute the lipid chemoattractant, the methanol-lipid solution was evaporated over a steady stream of compressed nitrogen and resuspended with HBSS. The isolated lipid-HBSS was then applied to the apical surface of naïve H292 cells during a PMN transmigration assay. As expected, resuspended lipid-isolates from uninfected cells yielded no PMN migration, indicating there is no chemoattractant produced by the cells without infection (Fig. 2.9B). When we applied resuspended lipid chemoattractant isolated from infected cells to the apical surface of H292 cells during a PMN transmigration assay, we induced PMN migration (Fig. 2.9B). Extracts isolated from H292 monolayers with reduced MRP2 expression were less effective at inducing PMN transmigration than H292 cells transfected with a scrambled shRNA sequence, in a manner similar to data reported in Figure 3 for Probenecid, indicating a direct correlation between MRP2 expression and PMN migration (Fig. 2.9B).

On the basis of reduced MRP1 surface expression during pneumococcal infection, we further hypothesized that MRP1 is involved in an anti-inflammatory cascade that suppresses PMN transepithelial migration. To test this theory, we once again resuspended the isolated lipid chemoattractant from Figure 2.9A to conduct a PMN migration assay. Instead of resuspending the chemoattractant with conventional HBSS, we conditioned HBSS with apical supernatants from either scrambled-control or MRP1-deficient knock-down cells. We expected MRP1 to secrete a molecule or molecules during basal,

uninflamed states (when MRP1 was highest) that would directly inhibit PMN transmigration. Media conditioned with MRP1 competent cells, then, would reduce PMN migration. Media conditioned with apical supernatants from MRP1 KD cells would show no such inhibition.

When examining the results of conditioning the media with uninfected apical secretions, the resulting PMN migration with normal HBSS without isolated lipids induced no PMN migration, as expected (Fig. 2.9C). Lipids resuspended with media conditioned with wild-type, MRP1-competent cells inhibited PMN migration when compared to lipids resuspended with unconditioned HBSS (Fig. 2.9C). When conducting a PMN migration with lipids conditioned with MRP1-deficient cells, we lost the inhibition observed with cells that had intact MRP1 expression (Fig. 2.9C). When we again used fMLP to examine the HXA_3 dependency, we again failed to observe a reduction in PMN migration (Fig. 2.9D). In addition, we saw no changes in TNF, IL8, CXCL2, or IL-10 signaling in MRP1 knockdown cells either prior-to or post-infection as measured by ELISA (Fig. 2.10). Thus, it appears that MRP1 inhibits HXA_3-specific PMN migration *in vitro* and by reducing MRP1 expression, we diminished the inhibition on the PMN migration that we observed with wild-type cells.

Fig 2.9 A.

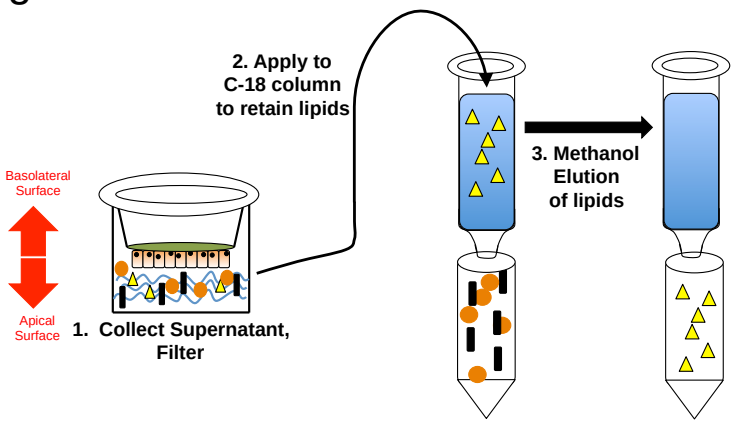
2. Apply to
C-18 column
to retain lipids
3. Methanol
Elution
of lipids
Basolateral
Surface
Apical
Surface
1. Collect Supernatant,
Filter

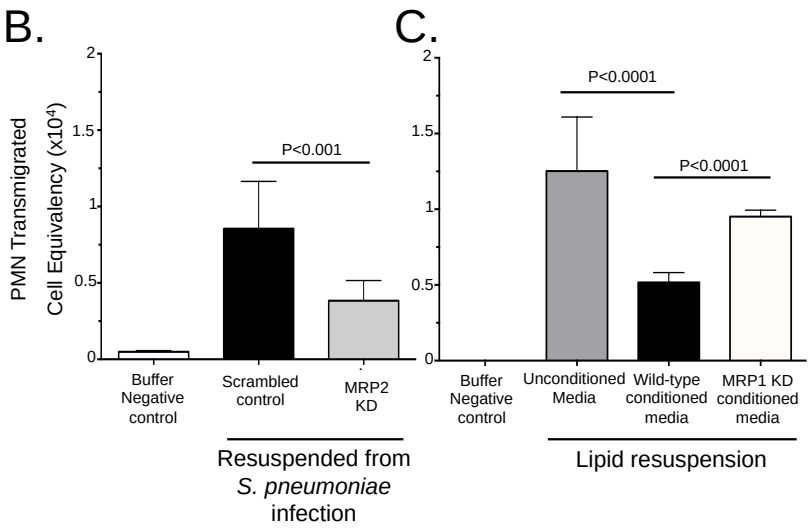
B.
C.
PMN Transmigrated
Cell Equivalency (x10⁴)
P<0.001
P<0.0001
P<0.0001
Buffer
Negative
control
Scrambled
control
MRP2
KD
Resuspended from
S. pneumoniae
infection
Buffer
Negative
control
Unconditioned
Media
Wild-type
conditioned
media
MRP1 KD
conditioned
media
Lipid resuspension

D.

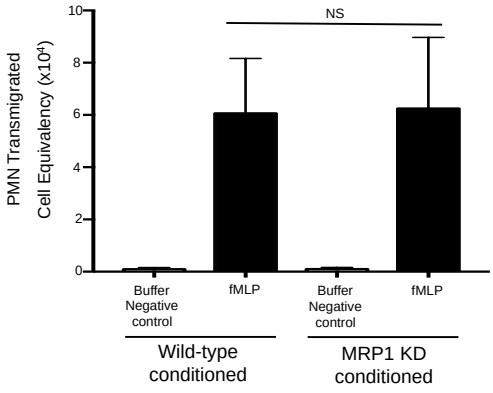
PMN Transmigrated
Cell Equivalency (x10⁴)
NS
Buffer
Negative
control
fMLP
Buffer
Negative
control
fMLP
Wild-type
conditioned
MRP1 KD
conditioned

Figure 2.9. MRP2 and MRP1 promote the secretion of proinflammatory lipids and anti-inflammatory molecules, respectively

(A) Pro-inflammatory lipids were isolated from apical supernatants of pneumococcus-infected H292 monolayers. HBSS subjected to the apical surface of pneumococcal-infected H292 were enriched on C-18 columns, which retain the pro-inflammatory lipids, and eluted in methanol for storage (see Materials and Methods). Yellow triangles represent proinflammatory lipids. **(B)** Lipids from MRP2-competent (Scrambled-control) and MRP2-deficient (MRP2 KD) cells were enriched and eluted with methanol. This methanol/lipid solution was evaporated under a constant stream of nitrogen and resuspended in HBSS to be used as PMN chemoattractant during a PMN migration assay through a monolayer of naïve wild-type H292 cells.

(C) Proinflammatory lipids isolated from wild-type cells infected with *S. pneumoniae* from (A) were resuspended with either unconditioned media (Unconditioned media), conditioned media from MRP1-competent scrambled-control cells (Wild-type conditioned media), or conditioned media from MRP1-knockdown cells (MRP1 KD conditioned media) and applied to the apical chamber of naïve cells to act as a chemoattractant during a PMN migration assay. HBSS without any lipid acted as negative control (Buffer Negative control). **(D)** MRP1-conditioned media failed to inhibit HXA_3-independent PMN-migration produced using formyl-methionyl-leucyl-phenylalanine (fMLP). NS represents “No significance” when examining student’s T-test.

Fig. 2.10

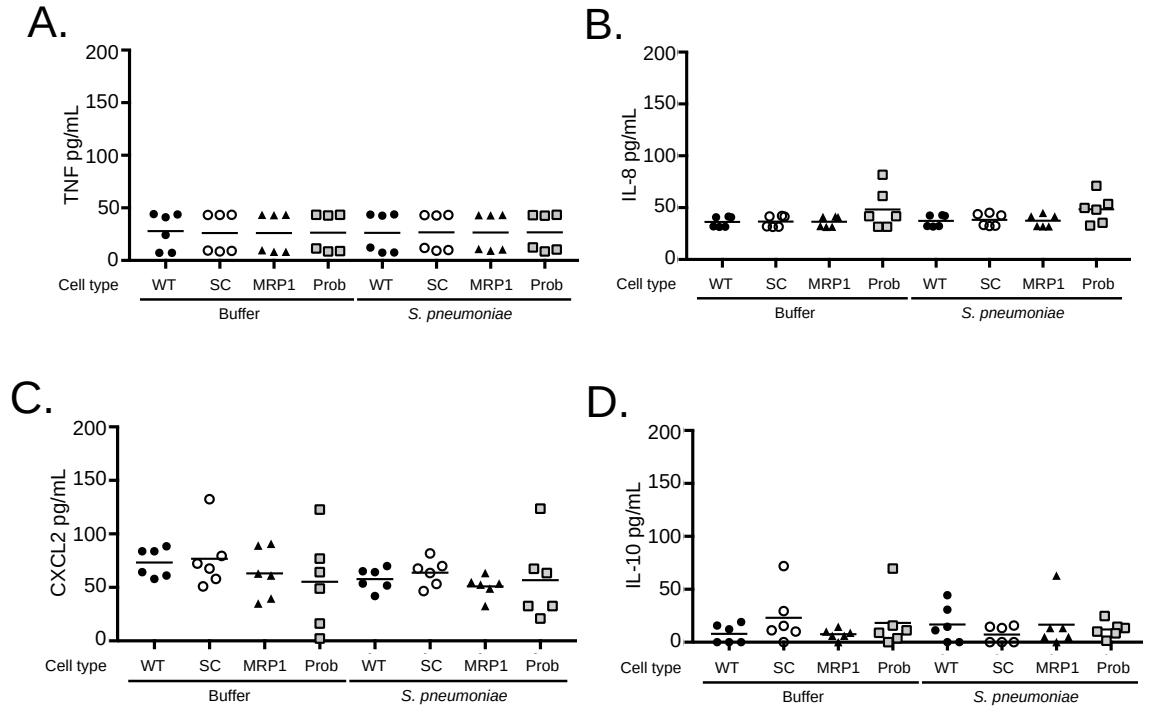

Figure 2.10. Neither MRP1 knockdown nor probenecid treatment significantly changes the ELISA profile of tissue culture cells within 1 hour of infection

Wild-type (WT, Black circles), Scrambled-control (SC, Open circles), MRP1 knockdown (MRP1, Triangles), and probenecid-treated (Prob, Grey squares) H292 cells were subjected to ELISA sample collection. HBSS+ was incubated for 1 hour post-infection in either mock-treated cells (Buffer) or *Streptococcus pneumoniae*-infected cells (*S. pneumoniae*) and collected from the apical surface for ELISA. No significant changes were observed in TNF **(A)**, IL8 **(B)**, CXCL2 **(C)**, or IL10 **(D)** when comparing Scrambled-control cells to MRP1 knockdown cells or wild-type to any of the other conditions. Shown are 2 separate runs pooled together and experiments were repeated with similar results.

2.3 Discussion

Lower respiratory tract infections are among the leading causes of death worldwide, and *S. pneumoniae* remains the deadliest bacterial agent causing this affliction. Infection of the lung with *S. pneumoniae* induces a variety of inflammatory responses, the pathological hallmark of which is massive influx of PMNs. In this role, PMNs are signaled to navigate to the site of infection and are charged with the task of pathogen eradication. Outright neutropenia or elimination of PMN activity at this step is detrimental to the host, as a full adaptive immune reaction has not had time to activate and the bacteria are unabated. However, unchecked, PMN recruitment lacking resolution culminates in massive tissue destruction, and ultimately lung failure. Thus, one of the key challenges in treating lung inflammation lies in attenuating the inappropriate influx of PMN without compromising the ability of the patient to fight normal infections. We envisage that a better understanding of the mechanisms underlying the regulation of PMN influx during pneumococcal infection is essential to designing improved therapies that dampen detrimental lung inflammation. This is a logical approach for *S. pneumoniae*, as this bacterium is encapsulated, countering PMN as a critical host defense mechanism. Thus, the cost of host tissue damage as a result of PMN infiltration of the airway epithelium during pneumococcal infection significantly outweighs any benefit PMNs may have in defense of this particular infection.

Although several studies have probed aspects of PMN recruitment to the airspace using a range of *in vitro* and *in vivo* models, many molecules mediating innate immune responses during pneumococcal pneumonia infection are redundant and/or dispensable

for PMN recruitment (100-107). As shown herein, we have uncovered a system of checks-and-balances in which eukaryotic ABC efflux transporters facilitate the coordination of PMN transepithelial migration across lung epithelia in response to pneumococcal infection. We have found that expression of the efflux transporter MRP1 on the apical surface of the lung epithelium is high in a normal basal state. The action of MRP1 at this site is to maintain homeostasis through efflux of immunosuppressive bioactive molecules that we have termed L- AMEND (Lung-Activity Modulating Epithelial-Neutrophil Discourse). Under the same homeostatic state, expression of another efflux pump, MRP2 is quite low, reinforcing the anti-inflammatory arm of this pathway. However, upon introduction of a foreign invader, such as *S. pneumoniae*, expression of MRP1 is decreased, reducing the effective concentration of anti-inflammatory molecules at the site of infection. MRP1 reduction is accompanied by an increase in the apical expression of MRP2, which facilitates the efflux of the proinflammatory eicosanoid, hepoxilin A_3; a potent PMN chemoattractant that in turn, attracts PMNs to the site of infection/injury (Fig. 2.11).

Critically, while it is known that HXA_3 is necessary in pneumococcal-induced PMN translocation (19) and lung infection (18), no studies have ever shown the link between MRP2-dependent HXA_3 efflux and Gram-positive bacteria, highlighting the conservative nature of the HXA_3/MRP2 axis. Additionally, we found that blockade of MRP2 by Probenecid during *S. pneumoniae* infection profoundly decreased PMN influx into the lungs of infected mice and, in turn, reduced the extent of systemic bacteremia. Our discovery that MRP1 effluxes L-AMEND, which suppresses PMN migration,

Fig. 2.11.

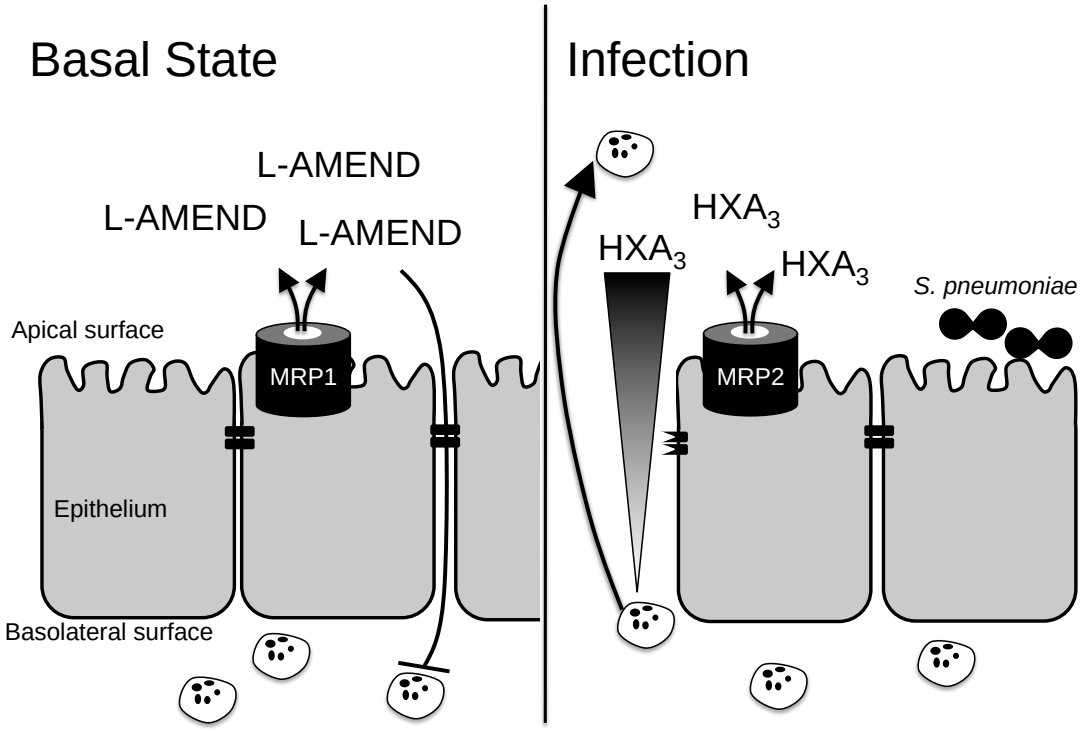

Figure 2.11. Epithelial MRPs assist in controlling pro- and anti-inflammatory states

Shown by this work, lung epithelium expresses high amounts of MRP1 and low amounts of MRP2 at basal (uninfected) states. MRP1 effluxes molecules with anti-inflammatory activity, here termed L-AMEND, which acts to suppress PMN migration. During infection with *Streptococcus pneumoniae* MRP1 is reduced and MRP2 increases on the apical surface of the epithelium. MRP2 mediates release of the pro-inflammatory molecule Hepoxilin A3 (HXA_3), which creates a chemotactic gradient to draw PMNs to the site of infection. By both reducing MRP1 and increasing MRP2, the epithelium works to maximize the transepithelial PMN migration; however, this PMN migration also disrupts epithelial tight junctions and can lead to infiltration of the intruding *S. pneumoniae*.

provides two potential and independent treatments strategies to reduce PMN migration and, thus, limit development of bacteremia: apical presentation of exogenous L-AMEND or local inhibition of MRP2. It remains to be seen as to what, exactly, makes up the components of the L-AMEND. When examining efflux supernatants from MRP1 knockdown cells or probenecid treated cells, we saw no discernable differences in the conditioned milieu as examined by ELISA (Fig 2.10).

We chose an intratracheal administration of bacteria in our studies to highlight the transition from lung- to blood-infection. One of the major focuses of this study was to examine whether MRP2 inhibition would augment PMN infiltration to the lungs during infection. Secondary to this, we sought to confirm that the PMN infiltration correlated with the development of bacteremia over the course of infection. Intratracheal infection seemed the most direct route to test this, bypassing any bottleneck in intranasal application, and guaranteeing bacteria enter the lung. Histology revealed that lung pathology does not appear different between Probenecid-treated and PBS-treated animals (Fig. 2.12A), seeming to indicate that all of the mice had equal opportunity to develop bacteremia. Because the infection is delivered almost directly to the lung in a bolus, it seemed reasonable that both cohorts exhibited similar lung pathology – the major difference between the two seems to be the induction of bacteremia and PMN infiltration, not the lung infection by itself. To that extent, one particular question that seemed interesting but unexplored was whether there might be fewer permissible passages of PMN entry or if fewer PMNs might be coming through in lesser numbers in Probenecid treated samples. The former seems more likely as HXA_3 has been demonstrated to be

critical in initial passage of PMNs but doesn't control the continued passage once the initial PMN passageway has been breached (108). In Probenecid treated mice, therefore, MRP2 blockade would lead to fewer paracellular openings and only slightly fewer PMNs but a significant reduction in the number of breakages by which bacteria pass through.

While our studies are the first to identify a push/pull interaction between MRP1 and MRP2 in PMN migration, there is another study examining MRP1 that presents an interesting paradox. Schultz et al. previously reported global *Mrp1* knockout mice were protected during intranasal pneumococcal (serotype 3) infection in a leukotriene B4 (LTB_4)-dependent manner whereas wild-type littermates succumb to infection (49). At 48 h post-infection, extracellular leukotriene C4 (LTC_4) in *Mrp1-/-* BALF was lower than in wild-type mice. Intracellular LTC_4, understandably, was found to be higher, leading to the conclusion that release of LTC_4 was inhibited by the elimination of murine MRP1(49). In a separate study, intracellular LTC_4 retention was suggested to be cytotoxic (35). Because PMNs express MRP1, a global knockout would yield MRP1-deficient PMNs. This could lead to PMN apoptosis and reduced numbers, exactly the observation in the Schultz study 48 h post-infection. With this explanation, it would appear that the previously reported *Mrp1* knockout data does not refute our stated results. Additionally, this is yet another communication reinforcing that fewer PMNs responding to bacterial infection actually can improve survival in *S. pneumoniae* infection.

Fig. 2.12

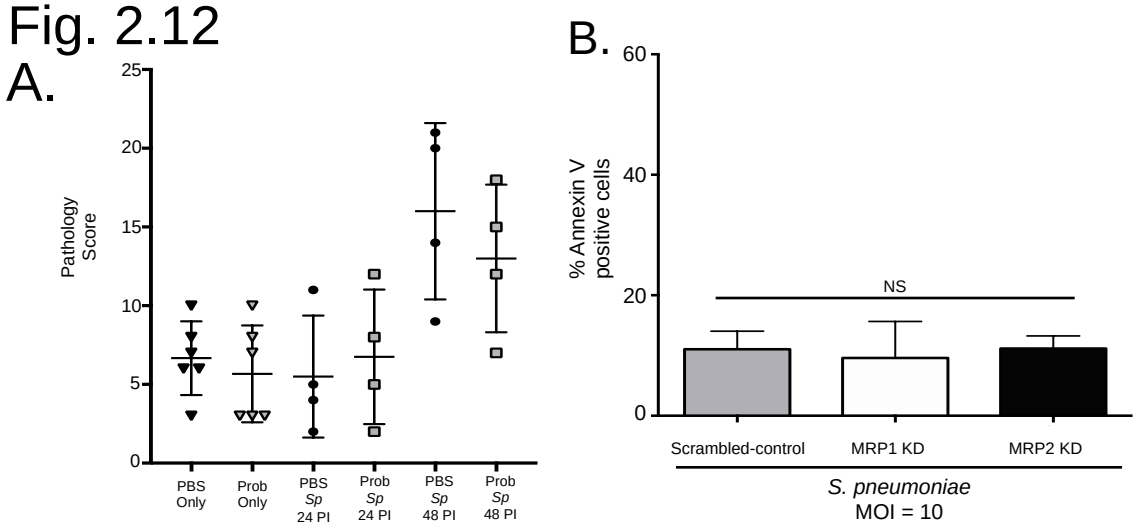

Figure 2.12. Histological examination shows little difference between Probenecid and PBS treatment during infection

(A) Mouse lungs were excised, sectioned, and underwent H&E staining. Slides were scored blindly. Although pathology scores worsened when comparing 24 and 48 hours post-infection, no statistically significant differences were observed between Probenecid- and PBS-treated animals. Prob abbreviation indicates 1 mg/kg intratracheal Probenecid treatment, *Sp* indicates animals were infected with *Streptococcus pneumoniae*. Lungs were excised either 24 (24 PI) or 48 (48 PI) hours post-infection. PBS and Probenecid treated animals without infection were scored and grouped whether sacrificed 24- or 48-hours post mock-infection. n=4 for infected animals, n=3 for PBS- and Probenecid-treated mock-infected animals for each time point. **(B)** H292 cells with control constructs, MRP1 shRNA, or MRP2 shRNA underwent staining for apoptosis post-infection. There were no significant increases in apoptosis between scrambled control and knockdown cells during the staining procedure. P-values calculated using students T-test.

There remains the possibility that epithelial-derived LTB_4 could influence PMN migration, however it has been shown that LTB_4 released by cells during *in vitro* PMN transmigration is almost exclusively PMN-derived (108), eliminating the possibility that the epithelium is coordinating PMN migration with LTB_4 in our MRP1 knock-down studies. To ensure that our infected epithelium do not undergo LTC_4-induced apoptosis, we tested Annexin V staining post-infection in MRP1-deficient epithelium when compared to control cells (Fig 2.12B), and found no differences, indicating that any increases in PMN migration associated with MRP1 deficiency is not caused by epithelial cytotoxicity.

Our hypothesis that MRP1/L-AMEND dictates an anti-inflammatory state while MRP2/HXA_3 assists in pro-inflammatory activity incorporates the concept that epithelial cells (through regulation of ABC efflux transporters) act as sensors that integrate signals to determine when and to what level to incite PMN transmigration (Fig. 2.11). Thus, a steady state, non-inflamed condition is established that limits inappropriate inflammatory responses but is poised to respond to pathogens, such as *S. pneumoniae*. Although this PMN response is critical in controlling the infection at hand, prolonged PMN activation also has deleterious effects on health, highlighting a cost-benefit relationship for the host. These findings regarding the nature of this anti-/pro-inflammatory balance could provide clinical targets for therapeutic control of dysregulated respiratory innate inflammatory responses that ultimately allow for containment of the infection but simultaneously dampen detrimental lung inflammation.

2.4 Materials and Methods

Cell culture

The human mucoepidermoid pulmonary cell line, NCI-H292 (H292), was cultured with RPMI (GIBCO #11875-093) supplemented with 10% FCS and subcultured using 0.05% Trypsin-EDTA (GIBCO #25300-054). Transmigration cells were prepared on 24-well inverted semi-permeable membranes (Costar #3421) and grown to confluency. Cells for RNA/protein assays were grown to confluency on 6-well membranes. MRP1, MRP2, and scrambled-control knockdown cell lines were developed by chromosomal integration of pLOK.1 shRNA constructs in wildtype H292 cells, selected with puromycin, and confirmed by western blot.

Bacteria

Streptococcus pneumoniae serotype 4 (TIGR4) was provided by Drs. John Leong and Andrew Camilli (Tufts School of Medicine). Bacteria were streaked overnight on 5% sheep-blood Tryptic Soy Agar (Northeast Laboratory Services #p-1100) and grown at 37℃, 5% CO_2 for 14-20 hours. On the day of infection, bacteria were resuspended with Todd-Hewitt-Yeast media and supplemented with oxyrase (#OB-0100, 5uL/mL culture). Cultures grew to ~$5x10^8$ CFU/mL. *In vitro* infections were diluted in Hanks Balanced Salt Solution (HBSS, GIBCO #14025-092). Mouse infection solutions were resuspended using filter-sterilized Phosphate Buffered Saline (PBS).

RT-PCR

Confluent H292 on 6-well membranes were rinsed with HBSS and infected apically with TIGR4 (~10 MOI) for 1 hour. Cells were washed with HBSS and RNA was collected using Qiagen RNeasy kits (Qiagen #74106) following suggested protocol. cDNA was obtained using Qiagen QuantiTect following manufacturers instructions. RT-PCR data was obtained using SybrGreen with custom primers for each transporter (in triplicate) normalized to expression of GAPDH.

Transmigration

Transmigrations were conducted as previously described (3) using H292 cells. Probenecid (Sigma #P8761-25G) was diluted in HBSS before being solubilized with NaOH and brought to pH 7.4 with HCl. Probenecid treatment at 100 μM was completed 1 hour prior to infection. H292s were infected apically with wild-type TIGR4 (~10 MOI) for 1 hour and washed. Human neutrophils were isolated from healthy donors using methods previously published (13). Freshly isolated neutrophils were applied to the basolateral chamber of infected membranes and allowed to migrate. Neutrophil migration was quantified using a myeloperoxidase assay. N-Formyl-methionyl-leucyl-phenylalanine (fMLP) was purchased from MP Bioscience (Cat# 151170) and used at a final concentration of ~150 nM during PMN migrations.

Biotinylation

H292 cells were grown on 6-well transmembranes to confluency, rinsed with HBSS, and infected with TIGR4 (~10 MOI) apically. Cells were washed and biotinylated

as previously described (109, 110). Cells were lysed and passed through 26½ -gauge needles, spun, and applied to streptavidin beads (Thermo Fisher #20347) or saved in tricine sample buffer (recipe from Bio-rad 161-0739). Biotinylated-bead samples were incubated at 4℃ overnight, washed, incubated at 40℃ for 20 mins in tricine sample buffer, then run on 4-20% TGX protein gel. Proteins were transferred on to nitrocellulose membranes, blocked, and incubated with the indicated antibodies: MRP1 (ABCAM ab24102), MRP2 (ABCAM ab3373), MRP3 (ABCAM ab3375), MRP4 (ABCAM ab56675), MRP5 (ABCAM ab77369), P (EMDMilipore 517310), GAPDH (EMDMilipore MAB374). HRP-conjugated secondary antibodies were used to visualize western blots.

Mouse infections

C57BL/6J mice were purchased from Jackson Laboratories. For lung immunofluorescence images, mice were anesthetized with isoflurane and mock-infected with PBS or infected with 50µL TIGR4 intratracheally (~$2.5x10^5$ CFU/infection). Infections progressed for 48 hours and mice were sacrificed. Lungs were re-inflated with 1mL 1:1 PBS/OCT mixture, frozen in OCT, and processed. For histological studies, mice were sacrificed and lungs were re-inflated and fixed with 10%formalin/PBS for a minimum of 24 hours. Lungs were processed, sectioned, and haemotoxylin and eosin (H&E) stained. Dr. Jerrold Turner, M.D., and associates scored pathology. CFU was calculated via lung homogenization and serial dilution plating.

For probenecid studies, mice were pretreated 3 hours prior to infection with 1mg/kg Probenecid, diluted in PBS, applied intratracheally. Mice were mock-infected with PBS or infected with $2.5x10^5$ CFU TIGR4, after which Probenecid was administered 3 hours post-infection. For bacteremia, 10 µL of blood was removed via tail vein lancet and diluted in anticoagulant for serial plating. ELISA samples and leukocyte panels were generated using a modified BALF isolation protocol (111). 1mL samples of PBS were applied to mouse lung via the trachea 3 times and spun in a centrifuge at 2000RPM. Supernatant was frozen for ELISA experiments and cells were washed and went to FACS processing. Following red blood cell lysis, cells and Fc receptors (Biolegend Cat# 101319) were blocked in PBS/0.5% FBS. Staining was achieved via incubation with Cd11b (Biolegend Cat#101236), Ly6G (Biolegend Cat#127618), or CD45 (Biolegend Cat#103130) and run on a MACSquant analyzer. Populations were analyzed via FloJo. ELISA kits were obtained from R&D systems (cat # DY453-05, DY452-05, DY217B-05, and DY410-05) and assays were completed using manufacturers instructions.

For survival curves, mice were sacrificed when exhibiting 3 of the following within 6-hours, according to our SOP: lethargy, shivering, loss of more than 10% body weight, and fur ruffling. In all survival experiments, animals showed no signs of pathology past 96-hours of infection. Repeated experiments going to 168-hours post-infection showed similar results. Survival curve statistics were calculated using Mantel-Cox test as well as Gehan-Breslow-Wilcoxon test. All experiments completed with approval of UMASS IACUC #1905.

Immunofluorescence

Immunofluorescence H292 samples were grown on inverted membranes and either mock-infected or infected with ~10MOI TIGR4 apically prior to fixation with 4% paraformaldehyde. Cells were washed, blocked with 3% BSA, and permeabilized with 0.01% Triton-X. Samples were stained with primary antibodies MRP1 (Santa Cruz sc-7773), MRP2 (Santa Cruz sc-5770), MRP3 (ABCAM ab3375), MRP4 (ABCAM ab56675), or MRP5 (ABCAM ab77369). Secondary-antibody incubations were with Alexa488/Phalloidin569 (Life Technologies #A12380) or Alexa568/Phalloidin488 (Life Technologies #A12379). Images were taken with a Leica SP-5 confocal microscope and calculations were completed using Image J. Images were converted to 8-bit, threshold was set for a given protein, and calculated for percent area in a given region of interest. All corresponding uninfected and infected images were infected, stained, and imaged on the same days as to reduce confounding factors and standardize the apical coverage calculations.

Mouse lung sections were fixed with 4% paraformaldehyde, blocked with 3% BSA, and permeabilized with 0.01% Triton-X. Slides were incubated with the indicated primary antibody, washed, and incubated with 1:1000 with the above secondary antibodies. Increases or decreases of signal were calculated using Image J to assign an arbitrary signal under parameters described with H292 immunofluorescence. Fold differences in Figure 2B were calculated by quantifying signal for specific antibodies and normalizing to surface area according to phalloidin staining. These ratios were averaged

and the buffer average was set to a ratio of 1. All samples were then standardized to the buffer average for each given antibody and fold increases or decreases were reported.

Lipid isolation

H292 and MRP2 KD cells were grown and infected as in biotinylation steps. HBSS applied post-infection was collected, debris removed via centrifugation, and solution was applied to a C-18 solid phase extraction column (Supelco Cat#52604-U). Lipids were eluted using methanol and stored at -80℃ for up to 1 month.

To analyze activity, lipid-methanol solutions were dried under constant nitrogen stream and resuspended in pre-warmed HBSS. HBSS/lipid was applied to the apical surface of inverted naïve H292s and PMN migrations were completed as described.

MRP1 inhibition was tested using pre-warmed HBSS applied to the apical surface of control or MRP1 KD cells for 5 hours, producing conditioned media. Lipid-methanol solutions from above were dried and resuspended with unconditioned HBSS, conditioned HBSS from MRP1-competent cells, or conditioned MRP1 knockdown media. Migrations were then conducted as described.

Human ELISA kits were obtained from R&D systems (DY210-05, DY217B-05, DY276-05, and DY208-05) and assays were completed using manufacturers instructions. To collect samples, 6-well filter-insert plates were seeded with H292 cells and grown to confluency. Cells were equilibrated in pre-warmed HBSS+ and either mock-treated or infected with 10 MOI of *Streptococcus pneumoniae* on the apical surface for 1 hour.

Cells were then washed and 1 mL HBSS+ was placed on the apical surface for 1 hour for sample collection.

Apoptosis

For apoptosis, inverted H292 constructs were infected with 10 MOI TIGR4 or Staurosporine (Santa Cruz #sc-3510a) as a positive control for one hour. Cells were washed and rested at 37° in HBSS for an additional two hours. Cells were lifted using 0.05% Trypsin-EDTA, washed, and stained with Annexin V-FITC and Propidium Iodide (Santa Cruz Cat#sc-4252 AK). Staining was visualized and enumerated using a MACSquant analyzer and FloJo. Three constructs per condition were pooled and data shown is the summation of 3 different infections.

Preface to Chapter III

Elucidating the *Streptococcus pneumoniae* virulence factors that modulate epithelial HXA_3 production and MRP2 plasma membrane enrichment

Work contained in this Chapter is unpublished data detailing experiments that attempt to elucidate how virulence factors from *S. pneumoniae* induce PMN migration and influence MRP2 localization during epithelial cell infection.

All experiments were completed by Andrew Zukauskas and significant intellectual contributions have been made by Andrew Zukauskas, Dr. Beth McCormick (UMASS Medical School), Dr. John Leong (Tufts University), Dr. Rudra Bhowmick (Oklahoma State University), Dr. Elsa Bou-Ghanem (Tufts University), and Dr. Walter Adams (Tufts University).

As indicated in the Materials and Methods, purified cytolysins were generously donated by Dr. Rod Tweten (Oklahoma University) through Dr. John Leong.

Chapter III

Elucidating the *Streptococcus pneumoniae* virulence factors that modulate epithelial HXA_3 production and MRP2 plasma membrane enrichment

3.1 Introduction

In the previous chapter, we demonstrated that the ABC-transporters, Multi-drug Resistance associated Proteins 1 and 2 (MRP1 and MRP2), coordinate pulmonary PMN transepithelial migration in response to *S. pneumoniae*. MRP1 effluxes a molecule or molecules that inhibit PMN transmigration at resting state (i.e. without inflammatory stimuli). During infection, MRP1 reduces while MRP2 increases and effluxes the pro-inflammatory PMN chemoattractant HXA_3 (Figure 2.11). This MRP2/HXA_3 effect is a conserved action coordinating PMN transepithelial migration to a variety of mucosal surfaces (i.e. lung, and gut) in response to bacteria including *E. coli, Salmonella,* and *Shigella* (4, 11, 12) and pulmonary infections with *Pseudomonas aeruginosa*. Since it appears that HXA_3 production and efflux is a conserved innate immune signaling pathway, there must be some convergent point in immune signaling that is common to these diverse bacteria. Likewise, there must be a consistent signaling pathway engaged by both pulmonary and intestinal epithelial cells. For instance, to advance the infection process, the Gram-negative *Salmonella* Typhimurium, *Shigella flexneri, E. coli,* and *P. aeruginosa* all inject bacterial effectors through a type-III secretion system to influence eukaryotic host-pathways to make the cell more amenable to bacterial survival and replication. *S. pneumoniae,* on the other hand, is a Gram-positive bacterium without a conventional secretion system and that relies on bacterial attachment, self-lysis, or

currently unidentified efflux processes to influence eukaryotic cells during infection. While most of the bacteria on this list possess some ability to invade eukaryotic cells, Enteroaggregative *Escherichia coli* are thought to be obligatory extracellular pathogens (112). We have previously reported that the virulence factor SipA, which reduces the expression of the efflux transporter P-gp (which conveys analogous activity to MRP1 in the lung), also increases the activity of pro-inflammatory MRP2 (13). Although the actions of SipA and interacting proteins have been described in some detail (109, 113, 114), no information on virulence factors coordinating the MRP2 activity in pulmonary infection have been elucidated. Identifying the factors by which *S. pneumoniae* initiates MRP2 enrichment on the apical surface of the plasma membrane and generates HXA_3, will provide valuable information that could be critical in identifying a more general mechanism of this HXA_3/MRP2 activation common to both the intestine and lung. Such an approach may also reveal potential therapeutic candidates, outside of HXA_3 and MRP2, which researchers could target with small molecule inhibitors.

This work is focused on two targets: 1) pneumolysin (PLY) and 2) bacterial-derived hydrogen peroxide (H_2O_2). Pneumolysin is a member of the pore-forming cholesterol-dependent-cytolysins. During bacterial growth, pneumolysin is released from *S. pneumoniae*, though there is contention as to whether this is due to bacterial autolysis or a currently unidentified secretion system (67, 115). PLY monomers are released from bacteria and multimerize on the epithelium surface. Pores of up to 44 subunits form a pre-pore ring at the base of the epithelial cilia and undergo a conformational change that excises a portion of the plasma membrane, forming the proper pore (116). Ciliary beating

slows, likely to allow for niche development, as the bacteria colonize the pulmonary system. Previous studies have indicated that PLY engages Toll-Like Receptor 4 (TLR4) and initializes NF-κB signaling to induce inflammation (117), though there is expectation that HXA_3/MRP2 activation is largely independent of NF-κB signaling (3, 4, 118). In mice, PLY-deficient bacteria are much less virulent in during experimental infection. Serotype-2 *S. pneumoniae* without PLY showed reduced burden compared to wild-type bacteria during intranasal administration (119), less outgrowth during intratracheal infection (120), and less ability to invade through the epithelial barrier to cause bacteremia (120).

Hydrogen peroxide is a by-product of ATP generation through the action of the pyruvate oxidase, SpxB (121). Because hydrogen peroxide has the potential to be detrimental to bacterial DNA, membrane, and proteins, most other bacterial species encode a gene to produce catalase, which neutralizes hydrogen peroxide into relatively harmless oxygen and water. *S. pneumoniae*, however, does not have a catalase gene, resulting in high concentrations of hydrogen peroxide during bacterial growth. In a process that is not completely understood, *S. pneumoniae* protects itself in other ways: it is suggested that DNA and iron (both sensitive to reaction with hydrogen peroxide) is sequestered to protect the organism (121). Bacterial glutathione peroxidase (PsaD) also assists in neutralizing oxidative pressure during growth (122). SpxB also somehow confers protection from hydrogen peroxide buildup (121). Hydrogen peroxide is not just a waste product, however; in the ever-evolving bacterial arms race, *S. pneumoniae* likely developed survival mechanism in high oxidative stress to combat another nasal

commensal bacteria, *Haemophilus influenzae*. If *H. influenzae* and *S. pneumoniae* are grown together in the presence of one another, *S. pneumoniae* continues to multiply while *H. influenza*e is unable to cope with the oxidative stress (66). Pericone and colleagues observed that pyruvate oxidase mutations or exogenous catalase in growth media allowed both *S. pneumoniae* and *H. influenzae* to grow at equal rates, without an inhibition on the *H. influenzae* (66). *In vivo* experiments show that hydrogen peroxide is a necessary virulence factor during infection. Notably, *spxB*-mutant bacteria were less virulent, exhibited less lung growth, were not as adept as wild-type at invading the circulatory system, and did not cause as much inflammation (123) when compared to wild-type bacteria.

Herein, we describe an intricate interplay between the pore-forming toxin PLY and bacterial-derived hydrogen peroxide. We reveal that eliminating either of these virulence factors prevents MRP2 enrichment on the apical surface of the epithelium and abolishes PMN transepithelial migration *in vitro*. The pneumolysin/H_2O_2 induction of HXA_3/MRP2 appears to be calcium dependent, as mutation in either pneumolysin or neutralization of hydrogen peroxide with catalase resulted in elimination of intracellular calcium increases. Disrupting calcium signaling, likewise, eliminated PMN migration and MRP2 translocalization.

These findings reveal that there are at least two bacterial factors modulating the epithelial HXA_3/MRP2 axis and transepithelial PMN migration and that both of these influence intracellular calcium. Although there are many bacterial species that induce HXA_3-dependent PMN transepithelial migration, only one virulence factor has been

identified as necessary: the *Salmonella* effector SipA (20). Additionally, ours is the first communication that reveals the necessity of calcium in MRP2 localization during PMN transepithelial migration. While our research identifies the necessity of PLY, it does not reveal the entire mechanism. Supplementing pneumolysin-deficient bacteria with the cytolysin perfringolysin O, instead of pneumolysin, results in similar PMN migration. The fact that two similar but distinct pore-forming toxins can mediate this activity may indicate a conserved mechanism of regulation for the HXA_3/MRP2 proinflammatory response.

3.2 Results

PMN migration is dependent on Pneumolysin

In Chapter II, we presented a model in which *S. pneumoniae* initiates HXA_3 synthesis and is subsequently vectorially effluxed from the cell via MRP2. While we demonstrated that MRP2 increases during infection, it remains to be determined what signal or signals from the *S. pneumoniae* promote the induction of MRP2 on the apical plasma membrane. The bacterial factors that we identify could be critical to elucidating a mechanism by which the epithelium activates the HXA3/MRP2 axis to assist in transepithelial PMN migration. To identify the signal or signals we took the following steps.

We chose first to examine whether the pore-forming toxin, PLY, could impact epithelial-directed PMN transmigration. It is well documented that PLY mediates pro-inflammatory signaling (124) and can mediate transendothelial diapedesis (125).

Moreover, it has been shown that sufficiently high concentrations of PLY can induce PMN migration (126). We therefore examined an *in vitro* model of transepithelial PMN migration that utilizes NCI-H292 cells that form a polarized monolayer on a semi-permeable membrane construct (19). We then infected the apical surface with a serotype-4, pneumolysin-producing strain of *S. pneumoniae* (TIGR4). Post-infection, the bacteria were washed away and freshly isolated human PMNs were placed in the basolateral chamber of the construct to simulate the basolateral-to-apical PMN migration through the epithelium. When infecting with a pneumolysin-deficient serotype-4 *S. pneumoniae* (ΔPLY) we saw a consistent 50% or greater reduction in PMN migration compared to wild-type bacteria (Figure 3.1A). To confirm that this is a pneumolysin-specific reduction we functionally complemented ΔPLY infections with purified pneumolysin.

In functionally complementing ΔPLY bacteria, it was necessary to first identify the amount of pneumolysin released by the wild-type *S. pneumoniae* at 10 MOI during a one-hour infection time. To measure this, we collected supernatant from the apical surface of infected H292 cells, removed the bacteria, and examined the free pneumolysin via Western blot against a standard of purified pneumolysin (Figure 3.1B). Our data revealed two facts: first, it confirmed that ΔPLY mutant bacteria were unable to generate detectable levels of pneumolysin; second, the amount of pneumolysin detected in the infection supernatant during exposure to H292 cells was approximately 33ng/mL. Separate experiments examining the ability of PLY alone to induce PMN migration revealed that concentrations of PLY upward of 1 μg/mL could cause PMN transepithelial migration and this effect was lost at concentrations less than 300 ng/mL (Figure 3.1C). In

assessing apoptosis, it was observed that concentrations of purified PLY over 300 ng/mL caused apoptosis one hour post-infection in a dose-dependent manner (Figure 3.1D). Since the previous one-hour, MOI 10 wild-type *S. pneumoniae* infectious dose failed to induce measurable apoptosis (Figure 2.5), we next supplemented the ΔPLY mutant infection with 33ng/mL purified PLY and examined the resulting phenotype.

During supplemented infections where ΔPLY bacteria were in solution with 33ng/mL of the purified PLY, wild-type levels of transepithelial PMN migration were regenerated, thus indicating pneumolysin activity is necessary for PMN migration in our model (Figure 3.1A). There was no significant PMN migration in treatments with 33ng/mL purified PLY by itself. Taken together, these results suggest that transepithelial migration is dependent on PLY to elicit PMN migration but 33ng/mL PLY is not sufficient by itself and likely requires at least one additional bacterial factor to stimulate a full, robust PMN transmigration at 10 MOI of *S. pneumoniae*.

Figure 3.1

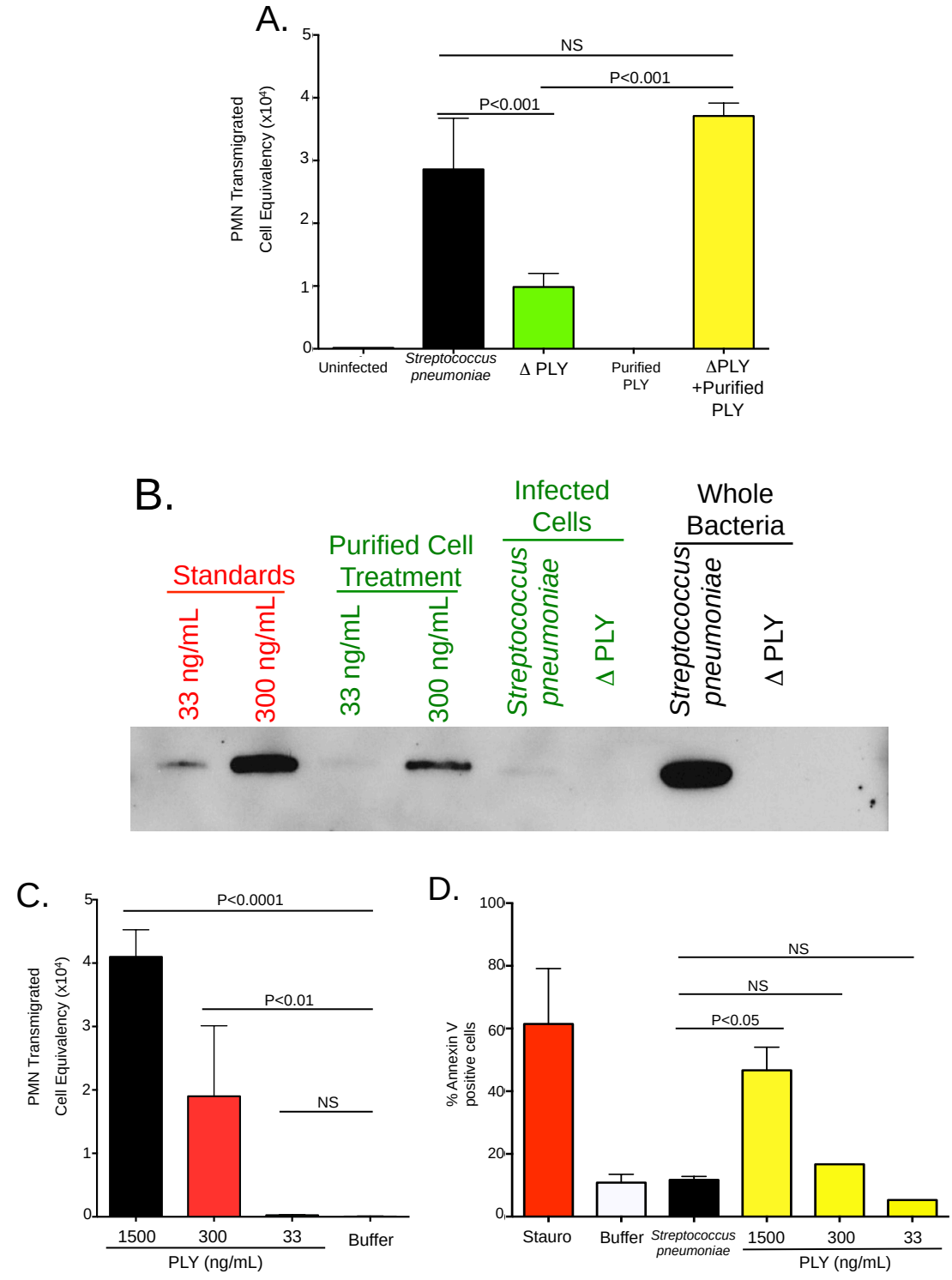

Figure 3.1 Transepithelial PMN migration is pneumolysin dependent

(A) PMN migration with either mock-treatment (Buffer), infected with *S. pneumoniae* (*S. pneumoniae*), infected with the ΔPLY mutant strain (ΔPLY), treated with 33 ng/mL purified PLY alone (Purified PLY), or infected with the ΔPLY strain supplemented with purified PLY (ΔPLY+Purified PLY). PLY-deficient bacteria induced significantly less PMN migration than wild-type bacteria. PMN phenotype was regenerated with functionally complemented infection. **(B)** Western blot quantifying the amount of PLY produced by wild-type bacteria during infection. Standards were loaded 33 ng/mL or 300 ng/mL purified PLY. Purified cell treatments were treated with 33 or 300 ng/mL of purified PLY and loaded into SDS-PAGE gel. Infected cells samples were infected with bacteria, supernatant was aspirated off, and then loaded into SDS-PAGE gel. Whole bacteria underwent bacterial cell lysis and loaded on to gel. Wild-type bacteria appear to release approximately 33 ng/mL of PLY. **(C)** PMN migration elicited after purified PLY treatment. As in (A), 33ng/mL was not a sufficient concentration to cause PMN migration alone. **(D)** Apoptosis as measured by Annexin AV staining. Concentrations of PLY greater than 300ng/mL caused increased apoptosis while wild-type 10 MOI infections with *S. pneumoniae* did not exhibit increases in apoptosis. Buffer indicates untreated cells. Staurosporine was used as a positive indicator of apoptosis. Statistics completed using Student T-test. NS refers to no significance. Shown are representative runs of at least 3 identical experiments.

Pore-forming Pneumolysin acts in conjunction with a signal from live bacteria

Our first attempt at identifying the second PMN-transepithelial migration-inducing signal involved heat-killed and UV-killed bacteria. We postulated that a general component of the bacteria, perhaps bacterial membrane, peptidyl-glycan, or lipoteichoic acid, might engage an immune receptor, together with PLY, to induce transepithelial PMN migration. For instance, heat-killed *S. pneumoniae* are still able to signal through TLR2, indicating some structural component engages even after the bacteria are dead (127). Similar to Figure 3.1A and C, monolayers of H292 were treated with suspensions of live bacteria or treated with killed bacteria together with purified PLY. Each treated monolayer was then subjected to the PMN transepithelial migration assay and assessed for PMN migration. In each case, whether the purified PLY was supplemented with *S. pneumoniae* killed with heat (Figure 3.2A) or UV (Figure 3.2B), the mixtures failed to induce PMN transepithelial migration. Likewise, wild-type *S. pneumoniae* that underwent heat-killing failed to induce any PMN transepithelial migration, even if supplemented with exogenous purified PLY (Figure 3.2C). Since none of the killed bacteria, mixed with purified PLY or not, were able to induce PMN migration we speculate that live bacteria were needed together with PLY to produce a full transepithelial PMN migration response.

Conceptually, PLY could be interacting with the epithelial immune sensors in a variety of ways. One could be that the PLY ring structure excises plasma membrane upon pore formation and allows sodium, calcium, or even a soluble “second virulence factor” to enter the epithelial cell, influencing stress pathways and commencing an immune

reaction that culminates in HXA_3/MRP2 activation. Another possible signaling mechanism is engagement of pneumolysin as a monomer or multimer at the plasma membrane surface through TLRs and other cell-surface receptors. Such receptors would signal upon being bound and subsequently induce the HXA_3/MRP2 axis.

To examine the possibility of whether pore formation was necessary or if the monomers/ring structure would suffice, we next sought to test mutations in PLY itself. We obtained a pore-forming mutant ("pre-pore") that is unable to form functional pores but instead multimerizes on the epithelium without excising the eukaryotic membrane from the center of the ring structure. (128, 129). The pore-forming mutant was supplemented at the same concentration as the purified PLY (33 ng/mL) and applied to the H292 cells as per previous experiments. We found that the ΔPLY bacteria was no longer complemented upon infection with the pore-forming mutant, suggesting that complementation requires functional pores to induce PMN transepithelial migration (Figure 3.3). We therefore inferred that functional pores were necessary to engage HXA_3 production and undergo efflux during infection.

Figure 3.2

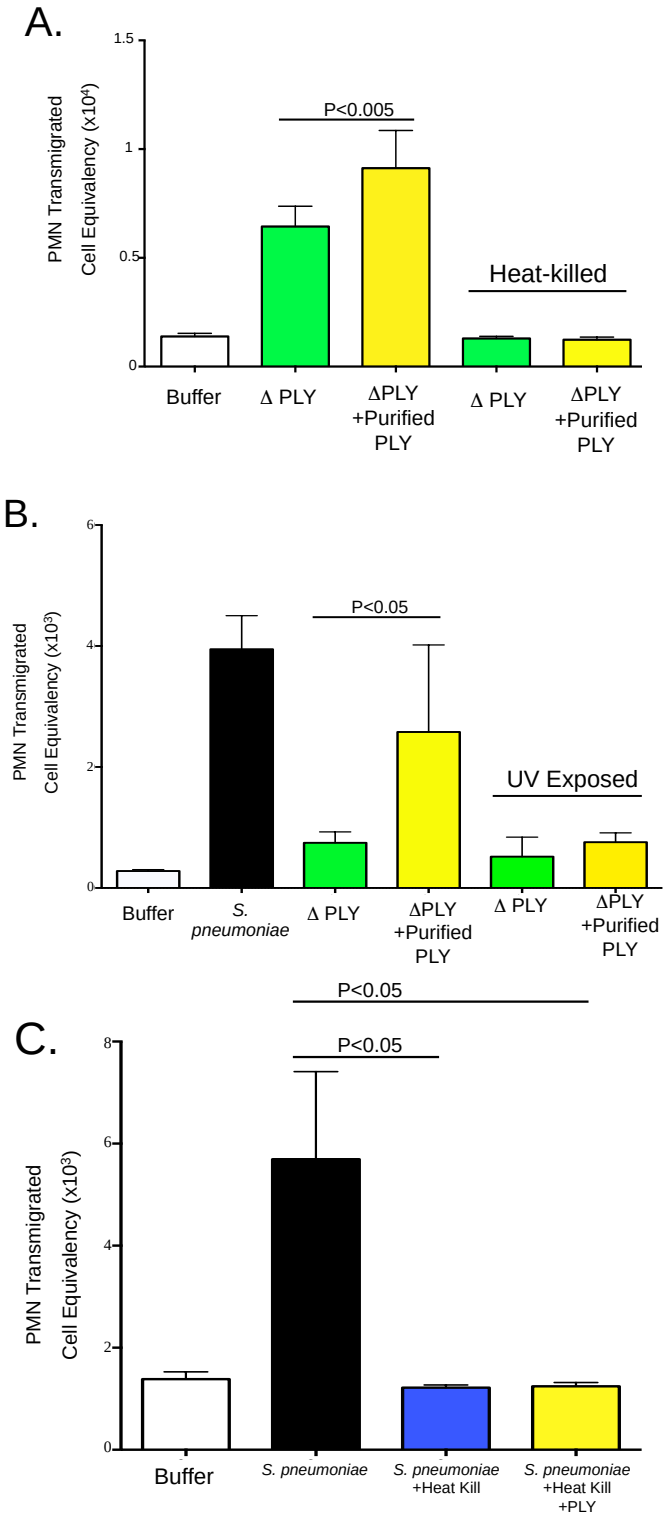
A.
PMN Transmigrated Cell Equivalency (x10⁴)
1.5
1
0.5
0
P<0.005
Heat-killed
Buffer
Δ PLY
ΔPLY +Purified PLY
Δ PLY
ΔPLY +Purified PLY
B.
PMN Transmigrated Cell Equivalency (x10³)
6
4
2
0
P<0.05
UV Exposed
Buffer
S. pneumoniae
Δ PLY
ΔPLY +Purified PLY
Δ PLY
ΔPLY +Purified PLY
P<0.05
C.
PMN Transmigrated Cell Equivalency (x10³)
8
6
4
2
0
P<0.05
Buffer
S. pneumoniae
S. pneumoniae +Heat Kill
S. pneumoniae +Heat Kill +PLY

Figure 3.2 PLY complement requires live bacteria

We examined the necessity of viable bacteria mixed with purified PLY to induce PMN migration. **(A)** Bacteria were grown to a given concentration and heat-killed by boiling for 30 mins. Killed bacteria were then washed and supplemented with purified PLY as in 3.1A. **(B)** Bacteria were UV killed after growing to a given concentration. Bacteria were exposed to UV light for 30 mins and supplemented with purified PLY. **(C)** Wild-type bacteria were heat-killed by boiling for 30 mins and supplemented with purified PLY. In all cases, killed bacteria were unable to regenerate PMN migration with or without exogenous PLY added to the infection solution. CFU plating confirmed that greater than 90% of bacteria were killed during boiling/UV exposure. Shown is a representative experiment. Experiments were conducted at least three times with similar results and statistics were conducted using a Students T-test.

Figure 3.3

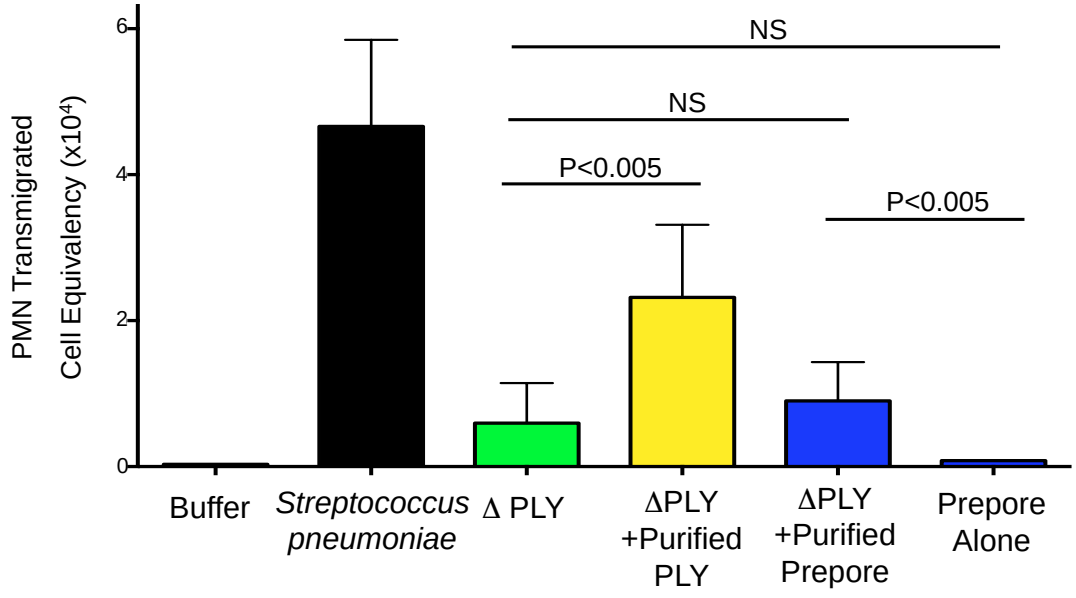

Figure 3.3 Functional pores are necessary for PMN migration

PMN migration conducted supplementing with either purified functional pneumolysin or a pre-pore lock that localizes to the plasma membrane but does not form functional pores. Pre-pore lock protein was isolated in a similar manned to purified PLY and applied at the same concentration. Pre-pore lock protein was unable to generate the PMN response by itself or mixed together with ΔPLY bacteria. Statistics were conducted using Student's T-test. Shown is one representative PMN transepithelial assay of at least 3 runs with similar results.

Pneumolysin acts in parallel or together with hydrogen peroxide to produce PMN migration

With the conclusion that live bacteria and PLY were necessary to initiate HXA_3 production, it seemed reasonable to examine bacterial factors that are produced by metabolically active *S. pneumoniae*. Actively dividing *S. pneumoniae* use a number of sources of carbon, such as sugars and pyruvate to generate ATP. SpxB, the *S. pneumoniae* pyruvate oxidase, is responsible for production of acetyl-phosphate, which can then be converted to acetate or acetyl-CoA during respiration (130). During pyruvate metabolism, hydrogen peroxide is produced in large quantities due to the lack of a *S. pneumoniae* catalase. Studies have indicated that bacterial-derived hydrogen peroxide, together with PLY, can induce apoptosis in neurons and inhibit ciliary beating in epithelial cells (131, 132). Other *Streptococcus* species also use hydrogen peroxide as a virulence factor during infection (133, 134). We postulated that bacterial-derived hydrogen peroxide could induce PMN transepithelial migration together with PLY. In the first step of this examination, we tested the extent to which *S. pneumoniae* produced measurable levels of hydrogen peroxide *in vitro*. We used a colorimetric assay in which we aspirated media after exposure to *S. pneumoniae* for the normal infection time of our *in vitro* assays at 10 MOI. Under these conditions, *S. pneumoniae* produced 250 to 500 μM hydrogen peroxide whether exposed to epithelial monolayers or incubated at 37 ℃ independent of epithelial exposure (Figure 3.4A). To neutralize hydrogen peroxide production, we treated *S. pneumoniae* resuspended in HBSS with 5 μg of catalase. It is possible to mutate the *S. pneumoniae spxB,* however, previous studies have shown that

this sensitizes the bacteria to killing with hydrogen peroxide. Additionally, genetic manipulation of *spxB* also reduces the amount of pneumolysin in experimental infection (115) – as such, we would not be able to examine whether reductions in PMN migration were due to hydrogen peroxide neutralization or pneumolysin reduction. The same studies showed that catalase treatment is effective at neutralizing *S. pneumoniae*-derived hydrogen peroxide without affecting the pneumolysin production during infection (115).

Upon treatment with catalase, hydrogen peroxide was undetectable during *S. pneumoniae* growth and infection (Figure 3.4B). Catalase treatment also appeared to have no effect on the *S. pneumoniae* growth, as bacteria in the presence or absence of catalase grew at equal rates during one-hour incubations (Figure 3.4C). To examine whether hydrogen peroxide acted on the epithelium to produce PMN transmigration, we applied catalase treated or mock-treated bacteria to epithelial cells and conducted an *in vitro* PMN migration assay.

After catalase treatment during infection steps, we observed a 90% reduction in PMN transepithelial migration as compared to mock-treated cells (Figure 3.5A). To ensure this effect was a *S. pneumoniae* specific occurrence, H292 cells were also exposed to catalase-treated *Pseudomonas aeruginosa*, a bacterium known to induce PMN migration in lung cells (18) but which possesses an endogenous catalase. We observed no difference in PMN migration between the *P. aeruginosa*-catalase-treated or mock-treated samples, leading us to conclude that catalase inhibition of the PMN migration appears to be specific to *S. pneumoniae* infection (Figure 3.5A). Pre-treating epithelial cells with catalase or including catalase during the post-infection PMN-migration step yielded no

such reduction, implying that the hydrogen peroxide is needed specifically during infection (Figure 3.5B). Due to the fact that catalase acts extracellularly and does not pass through the cell membranes, we favored the scenario that catalase was neutralizing *S. pneumoniae* derived hydrogen peroxide. Hydrogen peroxide is essential for *S. pneumoniae*-induced HXA_3 production and, as such, the epithelium can no longer induce PMN transepithelial migration in conditions where the hydrogen peroxide has been neutralized.

Figure 3.4

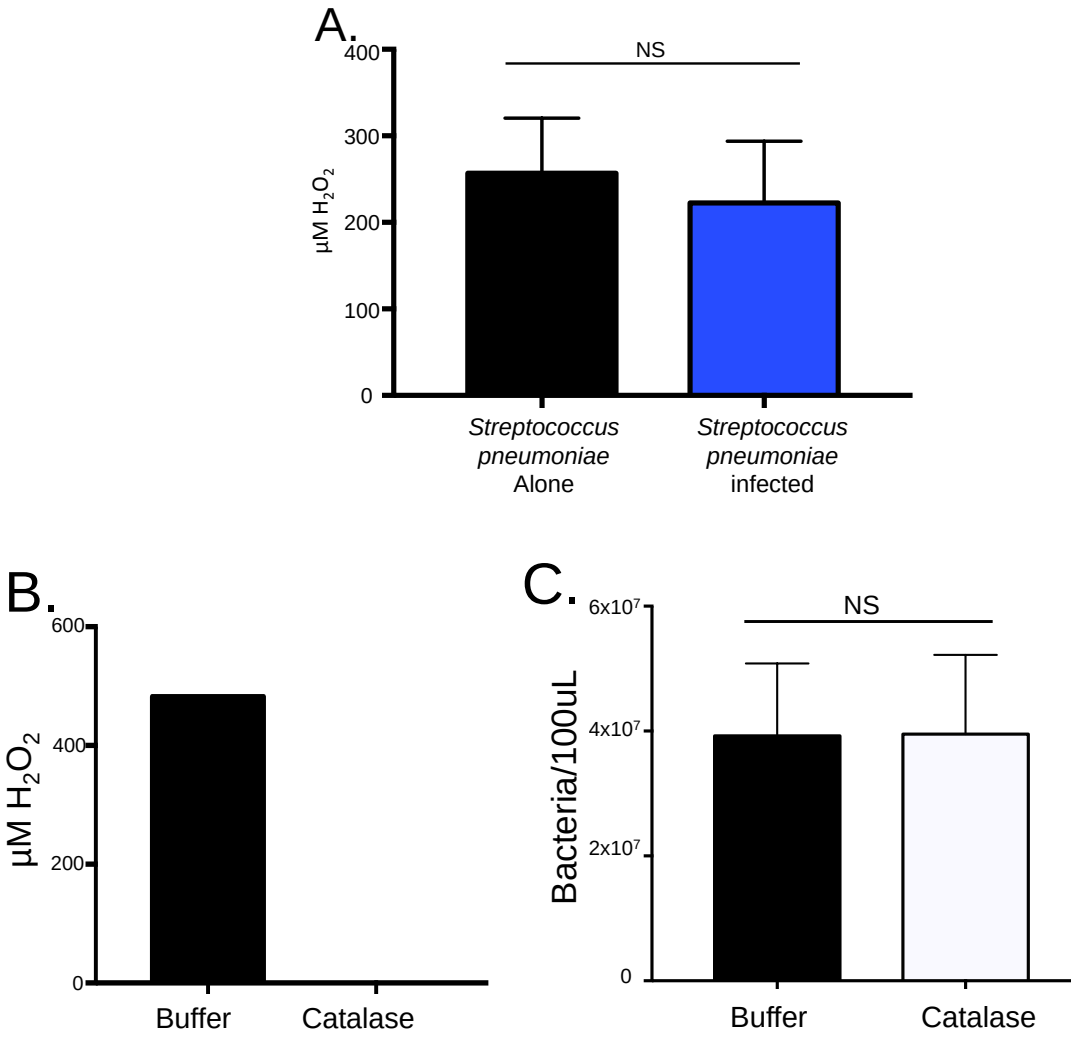
A.
NS
400
300
200
100
0
µM H_2O_2
Streptococcus pneumoniae Alone
Streptococcus pneumoniae infected
B.
600
400
200
0
µM H_2O_2
Buffer
Catalase
C.
NS
$6x10^7$
$4x10^7$
$2x10^7$
0
Bacteria/100uL
Buffer
Catalase

Figure 3.4 *Streptococcus pneumoniae* produces measureable amounts of hydrogen peroxide

(A) Hydrogen peroxide concentrations were measured in HBSS that contained bacteria for 1 hour (See Materials and Methods). Bacterial solutions were either incubated with bacteria alone (*Streptococcus pneumoniae* Alone) or incubated as during an *in vitro* infection with H292 cells (*Streptococcus pneumoniae* infected). There was no significant difference between the amount of hydrogen peroxide produced by the bacteria alone or the hydrogen peroxide in infected samples. **(B)** 5ug/mL of catalase neutralized hydrogen peroxide production in bacteria (without infection) during 1 hour growth in HBSS. **(C)** Catalase treatment had no effect on bacterial growth during the 1 hour process.

Figure 3.5

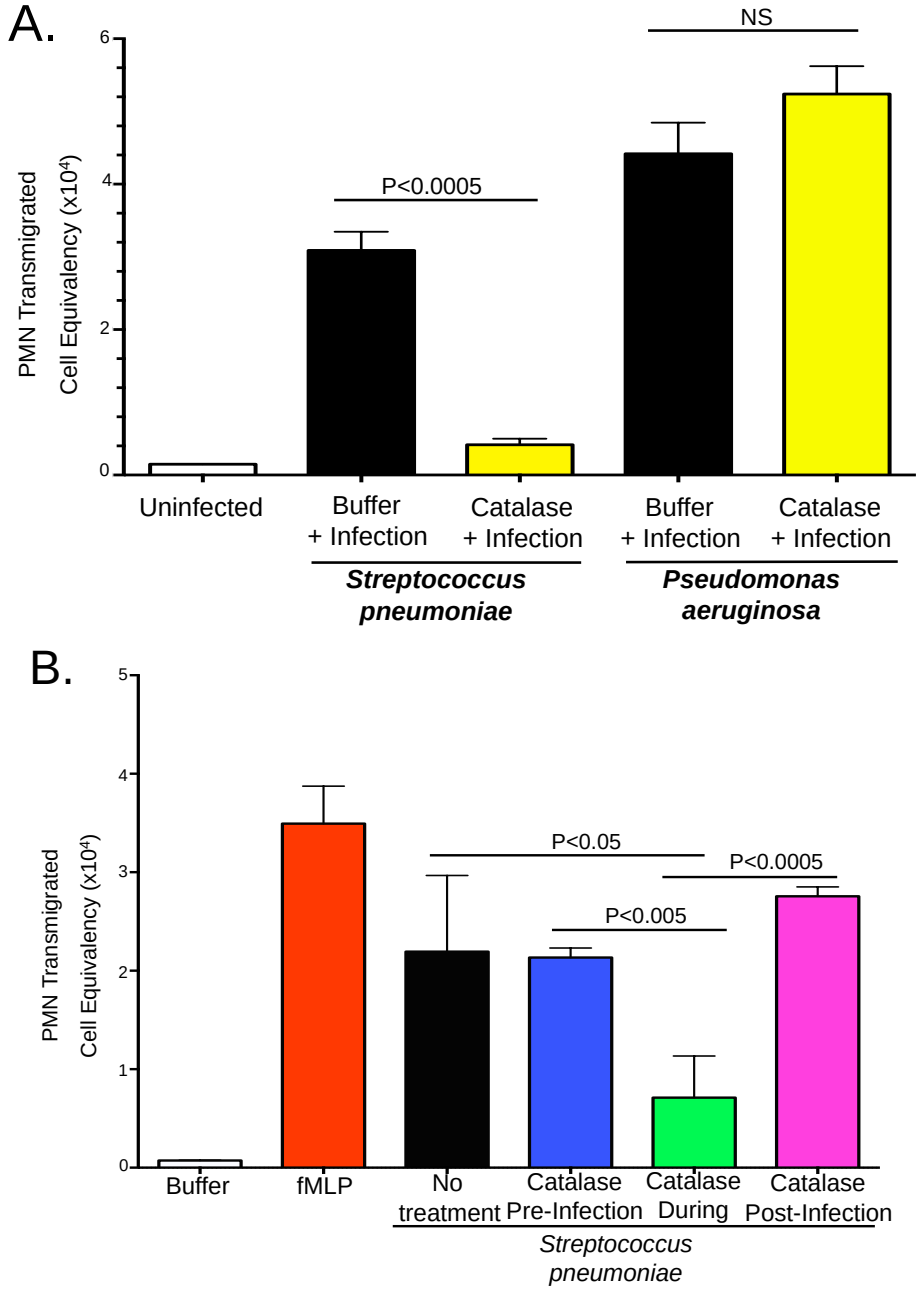
A.
PMN Transmigrated
Cell Equivalency (x10⁴)
0
2
4
6
P<0.0005
NS
Uninfected
Buffer
+ Infection
Catalase
+ Infection
Buffer
+ Infection
Catalase
+ Infection
Streptococcus
pneumoniae
Pseudomonas
aeruginosa
B.
PMN Transmigrated
Cell Equivalency (x10⁴)
0
1
2
3
4
5
P<0.05
P<0.0005
P<0.005
Buffer
fMLP
No
treatment
Catalase
Pre-Infection
Catalase
During
Catalase
Post-Infection
Streptococcus
pneumoniae

Figure 3.5 Catalase treatment inhibits PMN migration during *S. pneumoniae* infection

Transepithelial PMN migration **(A)** in which bacteria were either mock-treated or incubated with catalase during the infection step. Catalase (yellow) effectively reduced PMN migration of *Streptococcus pneumoniae* infected cells as compared to mock-treated (black) but was unable to reduce PMN migration of the catalase-competent *Pseudomonas aeruginosa*. **(B)** Catalase treatment had no effect when epithelial cells were pre-treated with catalase or treated post-infection during transepithelial PMN migration. Catalase was only effective if exposed during infection with *S. pneumoniae* indicating catalase is acting in a *S. pneumoniae*-specific manner. Statistics performed using Student's T-test. Shown is one representative PMN transepithelial assay of at least 3 runs with similar results.

Neither hydrogen peroxide nor PLY are sufficient to induce PMN transepithelial migration

Earlier examination demonstrated that 33ng/mL of purified PLY, the equivalent amount of PLY produced by 10 MOI wild-type *S. pneumoniae* during a one-hour infection, was not sufficient to induce PMN migration in a transepithelial assay (Figure 3.1). With the identification of hydrogen peroxide as an essential virulence factor, we sought to test whether the combination of hydrogen peroxide and PLY would be sufficient to drive HXA_3 production in epithelial cells. We initially attempted to induce PMN migration by exposing H292 epithelium with a mixture of PLY and varying hydrogen peroxide conditions. PLY was either mixed with a single dose of 250 μM H_2O_2 or a gradually increasing dose beginning at 0 μM and increasing to 250 μM (Figure 3.6). Under both conditions, PLY with the purified hydrogen peroxide was unable to induce PMN migration. To ensure that the window of efficacy was not being missed, the gradual hydrogen peroxide concentration was increased from 250 μM to 1 mM, to no effect (3.6C).

The results of these experiments suggest a system in which hydrogen peroxide and pneumolysin work in conjunction with at least one other *S. pneumoniae* virulence factor to induce HXA_3. It is not clear if this third signal acts independently of the hydrogen peroxide/PLY determinants or if it works in concert with these other two virulence factors. To examine whether this might be a soluble factor, we conditioned HBSS by allowing bacterial growth for one hour. We removed the *S. pneumoniae*, and then treated naïve cells with the bacterial-conditioned HBSS. H292 cells were unable to

mediate PMN transepithelial migration under such conditions (3.6D), indicating that the additional signals are not exclusively soluble factors.

The physical attributes of cells tend to be preserved upon fixation with paraformaldehyde (PFA) and other fixative agents. We surmised that if the third signal required a physical interaction with the epithelium, in addition to hydrogen peroxide and PLY, fixed bacteria supplemented with H_2O_2 and PLY might induce transepithelial migration of PMNs. Therefore, ΔPLY bacteria were fixed with 4% PFA and (post-fixation) supplemented with 300 μM hydrogen peroxide and 33ng/mL pneumolysin. These conditions failed to produce a significant PMN transepithelial migration response, indicating that the bacteria require some kind of active interaction together with hydrogen peroxide and pneumolysin (Figure 3.7) or a combination between soluble factors and physical interactions. Thus, we can conclude that to obtain maximal PMN migration, we need pneumolysin, hydrogen peroxide production, and at least one other, as of yet unidentified, signal.

MRP2 localization is dependent on Pneumolysin and hydrogen peroxide

We previously showed in Chapter II that PMN transepithelial migration is dependent on the expression of the ABC-transporter MRP2 during infection (Figure 2.9). HXA_3 efflux is mediated by MRP2 and in the previous section we demonstrated that transepithelial PMN migration is dependent on both pneumolysin and hydrogen peroxide. Thus, we next sought to probe how PLY and hydrogen peroxide impact the trafficking of MRP2 to the plasma membrane.

Apical surface biotinylation allows us to track the proteins that localize exclusively to the apical portion of the plasma membrane. To examine the MRP2 plasma-membrane enrichment during infection, we conducted apical biotinylations of wild-type infected, ΔPLY-infected, PLY-treated, and catalase-treated wild-type infected H292 cells. When exposed to the ΔPLY mutant, MRP2 was no longer enriched on the apical surface of H292 as compared to uninfected and wild-type infected cells (Figure 3.8A). Much like the PMN transepithelial migration data, purified PLY at 33ng/mL treatment was insufficient to induce MRP2 build up on the apical surface, demonstrating it is also necessary but not sufficient to cause MRP2 translocation. When complementing the ΔPLY mutant with purified PLY, we regenerated the MRP2 enrichment (Figure 3.8A). Similar to ΔPLY infections, when hydrogen peroxide was quenched via catalase, MRP2 mobilization to the plasma membrane was eliminated (Figure 3.8B). MRP2 apical localization directly correlated with the results of the function in transepithelial PMN migration assay: i.e., MRP2 enrichment was observed during any condition in which PMN migration occurred. Any condition unable to induce PMN migration also exhibited no increase in MRP2 localization.

Figure 3.6

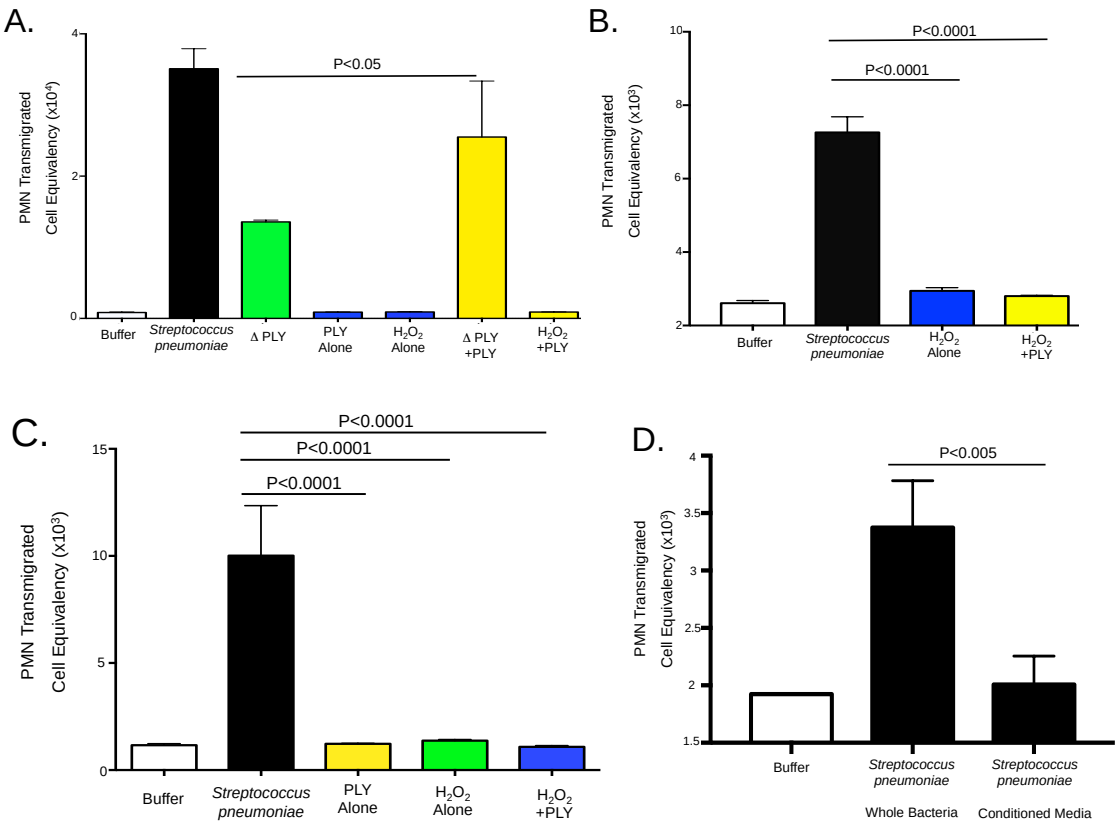

Figure 3.6 Purified PLY and hydrogen peroxide are both necessary but not sufficient alone or combined to induce PMN migration

PMN migrations with PLY, hydrogen peroxide, and the combination of the two yielded no PMN migration. PLY was spiked at time 0 at the concentration of 33ng/mL in all PLY samples and hydrogen peroxide was either spiked at 250μM (A), increased from 0 up to 250 μM every 10 minutes to replicate normal hydrogen peroxide production (B), or increased from 0 to 1mM every 10 mins (C). (D) HBSS was conditioned with *Streptococcus pneumoniae* for 1 hour and then bacteria were removed. Conditioned media was insufficient to induce PMN migration by itself. Statistics performed using Student's T-test.

Figure 3.7

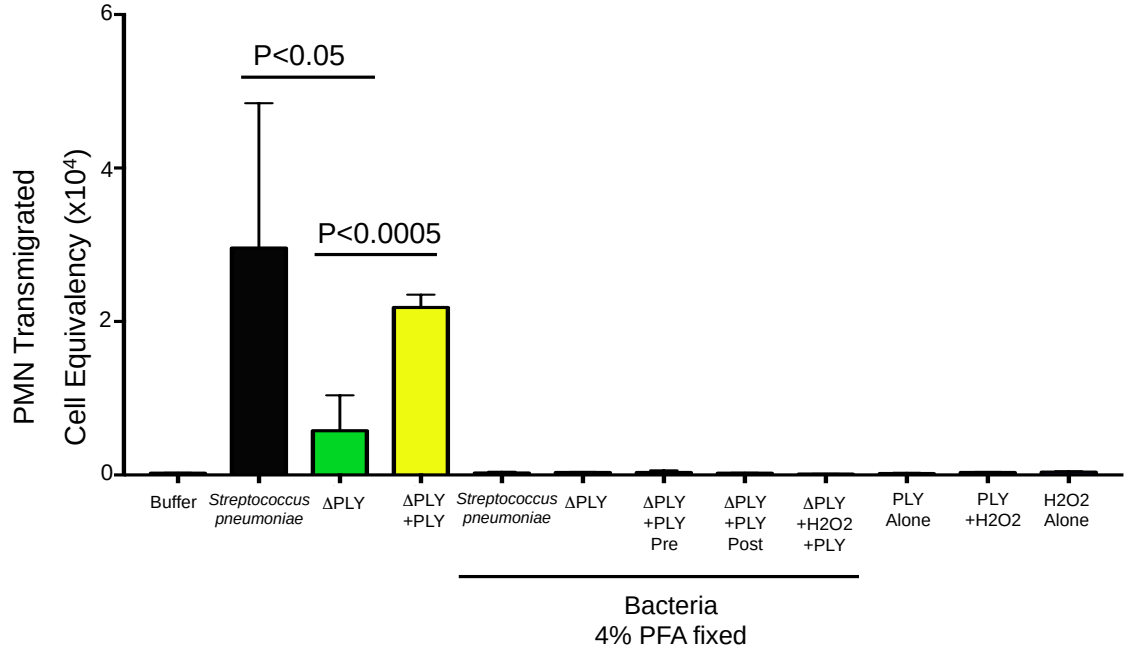

Figure 3.7 Hydrogen peroxide and PLY treatment are not complemented with fixed bacteria

Bacteria were fixed with 4% paraformaldehyde then combined with PLY pre- or post-paraformaldehyde fixation, thinking that the PLY might need a bacterial membrane anchor to activate. PLY was also applied post-fixation and mixed with hydrogen peroxide (ΔPLY+H2O2+PLY) to examine if earlier heat-killing or UV irradiation might be disrupting structures that might be necessary for PMN migration. None of the stated conditions induced observable PMN migration. Statistics were conducted using Student's T-test. Shown is one representative PMN transepithelial assay of at least 3 runs with similar results.

PMN migration and MRP2 apical enrichment are calcium dependent

Given that MRP2 and PMN transepithelial migration appeared to be dependent on both virulence factors, we saw an opportunity to examine the possible synergistic nature of hydrogen peroxide and pneumolysin activity. We therefore examined what secondary messengers might be impacted by either hydrogen peroxide or pneumolysin and how such factors might work together to coordinate MRP2 apical fusion. In addition to many pro-inflammatory responses, it has been shown that pneumolysin and hydrogen peroxide induce increases of eukaryotic intracellular calcium that can signal damage or distress in the cell (135, 136). As it has been demonstrated that wild-type *S. pneumoniae* infection increases intracellular calcium (136), we began to examine how calcium signaling might impact HXA_3-induced PMN transepithelial migration and MRP2 localization. First, we evaluated whether calcium increases in a detectable manner during our experimental process. Over a one-hour infection at 10 MOI, serotype TIGR-4 *S. pneumoniae* infection increased intracellular calcium concentrations in H292 cells by approximately 60% (Figure 3.9A).

Figure 3.8A

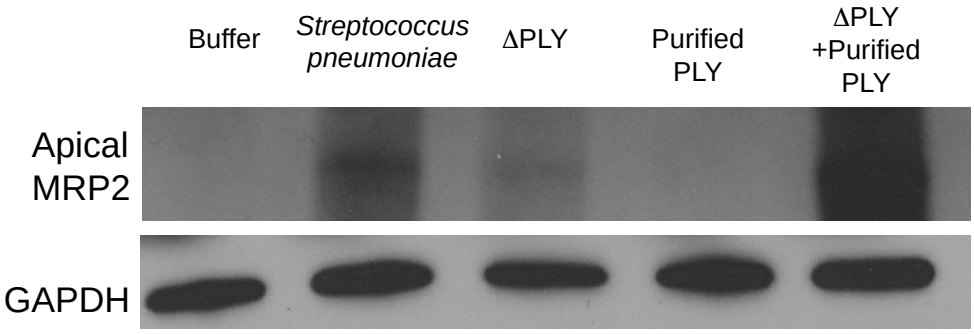
Buffer
Streptococcus pneumoniae
ΔPLY
Purified PLY
ΔPLY +Purified PLY
Apical MRP2
GAPDH

B.

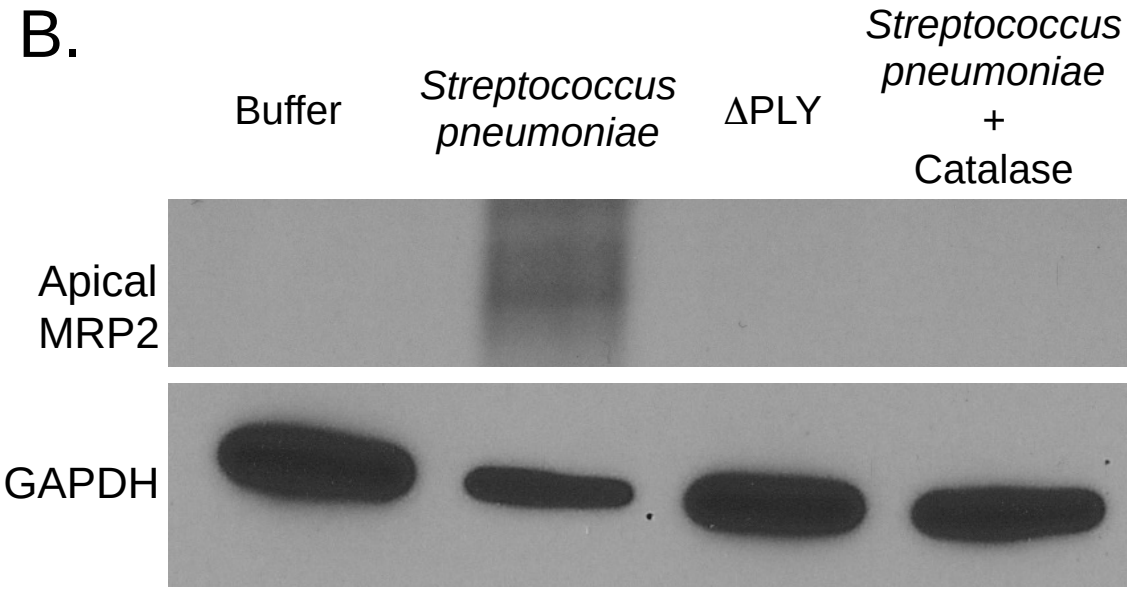
Buffer
Streptococcus pneumoniae
ΔPLY
Streptococcus pneumoniae + Catalase
Apical MRP2
GAPDH

Figure 3.8 MRP2 apical enrichment requires both hydrogen peroxide and PLY

H292 cells were treated with (**A)** HBSS (Buffer), wild-type infected (*Streptococcus pneumoniae*), ΔPLY infected (ΔPLY), PLY-treated (Purified PLY, 33ng/mL), or ΔPLY infected with PLY (ΔPLY+Purified PLY, 33ng/mL). ΔPLY infections were not able to elicit the same MRP2 localization that wild-type bacteria were able to. Like PMN migration, PLY alone at 33ng/mL was unable to induce MRP2 translocation but complementing ΔPLY infections with purified PLY was able to regenerate the MRP2 enrichment. **(B)** Catalase treatment also inhibited *S. pneumoniae*-induced MRP2 plasma membrane enrichment, showing that hydrogen peroxide is also necessary to induce wild-type levels of MRP2 on the apical surface. GAPDH used as loading control.

While calcium influxes are usually observed in much shorter time-scales than the one-hour infection, there is precedent in examining longer time-points of calcium increase (136). In uninfected cells, cells infected with pneumolysin-deficient bacteria, and cells infected in the presence of catalase, we saw no discernable increases in calcium. Hydrogen peroxide and pneumolysin treatment by itself at our experimental concentrations exhibited no increases either, leading us to conclude that there is likely a threshold event that must take place where calcium reaches specific concentration to initialize signaling.

While calcium signaling is critical in many processes, we sought to examine whether epithelial-specific calcium signaling might be critical in PMN migration. We chose to eliminate apical calcium post-infection to investigate whether calcium influx in the epithelium during the post-infection time point was necessary to induce PMN migration. We compared this to cells incubated with media in which magnesium had been eliminated to elucidate whether changes in phenotype might be specific to divalent-cations instead of solely calcium signaling. We could not eliminate calcium during the infection as *S. pneumoniae* virulence relies on calcium (137). Similarly, eliminating calcium in the basolateral chamber might impact PMN signaling and activity during the PMN migration step. Under these conditions, we observed a large reduction in the PMN migration phenotype when calcium-free HBSS was used instead of conventional HBSS (Figure 3.9B). This did not appear the case in samples with reduced magnesium, indicating to a calcium-specific effect.

To more subtly assess the necessity of calcium on the system, we sought to examine whether the MRP2 apical increase was impacted by calcium decreases. When treated with the cell permeable intracellular calcium chelator, BAPTA, cells were no longer able to increase induce PMN transepithelial migration or MRP2 on the apical surface during infection (Figure 3.10). This outcome supported the hypothesis that calcium signaling impacted both MRP2 plasma membrane enrichment and HXA_3 production.

Assuming that PLY only functions in inducing the HXA_3/MRP2 axis through calcium mobilization, we assessed whether infection-independent induction of intracellular calcium could trigger PMN migration. We therefore investigated whether thapsigargin, a drug that normally causes cytosolic calcium buildup, could complement our ΔPLY infection. H292 cells were either mock treated or pre-treated with thapsigargin, washed, subjected to ΔPLY infection, and either underwent a intracellular calcium measurement or PMN transepithelial migration assay. We found that thapsigargin induced similar calcium increases during the infection time-frame (Figure 3.11A), but did not rescue the phenotype, nor did it cause transepithelial PMN migration. Not only did thapsigargin not rescue the PMN phenotype, but it also inhibited PMN migration in wild-type infections (Figure 3.11B and C). Cells pretreated with thapsigargin, whether infected with ΔPLY or wild-type bacteria, were unable to mediate a PMN response. The thapsigargin observation seems to highlight that not only is calcium influx necessary, but specific types of calcium influx are important for pneumococcal-induce PMN transepithelial migration.

Figure 3.9A

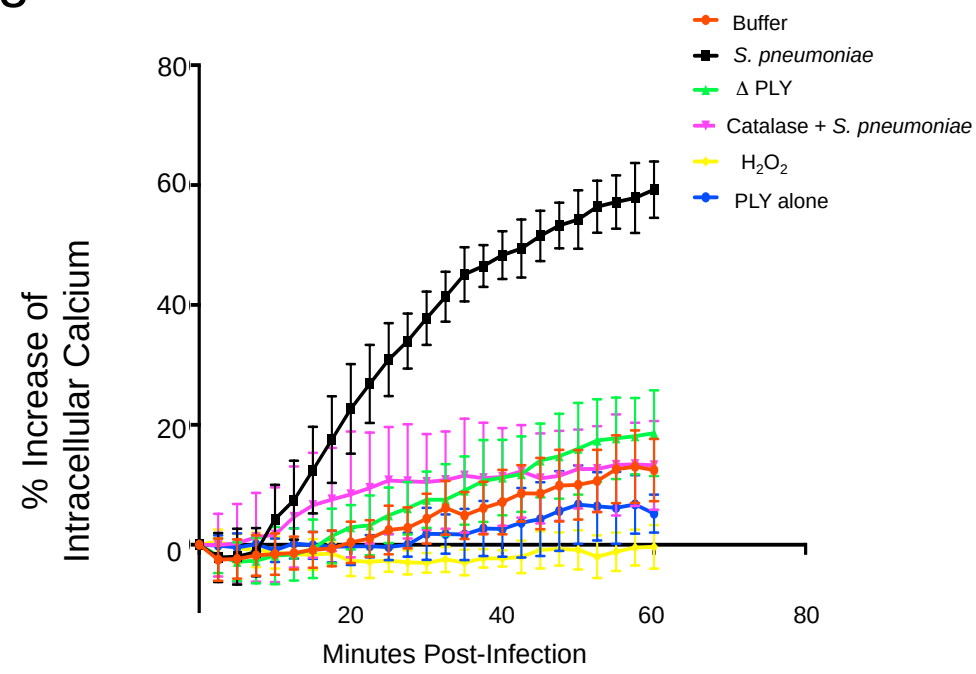
Buffer
S. pneumoniae
Δ PLY
Catalase + S. pneumoniae
H2O2
PLY alone
% Increase of Intracellular Calcium
0
20
40
60
80
20
40
60
80
Minutes Post-Infection

B.

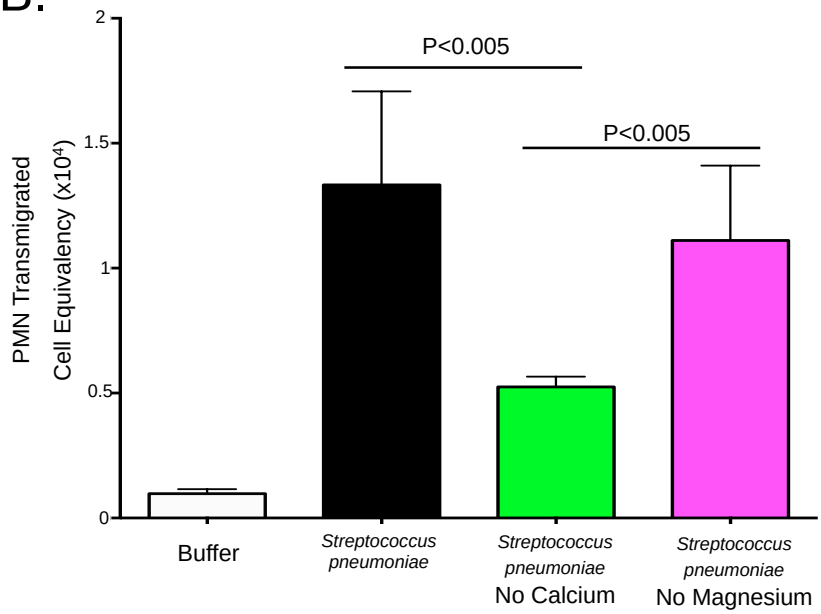
PMN Transmigrated Cell Equivalency (x10⁴)
0
0.5
1
1.5
2
P<0.005
P<0.005
Buffer
Streptococcus pneumoniae
Streptococcus pneumoniae No Calcium
Streptococcus pneumoniae No Magnesium

Figure 3.9 Intracellular calcium is a necessary component of transepithelial PMN migration

(A) H292 cells were loaded with Fura-2-AM, infected or treated with the indicated conditions, then measured for one hour to detect intracellular calcium increases. *S. pneumoniae* induced a consistent increase in calcium while hydrogen peroxide, PLY, ΔPLY bacteria, and catalase treatment all were insufficient to increase the calcium. **(B)** PMN transmigration in the presence of absence of calcium and magnesium. H292 cells were exposed to wild-type bacterial infection for one hour and then allowed to undergo a PMN migration assay where the apical surface was deficient in either calcium or magnesium. To avoid situations in which the bacteria or PMNs might not be activated because of lack of the cation, the infections and basolateral chamber of the migration construct was kept whole with the normal calcium and magnesium concentrations. This assay revealed the need for calcium during PMN migration.

The requirement for proper calcium signaling is further underscored when we investigated the role of a second calcium mobilizer, ionomycin. Unlike thapsigargin, ionomycin induces calcium influx both from extracellular calcium as well as release from intracellular stores via pore formation (138). After treating cells with ionomycin and infecting with ΔPLY, the cells were subjected to a transepithelial PMN migration assay. We noted a recapitulation in the transepithelial PMN migration phenotype when ΔPLY bacteria infected cells that had been treated with ionomycin (3.12A). Additionally, ionomycin alone caused no PMN migration. The ionomycin-induced supplement was dose-dependent, and transepithelial PMN migration was lost when the ionomycin concentration was reduced from 1μM to 0.5μM.

On the balance of these observations, we concluded that there was a threshold of stress specifically placed on cells in order to elicit signals that induced calcium increases and led to MRP2-mediated PMN transepithelial migration. Furthermore, the calcium buildup appeared to be dependent on hydrogen peroxide and pneumolysin. Yet, the calcium mobilization was also specific; if calcium signaling was reduced via chelation or perturbed via thapsigargin, PMN transepithelial migration was inhibited. However, normal bacterial infection or ionomycin induction of calcium buildup was productive to facilitate the HXA_3/MRP2 axis. One key similarity between ionomycin and pneumolysin is that both induce calcium across the plasma membrane by perturbing it by pore formation. Might other cytolysins send the same signal that PLY does? Perhaps the pore formation allowing for extracellular calcium signaling is a critical step in the infection to induce MRP2 localization and PMN migration.

To examine whether pore formation in general would produce a productive HXA_3 reaction, we supplemented our ΔPLY bacteria with perfringolysin O (PFO). Perfringolysin O is another cholesterol-dependent cytolysin produced by the Gram-positive bacterium *Clostridium perfringens* and behaves in a similar manner to PLY (139). When we mixed ΔPLY bacteria with 33ng/mL of PFO and conducted a PMN migration, we observed a similar phenotype as when ΔPLY was supplemented with purified PLY (Figure 3.12B). This verified that there was likely a conserved mechanism influencing transepithelial PMN migration.

Figure 3.10

A.

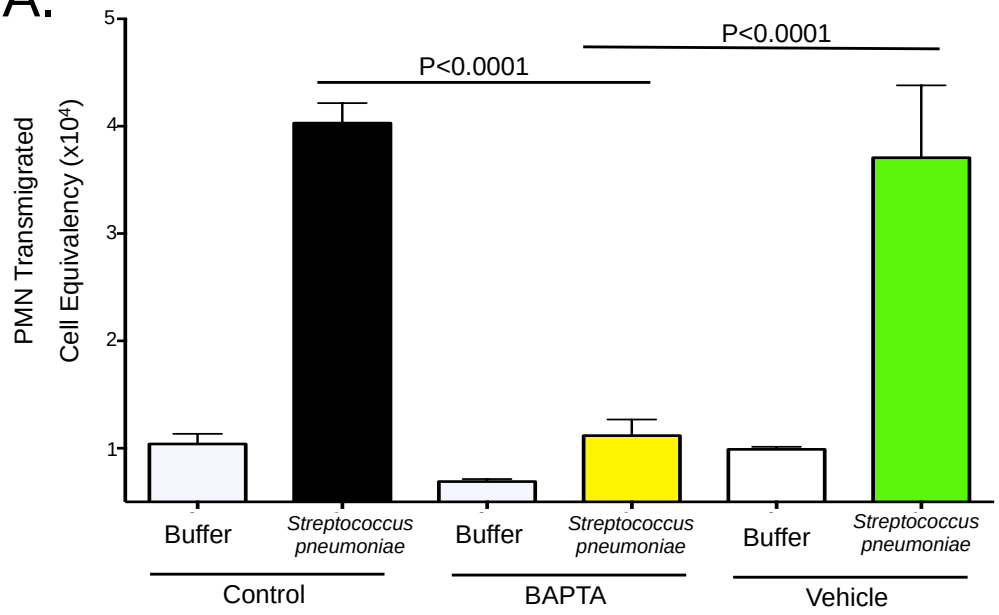

B.

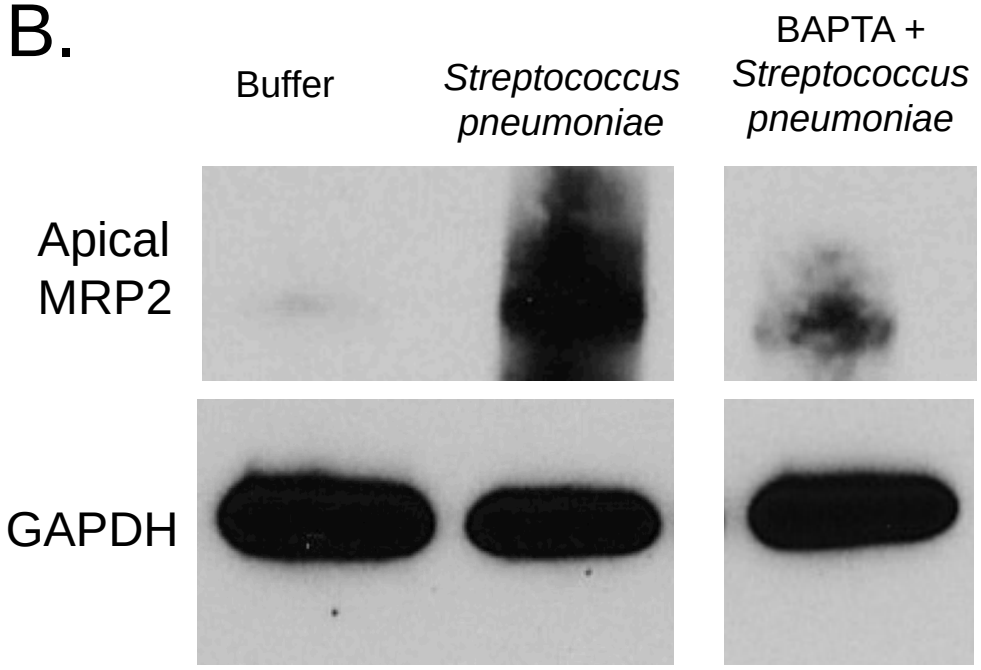

Figure 3.10 Intracellular calcium is necessary for PMN migration as well as MRP2 localization

Treatment of the H292 epithelium with the membrane permeable calcium chelator BAPTA resulted in reduction of intracellular calcium buildup and **(A)** reduced PMN migration after infection with wild-type *S. pneumoniae*. **(B)** Reduced the ability of MRP2 to reach the apical surface during *S. pneumoniae* infection as observed during a biotinylation experiment. Cells were pretreated with BAPTA, washed, and then infected for one hour as normal. Shown is one run of at least three that showed similar results.

Figure 3.11

A.

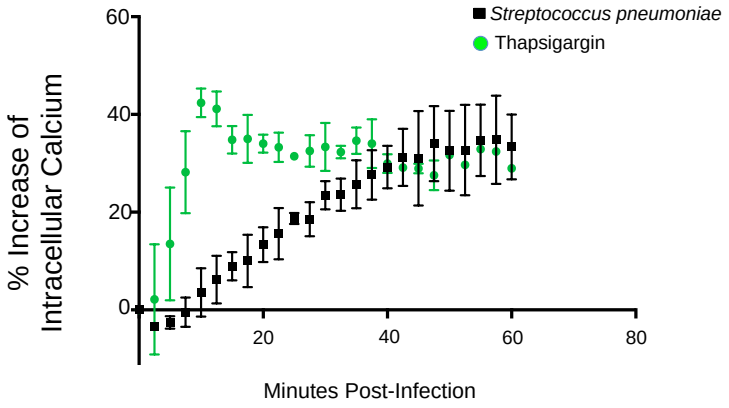

B.

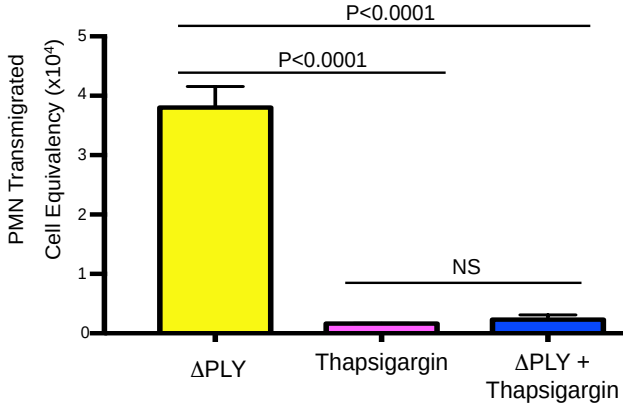

C.

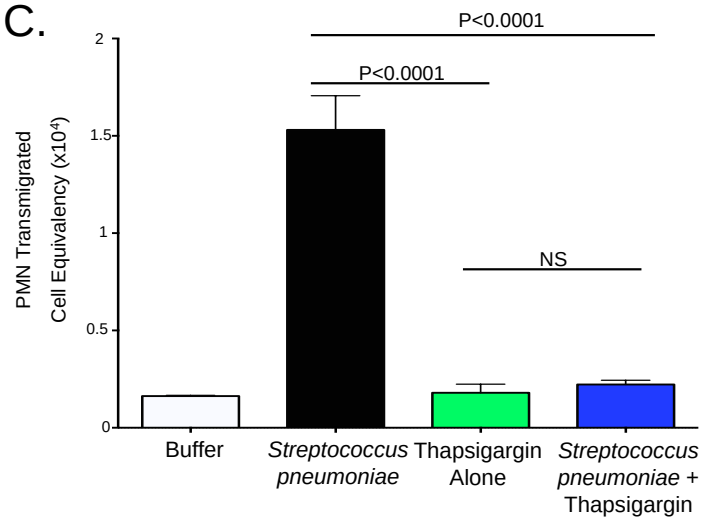

Figure 3.11 Intracellular calcium increases caused by thapsigargin reduces PMN migration

Thinking that artificially increasing intracellular calcium concentrations might recapitulate wild-type PMN migration during infection with the ΔPLY mutant, we first pretreated cells with thapsigargin. Thapsigargin increased calcium to similar levels as wild-type *Streptococcus pneumoniae* infection **(A)** but failed to complement ΔPLY infections during a PMN migration assay **(B)**. Similarly, if cells pretreated with thapsigargin are infected with wild-type bacteria, the cells are no longer permissible to inducing PMN migration **(C)**.

Figure 3.12

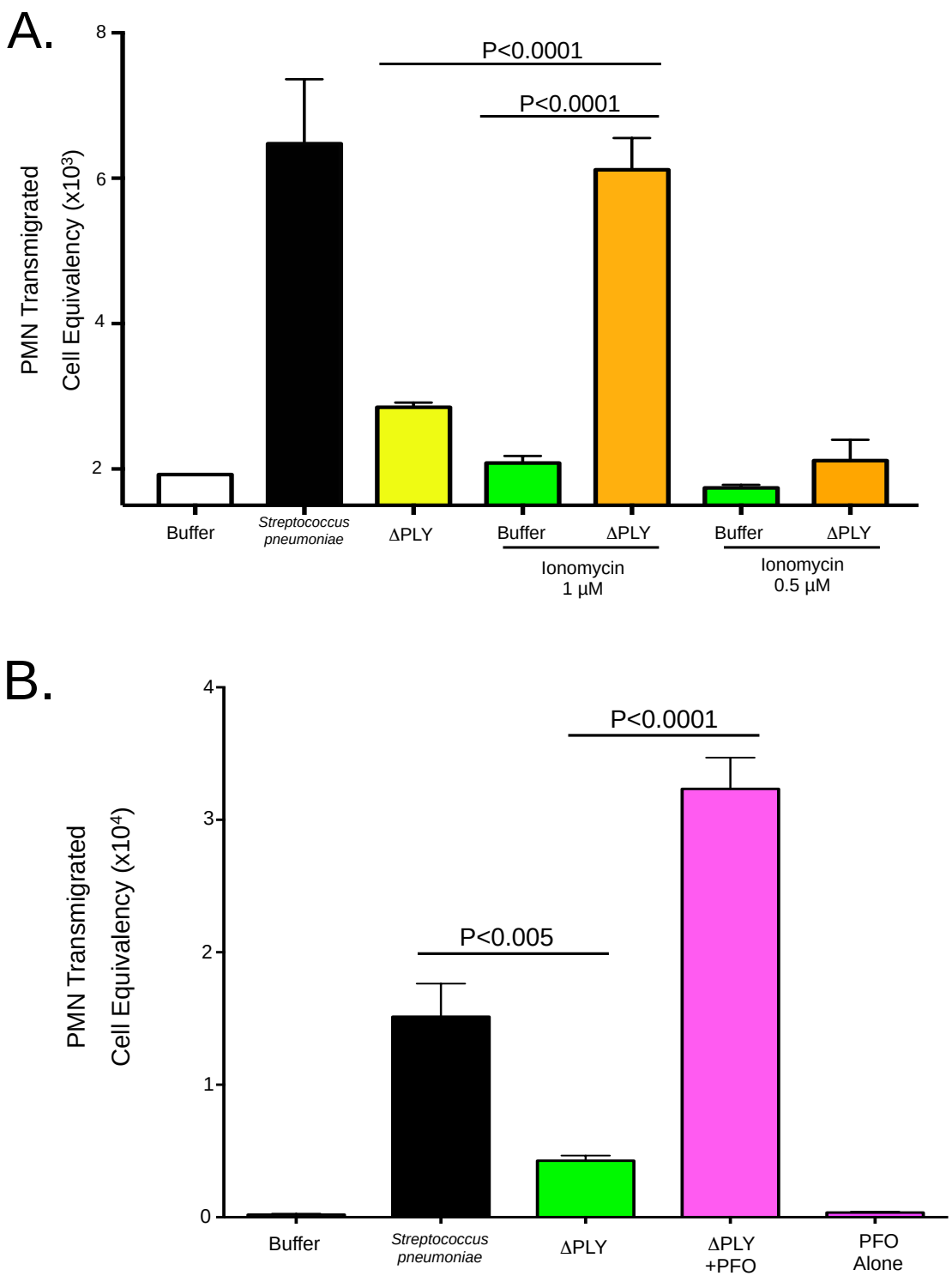
A.
PMN Transmigrated Cell Equivalency (x10³)
8
6
4
2
P<0.0001
P<0.0001
Buffer
Streptococcus pneumoniae
ΔPLY
Buffer
ΔPLY
Ionomycin 1 μM
Buffer
ΔPLY
Ionomycin 0.5 μM
B.
PMN Transmigrated Cell Equivalency (x10⁴)
4
3
2
1
0
P<0.0001
P<0.005
Buffer
Streptococcus pneumoniae
ΔPLY
ΔPLY +PFO
PFO Alone

Figure 3.12 Calcium induction by Ionomycin complements ΔPLY infections

(A) As expected with thapsigargin, pretreatment with the ionomycin increased PMN migration when infected with ΔPLY bacteria. This occurred in a dose-dependent manner and did not induce PMN migration by itself. **(B)** Likewise, replacement of PLY with another cholesterol-dependent-cytolysin, Perfringolysin O, at 33 ng/mL also complemented the ΔPLY infection during PMN migration assays. Statistics calculated using Student's T-test. Shown is a representation transepithelial PMN migration of at least 3 runs exhibiting similar results.

3.3 Discussion

We have previously demonstrated that there is a conserved innate immune reaction in both the intestinal and pulmonary systems that reacts to bacterial infection by initializing efflux of the PMN chemoattractant Hepoxilin A_3. Active efflux of HXA_3 is dependent on the ABC-transporter MRP2. There have been few reports about specific virulence factors and the upstream targets that assist in production and efflux of HXA_3. Garnering this information is an important task because the HXA_3/MRP2 axis appears to be conserved in both the intestinal and pulmonary organ systems. Additionally, there is evidence that HXA_3 and MRP2 have a role in intestinal dysbiosis and autoimmune diseases – therefore identifying virulence factors and conserved epithelial response molecules underlying this pathway would shed light into how undesired PMN migration might be targeted or interrupted to disrupt aberrant inflammation.

Herein, we demonstrate that PMN transepithelial migration to the site of an active *S. pneumoniae* infection is reliant on the virulence factors pneumolysin and hydrogen peroxide. PLY and hydrogen peroxide are both necessary but not sufficient either alone or in combination to induce PMN transepithelial migration *in vitro*. *S. pneumoniae*-conditioned media was unable to induce PMN migration alone (Figure 3.6D), pointing to the necessity of either live *S. pneumoniae* or a physical host-pathogen interaction. Mixture with PFA-fixed *S. pneumoniae*, hydrogen peroxide, and PLY also yielded no PMN migration, indicating a need for either live bacteria or a combination of soluble and structural *S. pneumoniae* components.

As stated, the MRP2/HXA_3 axis is conserved in both the intestine and the lung, indicating the eukaryotic signaling processes detecting these virulence factors is likely also conserved, though it remains to be seen whether enteric bacterial virulence factors signal in a similar manner. To date, HXA3-dependent PMN transepithelial migration has been described in the context of infections including *E. coli*, *Salmonella* Typhimurium, *Shigella*, and *Pseudomonas aeruginosa* (4, 11, 12, 18). These bacteria do not produce pore-forming toxins or excessive amounts of hydrogen peroxide during their infection cycles, so it is exceedingly unlikely the same bacterial detectors would trigger PMN transepithelial migration. When assessing similarities between these bacteria, we find that there are few similarities to *S. pneumoniae.* In contrast to *S. pneumoniae*, these other bacteria are Gram-negative, encode type-III-secretion systems, and all harbor catalase, which will quench hydrogen peroxide. However, one particular trait common to all these bacterial pathogens is that they coopt host cell machinery to induce alterations in how membranes and vesicles are utilized in the cell. Pore-forming toxins need additional membrane fusions to repair *S. pneumoniae*-induced pores. Hydrogen peroxide can also mediate the Fenton reaction, requiring membrane repair. *Salmonella*, *E. coli*, and *Shigella* all hijack membrane components to allow for bacterial entry or niche development (via *Shigella* entry, *Salmonella*-containing-vacuole development, or *E. coli* pedestal formation). Although there are no readily identified membrane-manipulating virulence factors during *Pseudomonas* infection, it remains possible that the endosome/vesicle trafficking mechanisms might have perturbations leading to similar signaling. The Type-III secretion apparatus, itself, may initialize immune function upon interaction with the

eukaryotic membrane. Observations that PLY-like cytolysins such as PFO can effectively complement pneumolysin-deficient *S. pneumoniae* reactions during PMN migration assays support the hypothesis that membrane perturbation may be linked to HXA_3/MRP2 activation (Figure 3.12B). Similarly, ionomycin, a molecule that increases intracellular calcium through pore formation, can complement ΔPLY infections.

Our hypotheses concerning membrane-trafficking manipulation go hand-in-hand with increases and decreases of the ABC-transporters on the plasma membrane surface. We have shown previously that increases of MRP2 on the apical surface of the lung epithelium is independent of new protein generation. Instead, it is likely that existing stores of the protein, held in endosomal vesicles, fuse with the plasma membrane and increase on the apical surface in this manner. There are current theories that plasma membrane repair during bacterial infection is paired with MRP2 increases through endosomal fusion at the plasma membrane. PLY-induced pores are excised as new membrane containing MRP2 is fused to the apical surface of the pulmonary epithelium, allowing for efficient membrane repair and initializing the pro-inflammatory response through HXA_3 via MRP2.

One other common signaling molecule is intracellular calcium. It is known that a number of eukaryotic signaling events occur via calcium-mediated signaling, including production of IL-8 in *Salmonella* Typhimurium infections. Calcium, however, is a relatively common and ubiquitous secondary messenger and more specific signaling has yet to be elucidated with the MRP2/HXA_3 axis. Nevertheless, our work identifies that both MRP2 translocation and corresponding PMN transepithelial migration are

dependent on pneumolysin, hydrogen peroxide, and specific calcium signaling. These factors likely link HXA_3 generation and MRP2 activation through a conserved messenger system present in mucosal surface epithelial cells to induce PMN migration. It is likely that one common link is membrane perturbation or membrane repair and it is this particular activity that we may want to focus further work to elucidate the active players in MRP2 plasma membrane enrichment.

3.4 Materials and Methods

Cell culture

The human cell line, NCI-H292 (H292) was cultured with RPMI (GIBCO #11875-093) supplemented with 10% FCS and subcultured using 0.05% Trypsin-EDTA (GIBCO #25300-054). Transmigration cells were prepared on 24-well inverted semi-permeable membranes (Costar #3421) and grown to confluency. Cells for protein assays were grown to confluency on 6-well membranes.

Bacteria

Streptococcus pneumoniae serotype 4 (TIGR4) and Pneumolysin-deficient mutants (ΔPLY) were provided by Drs. John Leong and Andrew Camilli (Tufts School of Medicine). Bacteria were streaked overnight on 5% sheep-blood Tryptic Soy Agar (Northeast Laboratory Services #p-1100) and grown at 37℃, 5% CO_2 for 14-20 hours. On the day of infection, bacteria were resuspended with Todd-Hewitt-Yeast media and supplemented with oxyrase (#OB-0100, 5uL/mL culture). Cultures grew to ~$5x10^8$

CFU/mL, as confirmed post-infection by CFU counting 18-24 hours later. ΔPLY complement with purified cytolysin, such as PLY, provided by Dr. Rod Tweten through Dr. John Leong, was performed by adding given amount to dilute to a final concentration as reported. Purified PLY procedure previously published (128, 140). *In vitro* infections were diluted in Hanks Balanced Salt Solution (HBSS, GIBCO #14025-092). Hydrogen peroxide (Sigma Aldrich Cat# H1009-100mL) treatments and supplements were at indicated concentrations. Catalase treatments were conducted by initially diluting catalase (Sigma Aldrich Cat#C1345-10G) in HBSS+ at 5µg/mL. This solution was then diluted 1:10 in the infection solution and applied to epithelial cells.

Bacterial killing assay

Wild-type and ΔPLY *Streptococcus pneumoniae* were cultured as above and washed with HBSS+ once. While in clear eppendorf tubes, bacteria were either exposed to UV light for 30 mins, boiled for 30 mins, or resuspended in paraformaldehyde (4% in Phosphate Buffered Saline [PBS]) for 30 mins. Bacteria were then centrifuged and resuspended with HBSS+ together with indicated conditions. CFU counting confirmed that >90% of bacteria had been killed by comparing to unkilled counterparts.

Transmigration

Transmigrations were conducted as previously described (3) using H292 cells. H292s were infected apically with wild-type TIGR4 (~10 MOI) for 1 hour and washed. Human neutrophils were isolated from healthy donors using methods previously

published (13). Freshly isolated neutrophils were applied to the basolateral chamber of infected membranes and allowed to migrate. Neutrophil migration was quantified using a myeloperoxidase assay.

Biotinylation

H292 cells were grown on 6-well transmembranes to confluency, rinsed with HBSS, and infected with TIGR4 (~10 MOI) apically. Cells were washed and biotinylated as previously described (109, 110). Cells were lysed and passed through 26½ -gauge needles, spun, and applied to streptavidin beads (Thermo Fisher #20347) or saved in tricine sample buffer (recipe from Bio-rad 161-0739). Biotinylated-bead samples were incubated at 4℃ overnight, washed, incubated at 40℃ for 20 mins in tricine sample buffer, then run on 4-20% TGX protein gel. Proteins were transferred on to nitrocellulose membranes, blocked, and incubated with the indicated antibodies: MRP2 (ABCAM ab3373), GAPDH (EMDMilipore MAB374). HRP-conjugated secondary antibodies were used to visualize western blots.

Calcium examination

Thapsigargin (Sigma Aldrich Cat#T9033-1MG), Ionomycin (Sigma Aldrich Cat#IO634-1MG), and BAPTA (Molecular Probes Cat#B1205) were diluted in HBSS+ and applied to H292 cells after initial wash prior to infection. Thapsigargin working solution 10 µM, diluted in HBSS. Cells were exposed for up to one hour and washed before assay. Ionomycin working solution 1µM and 0.5µM, cells were exposed for up to

one hour and washed before assay. BAPTA working solution was 25μM, cells were exposed to HBSS-diluted BAPTA for 30 mins, washed, infected as normal (for PMN migration) or biotinylated (For biotinylation). Solutions were added to the apical surface (600 μL) as well as the basolateral surface (100 μL) for 1 hour and washed away for transmigration assays. Similar steps were conducted for biotinylation assays.

Intracellular calcium was measured by loading H292 cells with Fura-2-AM (Molecular Probes Cat#F1221) per manufacturers instructions. Cells were either pre-infection treated, treated with bacterial solution, or treated with cytolysin/hydrogen peroxide. For time course H2O2 experiments, cells were removed from their initial wells in a 24-well plate and added to a separate well containing the given concentration of hydrogen peroxide in pre-warmed HBSS+. Samples run every 2.5 mins for 1-hour. Increases of calcium were calculated by examining the excitation of 340 vs. 380 nm and emission at 510nm by an H4synergy plate reader.

Hydrogen peroxide measurement

Hydrogen peroxide was measured using a colorimetric assay as previously described (141). Briefly: Solutions were mixed with 1mL, 2% Potassium Iodide; 1mL, 2M HCl and mixed thoroughly. To this, we added 0.5mL, 0.01% Toluidine Blue, followed by 2mL Sodium Acetate. Final solution was measured at 628nm and measured against a blank containing only HBSS.

Chapter IV: Discussion and importance

4.1 Introduction

The following section restates the general findings of the thesis and discusses some of the alternative theories that were tested during the completion of this work. In it and the following appendix, I will discuss similarities and contrasts between pulmonary and intestinal infections and attempt to infer universal mechanisms controlling HXA_3-dependent PMN transepithelial migration and MRP2 enrichment on the plasma membrane. I will also discuss certain caveats that need to be addressed to give a complete picture of the work presented.

4.2 Restating the Thesis findings

At the beginning of this thesis work, PMN infiltration was known to be HXA_3 dependent in Gram-negative infections with *Salmonella serotype* Typhimurium (4), *Shigella* (11), and *Pseudomonas aeruginosa* (18) at a variety of mucosal surfaces. Ongoing research completed during my first few years of experimentation expanded this list to *E. coli* (12) infection in the intestinal tract and, finally, *Streptococcus pneumoniae* in pulmonary infections (19). Although reported critical in bacterial pulmonary infections, it remained to be seen how HXA_3 was exported to the site of infection and whether mediation of HXA_3 efflux was similar to the intestinal trafficking. We sought to examine whether mechanisms comparable to that in the gut, mediated by ABC-transporters, might be key to HXA_3 efflux. We initiated these studies in a semi-biased

approach, examining a variety of ABC-transporters for increases on the apical surface of the epithelium during infection, a hallmark of an HXA_3 efflux transporter. As detailed in the introduction, there have been few reports that have assessed expression and activity of ABC-transporters in the lung under normal, basal states, so our goal was to help illuminate some of these details throughout our studies.

Another specific goal during this investigation was to probe the correlation between inflammation, especially ABC-transporter-mediated PMN transepithelial migration, and infiltration of *S. pneumoniae* in to the blood. Previous studies had demonstrated a distinct relationship between PMN transepithelial migration and the ability for *S. pneumoniae* to disseminate and it was our desire to hone in on the transition from pulmonary infection to bacteremia. The greater goal was to examine whether obstruction of HXA_3 efflux by targeting transporters for inhibition could lessen PMN infiltration and reduce bacterial entry into the blood.

Our initial observation was that, similar to efflux of HXA_3 in the gut, MRP2 increases on the apical surface upon infection with *S. pneumoniae*, as measured by apical immunofluorescence and apical biotinylation (Figure 2.2). Other ABC-transporters either decreased (MRP1) or showed no change (MRP4, MRP5). Still, others, were undetectable by both methods and were determined to either not be expressed by our *in vitro* cell lines or were too low to be detectable and, therefore, disregarded for future experimentation. Both MRP4 and MRP5 have been implicated in pulmonary reactions (27), though it did not appear they took part in HXA_3-mediated transepithelial PMN migration, as there were no increases in MRP4 or MRP5 expression or enrichment on the membrane.

During functional studies, MRP1 was shown to efflux an anti-inflammatory molecule or molecules that we have termed L-AMEND (Chapter II). Similar effects correlating MRP1 and protection from inflammation have been reported in the intestine (35) as well as pulmonary conditions such as COPD (47). Our work correlates MRP1 activity with reduction of PMN infiltration during bacterial infection. Similar activities have been reported in the intestine where eukaryotic P-gp effluxes a PMN-inhibiting molecule AMEND (159). In contrast, MRP2 effluxes the pro-inflammatory HXA_3 during infection.

The MRP2 increase on epithelial cells appears dependent on both presence of the cholesterol-dependent cytolysin, pneumolysin, and bacterial-derived hydrogen peroxide (Chapter III). Eliminating either of these virulence factors limits PMN migration during *in vitro* studies, though neither appear to be sufficient in generating the PMN migration phenotype by themselves. Additional communications have detailed that pneumolysin and hydrogen peroxide work together to promote neuronal apoptosis during meningitis (131). When measuring the number of apoptotic cells during infection, it was shown that *S. pneumoniae* does not appear to induce wide-scale apoptosis during one-hour *in vitro* assays. Schreiber et al. reported similar observations that neither *S. pneumoniae* nor *P. aeruginosa* caused epithelial apoptosis during infection – the majority of apoptotic cells observed during the experiments were leukocytes (142). There has been a report that hydrogen peroxide causes DNA damage leading to apoptosis, however this study reported no increases of apoptosis prior to a 7-hour time-point when infecting with 200-400 MOI, well above our *in vitro* experiments (123). Similarly, Schmeck et al. examined

caspase-6 associated apoptosis during infection with a pneumolysin-competent serotype 2 pneumococcus and observed no increases prior to 8 hours of infection (97). Both PLY and hydrogen peroxide work together with live *S. pneumoniae* to induce an intracellular calcium increase that remains detectable 1 hour post-infection and which, if disrupted, completely abrogates PMN migration.

4.3 MRP1 activity reduces PMN migration

We have demonstrated in our *in vitro* model of PMN transepithelial migration that MRP1-mediated efflux of a substance we have termed "L-AMEND" reduces PMN transmigration. Likewise, we showed via biotinylation and immunofluorescence that MRP1 is not as abundant on the apical of *in vitro* tissue culture cells and *ex vivo* murine pulmonary tissue during infection with *S. pneumoniae*. Previous studies conducted by Schultz et al. have examined MRP1 deficiency in murine models of pneumococcal infection, resulting in increased survival when MRP1 is absent (49). As noted previously in Chapter 2, these studies used a slightly different infection model (intranasal infection, versus our infection method of intratracheal application) with serotype-3 bacteria. Nevertheless, the apparent dichotomy that the authors report *Mrp1*-deficiency reduces mortality and PMN infiltration actually might reveal a subtlety of the complexity of the system that we are studying. MRP1 reduction in cells has been suggested to be cytotoxic during pro-inflammatory reactions (35). PMNs, which express MRP1 on cellular membranes, might actually undergo early apoptosis, reducing numbers of infiltrating PMNs and resulting in the observations made in Schultz et al.

Reductions in intestinal MRP1 during DSS-modeled inflammation have been shown to increase intestinal damage, indicating that that MRP1 may be protective during intestinal inflammatory events (36). Similarly, in COPD studies, lower MRP1 expression in lungs has correlated with increased inflammation (47). Both these conditions have a hallmark of significant infiltration of PMNs, a similar phenotype observed when we reduce MRP1 expression in our experimental models of pneumococcal disease. These observations all indicate a possible anti-inflammatory activity conferred by MRP1 that seems reduce PMN infiltration and inflammation.

The reduction of MRP1 closely resembles a reduction in P-gp in the intestine as observed by our lab (159)(34). In this work, P-gp effluxes an anti-inflammatory endocannabinoid that reduces PMN migration in stable, uninfected states. P-gp is undetectable in NCI-H292 cells and our observations concerning MRP1 in pulmonary tissue mirrors the activity of P-gp in the intestine; therefore, it seems reasonable to hypothesize that MRP1 might occupy the same or a similar role in the lung to maintain homeostasis and resolve inflammation. Although there is indication that P-gp expression is increased due to the presence of the microbiota, there is no such study that indicates MRP1 needs similar priming by bacteria.

4.4 Addressing MRP1 localization and reduction

Classically, MRP1 is thought to be basolaterally located while MRP2 is apical. As mentioned in Chapter 1, there are conflicting reports in the literature about where each transporter localizes in the lung in uninfected, basal states and very little information as

to how these transporters are regulated during inflammation. While our *in vitro* immunofluorescence and biotinylation data specifically looks at the apical surface, our *in vivo* immunofluorescence does not distinguish between the two; meaning that some pulmonary MRP1 may localize to the basolateral surface. Regardless, the immunofluorescence signal reduces during infection in mouse tissue, which is consistent to observations made *in vitro*. Conceptually, whether MRP1 is also on the basolateral portion of the epithelium does not adversely impact our findings that it acts as an immunosuppressant mediator.

MRP1 reduction mirrors reduction of P-gp in the intestine during *Salmonella* infection (34, 143). This has been shown to be a caspase-3 mediated event where intracellular portions of P-gp are cleaved at a -DXXD- motif, degrading the protein and reducing its effective concentration through a mediator known as “P53 apoptosis Effector Related to PMP-22” (PERP) (113). Although there is no information regarding caspase-mediated cleavage of MRP1 in the current literature, there are 2 prospective sites: DXXD motifs at amino acid sequences 1081 and 1417 (DTVDS and DKLDH). It is possible that caspases are activated during *Streptococcus pneumoniae* infection and reduce MRP1 through cleavage events, thus eliminating concentrations of L-AMEND and increasing the potency of proinflammatory modulators that attract PMNs from the basolateral surface.

4.5 Isolating and validating HXA_3

This thesis makes the supposition that there is interplay between MRP1, which effluxes anti-inflammatory molecules reducing PMN infiltration, and MRP2, which effluxes pro-inflammatory lipids, namely HXA_3. When examining the activity of substances effluxed by MRP2, we have used a previously described method of isolating lipids that has been shown to enrich for HXA_3 using a C-18 column followed by a functional assay, demonstrating the ability of these lipids to induce PMN migration on naïve epithelial cells (4, 11, 12).

Present day, one of the most effective techniques to quantify HXA_3 is by Mass Spectrometry. Current commercially available HXA_3 actually contains a great deal of the degradation product of HXA_3, which is biologically inactive in our assays. This has left very few options for identifying HXA_3. To ensure our bioactive lipids were enriched for hepoxilin, we relied instead on the chemical composition of HXA_3 to assist in identification. HXA_3 is an eicosanoid that contains an epoxide ring (Figure 4.1A). HXA_3 is the only known lipid PMN chemoattractant with an epoxide ring. Soluble epoxide hydrolases are chemicals that break these three-member rings, degrading them to alcohol groups and hydrocarbons. The epoxide hydrolase renders HXA_3 unable to function, thereby giving us a measureable output for a functional HXA_3 assay. When we applied epoxide hydrolase to our isolated lipids (Figure 2.9A) and then tested the ability of those lipids to induce transepithelial PMN migration, we observed a sharp decline in the number of PMNs that traversed the epithelial layer compared to mock-treated lipids (Figure 4.1B). This demonstrated that the C-18 isolation method provides for significant enrichment of an epoxide-containing lipid that induces PMN migration, namely HXA_3.

There was one other possible epoxide-containing lipid that we identified through a literature search: Thromboxane A_2 (TXA_2). TXA_2 is a ubiquitous lipid reagent that activates platelets. While there is no evidence that TxA_2 acts as a PMN chemoattractant, we treated the apical surfaces of polarized H292 cells with TxA_2 inhibitors and conducted a PMN migration assay to ensure the epoxide hydrolase effect wasn't TxA_2 dependent. No differences were observed between wild-type *S. pneumoniae* infection or those cells treated with TxA_2 inhibitors (Figure 4.1C), therefore we concluded that HXA_3 is most likely the source of lipid PMN chemotactic activity.

4.6 Global MRP2 protein remains static while MRP2 protein localization at the epithelial surface increases

We have reported that total MRP2 protein from cell lysis does not change during infection as measured by western blot (Figure 2.1) and that it is protein enrichment of MRP2 on the plasma membrane that increases in the context of *S. pneumoniae* infection (Figure 2.2). Total cellular content of MRP2 protein in intestinal epithelial cells during *Salmonella* infection, in contrast, seems to increase (13), although this increase occurs absent of transcriptional increase. MRP2 is able to undergo a number of different post-translational modifications, which may increase protein stability and, thereby, increase protein availability. One explanation as to how MRP2 increases on the apical surface absent of new protein synthesis is that during infection MRP2 is directed from a different subcellular location to the plasma membrane. Due to MRP2 identity as an integral membrane protein, it is likely that MRP2 sequestered from the plasma membrane is,

instead, stored in endosomal vesicles and awaits a directed signal to fuse to the plasma membrane, effectively increasing its concentration on the cell surface. Enrichment of this kind can be mediated by a family of Ezrin-Radixin-Moesin (ERM) proteins. ERM proteins are chaperones that assist directed transport of integral membrane proteins contained in endosomal vesicles. Previous reports have identified that both ezrin and radixin assist in directing MRP2 to the apical surface of the plasma membrane in *in vitro* intestinal cells (144). Furthermore, Agbor et al. demonstrated that Ezrin assists MRP2 in apical enrichment during *Salmonella enterica* Typhimurium infection (109). It is our expectation, therefore, that lung epithelial cells selectively increase MRP2 on the apical surface through a coordinated endosomal fusion activity directed by one of the ERM family proteins, most likely Ezrin.

Figure 4.1 A.

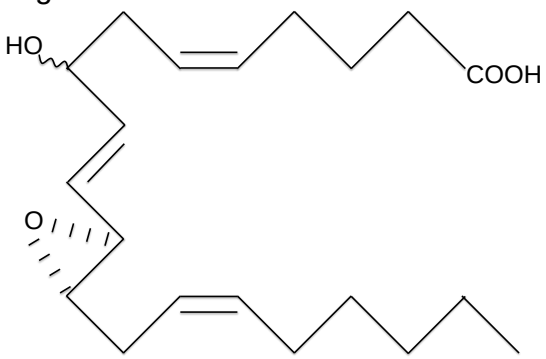

B.

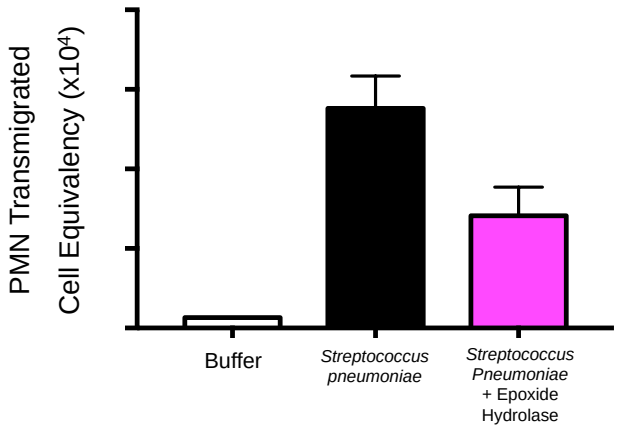

C.

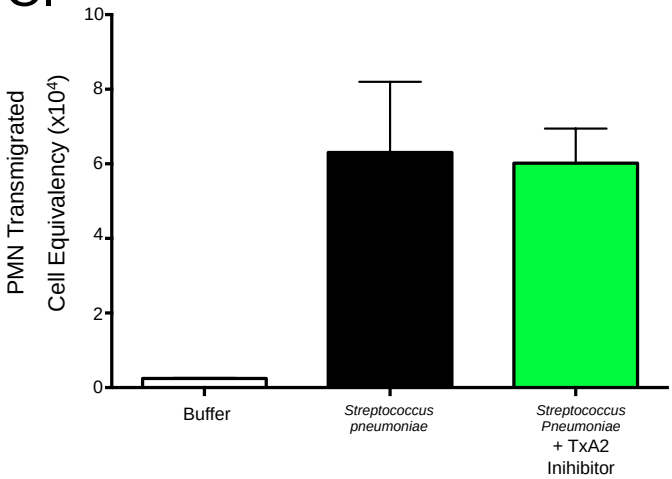

Figure 4.1 Isolating and enriching HXA_3 from infected H292 cells

(A) Structure of Hepoxilin A_3. HXA_3 is the only known lipid that contains an epoxide ring and confers PMN chemoattractant activity. **(B)** Classically, HXA_3 has been identified using LC/MS/MS together with functional assays that induce PMN migration. A functional assay using lipids isolated from *S. pneumoniae* infection, however, identifies the majority of PMN chemoattractant as a proinflammatory lipid with an epoxide ring. **(C)** Although HXA_3 is currently the only lipid chemoattractant that fits that description, there is another epoxide-containing lipid, Thromboxane A_2 that is a candidate although there is no information supposing that TXA_2 acts as a PMN chemoattractant. When we treat our infection milieu with a TXA_2 inhibitor, we see no inhibition, making it all the more likely that the efflux payload of MRP2 during infection is HXA_3.

4.7 Reasoning for Probenecid usage and dosing strategy

In studying MRP2 inhibition during experimental *S. pneumoniae* infection, we settled on a single intratracheal dose of conventional Probenecid pre- and post-infection after optimization indicated that this was the method most efficacious in limiting PMN infiltration. Although MRP2 knockout mice are commercially available, genetic manipulation of the ABC transporters has caused compensatory increases in other transporters (145). In addition, a global knockout of MRP2 in mice could have trans effects from liver or immune function that is avoided by local application of Probenecid.

Although Probenecid could possibly affect other MRPs, it has been shown to have high affinity for MRP2 but not P-gp. It is also possible that higher concentrations of Probenecid inhibit other anionic transport systems, such as MRP5 and MRP4 (29, 81, 92) (5mM for MRP5; 500 μM MRP4, 50mg/kg in vivo), but our *in vitro* concentration of 100 μM is well short of these concentrations. Additionally, *in vivo* application of 1 mg/kg of Probenecid intratracheally is unlikely to inhibit MRP4 or MRP5. MRP1 exhibits a decrease in plasma membrane protein content during infection when we observe an increase in PMN migration, so it is unlikely a further reduction during Probenecid treatment in MRP1 activity would reduce PMN migration.

4.8 Intratracheal application of *S. pneumoniae* is most effective in assaying lung-to-blood transmission and development of bacteremia

Intratracheal application of *S. pneumoniae* ensured that we assessed the possible bacterial lung-to-blood transition that may have been absent during intranasal infection.

Although intratracheal delivery may have caused more physical irritation than intranasal application of the bacteria, there were no discernable differences between Probenecid-treated and PBS-treated uninfected mice, meaning any irritation caused by intratracheal application of the bacteria seemed to be minimal and normalized between the two treatments. When measuring different cytokines and leukocyte infiltrations to the lung, we saw no discernable differences between Probenecid and PBS-treated mice, besides PMN infiltration to the lumen of the lung (Figures 2.5, 2.6, and 2.7).

It seems prudent to emphasize that Probenecid inhibition of MRP2 is not meant to reduce PMNs or PMN activity, per se. The goal of MRP2 inhibition via Probenecid was to reduce the transepithelial migration of PMNs from the basolateral-to-apical surface of the epithelial cells. The expectation was that there would be fewer PMNs infiltrating the lumen but all other signals, such as IL-8, TNF, IL-1β, and other leukocytes would remain consistent between PBS- and Probenecid-treated mice. In addition, the signals governing PMN extravasation and traffic to the basolateral portion of the epithelium remain intact. With the fact that Probenecid is limiting only the physical exit of the PMNs from the basolateral portion of the epithelium, it is remarkable that we observe such a reduction in bacteremia and increase in survival. These observations, however, highlight the importance of PMN infiltration kinetics.

4.9 Purified PLY forms functional pores that successfully supplement ΔPLY mutations

We received the purified pneumolysin, pre-pore lock mutant protein, and perfringolysin from the lab of Dr. Rod Tweten (129). The purification methods have previously been described (128, 140). Briefly, the cytolysins are produced in *E. coli*, isolated, and resuspended in storage buffer to freeze at -80 ℃. We identified that PLY is necessary but not sufficient in Chapter III (Figure 3.1) with use of a pneumolysin-deficient mutant (ΔPLY) and functional complement with the purified pneumolysin. One caveat to this study is whether the protein, purified from *E. coli* and supplemented during infection, forms pores and mimics the wild-type protein. All controls indicated that when supplementing the ΔPLY mutant with amounts of purified PLY equal to those previously measured during wild-type infections (33 ng/mL, Figure 3.2), the PMN phenotype is restored. The pre-pore mutant protein, purified in the same manner and supplemented at the same concentration, did not rescue the PMN migration phenotype, indicating that any component of the sample preparation or buffer was unlikely contributing to the induction of transepithelial PMN migration (Figure 3.3). Data indicating the pre-pore lock protein does not supplement ΔPLY infections also would indicate that the unmutated cytolysins form functional pores able to replicate the wild-type activity.

It has previously been described that PLY can interact with TLR4 (117), and a lesser extent TLR2 (146), to induce immune function. We, therefore, tested different neutralizing antibodies to TLR2 and TLR4 during a PMN transepithelial migration. There were no differences between isotype controls and the specific antibody-treated samples,

leading us to conclude that the HXA_3-dependent PMN transepithelial migration did not require TLR2 or 4 (Figure 4.2). This is not to say that TLR2 or TLR4 are completely dispensable for PMN migration: this particular assay specifically investigates the necessity of TLR2 and 4 in the context of HXA_3. Additionally, there is likely some non-specific activity conferred by PLY, as it was observed that administration of ΔPLY-mutant bacteria together with another of the cholesterol-dependent-cytolysin, perfringolysin O, recapitulated the PMN migration phenotype (Figure 3.12B).

Our initial studies investigating wild-type *S. pneumoniae* infection for one-hour at 10 MOI revealed no increase in apoptosis (Figure 2.12B and 3.1D). We observed, however, that increasing concentrations of purified PLY were effectively inducing apoptosis after one hour of treatment at concentrations of 300 ng/mL and higher. Although some previous studies have reported epithelial apoptosis and cell death (97, 123) during *S. pneumoniae* infection, these studies have infected *in vitro* cells at 200-400 MOI for extended periods of time, up to 16 hours. In addition, Schreiber and colleagues noted that the majority of apoptosis in the lung during *S. pneumoniae* infection actually appeared to be dying macrophages and that the epithelium remained largely viable, albeit injured (142). In context of examining transepithelial PMN migration, it is not entirely understood how epithelial apoptosis might affect the number of traveling leukocytes, which was why we focused on PLY concentrations that did not independently induce apoptosis (Figure 3.1C and D).

4.10 Catalase neutralizes bacterial hydrogen peroxide production

Catalase treatment of *S. pneumoniae*-containing media resulted in neutralization of hydrogen peroxide. Catalase had no effect on epithelial cells prior-to or post-infection, indicating that treatment only affects the transepithelial PMN migration when catalase is mixed with *S. pneumoniae* during infection (Figure 3.5B). Additionally, hydrogen peroxide is required during *S. pneumoniae* induced MRP2 enrichment on the plasma membrane (Figure 3.8B). Catalase had no effect on bacterial growth (Figure 3.4C) and has been shown to have no effect on pneumolysin production (115), thus the effects of catalase should be hydrogen peroxide specific. This indicates that bacterial hydrogen peroxide is a factor that contributes to MRP2-mediated transepithelial PMN migration.

The main virulence factor contributing to hydrogen peroxide production is the *S. pneumoniae* pyruvate oxidase gene *spxB*. *spxB* mutant bacteria are known to be deficient in virulence (123), more sensitive to oxidative stress (121), and produce less pneumolysin that its wild-type counterparts (115). For this reason, we chose to eliminate hydrogen peroxide stress using catalase instead of genetic manipulation. In contrast to *spxB* manipulation of *S. pneumoniae*, catalase treatment does not influence pneumolysin production (115). Additionally, a number of different studies have used catalase to eliminate hydrogen peroxide stress and none have reported off-target side-effects (66, 115, 123, 132, 147, 148).

Figure 4.2

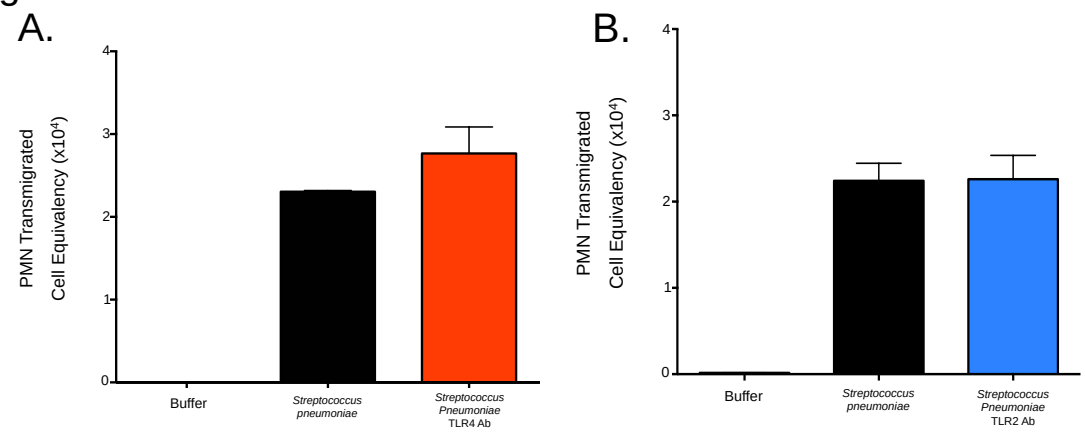

Figure 4.2 Neither TLR2 nor TLR4 blocking antibodies reduce PMN transepithelial migration during *S. pneumoniae* infection

H292 cells were pre-treated with TLR2 and TLR4 neutralizing antibodies and then underwent a PMN transmigration assay. Neither TLR2 nor TLR4 blocking seemed sufficient to reduce PMN migration.

4.11 Live bacteria are needed to induce Transepithelial PMN migration

During infection, *S. pneumoniae* are undergoing active growth processes, meaning production of both the pneumolysin and hydrogen peroxide is dynamic, not static. Original inspection on the necessity of PLY demonstrated that a single, one-time addition of purified PLY allowed for complement of the ΔPLY bacterial infection (Figure 3.1A). Due to the fact that a single, spiked addition of 33 ng/mL of PLY was sufficient to complement the ΔPLY infection, subsequent experiments examining a range of hydrogen peroxide concentration used the single-dose application of 33 ng/mL PLY. PLY mixed with a single-dose of 250μM H_2O_2 (Figure 3.6), time-course increase to 250μM H_2O_2 (Figure 3.6), time-course to increase to 1mM H_2O_2 (Figure 3.6), and time-course increase to 300μM H_2O_2, together with PFA-fixed bacteria (Figure 3.7) all yielded no observable increases in PMN transepithelial migration. It was our conclusion that PLY, hydrogen peroxide, and a third signal from live bacteria were needed to fully induce HXA_3-mediated transepithelial PMN migration.

There remains a second possibility: there may be a need for a combination of PLY, hydrogen peroxide, at least one other soluble factor from live bacteria, and at least one physical interaction between *S. pneumoniae* and host. Presumably if only soluble factors (PLY, hydrogen peroxide, and the aforementioned unidentified soluble factor) were needed, media conditioned with *S. pneumoniae* for one hour would induce PMN migration during treatment with naïve H292 cells during a PMN migration assay (Figure 3.6 D). A similar argument can be made with the mixture of PLY, hydrogen peroxide, and PFA-fixed bacteria: if there were a necessary fourth soluble signal, that would

explain why we observe no PMN migration with the PLY, hydrogen peroxide, and PFA-fixed bacteria.

4.12 Speculating how intracellular calcium increases interact with PLY/hydrogen peroxide-specific induction of PMN migration

While we know eukaryotic intracellular calcium increases during *S. pneumoniae* infection, it remains to be seen how calcium specifically affects the MRP2/HXA_3 axis. We reasoned that calmodulin might influence downstream signaling due to the calcium increases. This did not appear the case, however, as calmodulin inhibition by the drug W-13 had no effect on migration (Figure 4.3). Likewise, we postulated that PLY and hydrogen peroxide might induce calcium-dependent signaling in the unfolded-protein response that occurs in some cellular stress responses. Inhibition of the stress response with salubrinal showed no impact on the ability of epithelial cells to mediate PMN migration (Figure 4.3B), indicating that calcium signaling appears independent of these two processes. There remain other possibilities:

1) Calcium signaling assists in activation of PKC and PLA_2, which is important in HXA_3 formation
2) Calcium and potassium influx influences cell-stress processes
3) Calcium influx specifically from the extra-cellular space induces annexins which, in turn, activate MRP2 fusion and HXA_3 production

The Annexin possibility is particularly intriguing. Annexins are most widely known for their association with apoptosis; however, at earlier stages of cellular insult, Annexins 1,

2, and 6 are helpful inflammatory/cell survival signals (149). Annexin A1 and A2, in fact, have been theorized to assist in cell membrane repair during cholesterol-dependent cytolysin injury, of which PLY is a member. Annexin mediated pore repair is calcium dependent. Our data reflecting that calcium chelation and thapsigargin both interfere with PMN migration (Figures 3.10A and 3.11C) is provocatively reminiscent of observations communicating similar calcium dependency on membrane repair (150) .

There is a model of pore repair theorized in Andrews et al. in which the authors propose endosomal fusion of membrane to cytolysin-pore-damaged plasma membrane and microvesicle shedding as a method of cellular repair (151). While microvesicle shedding likely occurs (152), it still remains unclear whether endosomal fusion occurs. Endosomal fusion pore repair would be a rather favorable explanation for MRP2 increases on the plasma membrane. The process would begin with *S. pneumoniae* induced cell injury through PLY pore formation, calcium increase, and Annexin A2 activation. Annexin A2 would assist in guiding endosomes to the plasma membrane and MRP2-containing vesicles would fuse to the plasma membrane, excising the pore-containing membrane as a microvesicle. MRP2, now on the plasma membrane, would efflux HXA_3 from the apical surface and create the chemotactic gradient to draw PMNs through the epithelium to the site of infection. However, this does not account for the requirement of hydrogen peroxide. Hydrogen peroxide can also increase calcium influx (135) by itself and Annexin A2 is also known to be activated by hydrogen peroxide stress (153). The initiation of arachidonic acid release and MRP2 apical increase may only need to reach a certain threshold of calcium signaling by PLY, hydrogen peroxide, and the

third signal to fully activate the specific AnnexinA2. We will further discuss these possibilities in the Appendix.

4.13 Future focus

The most glaring piece of the *S. pneumoniae* infection puzzle is the missing identity of the third virulence factor necessary to induce PMN migration. Media conditioned with *S. pneumoniae* (that is, that contain PLY, hydrogen peroxide, and additional soluble virulence factors) does not elicit PMN migration (Figure 3.6D). This observation, together with data that a mixture of purified hydrogen peroxide, PLY, and UV-killed bacteria did not induce PMN migration, indicates that the virulence factor(s) might be a surface exposed protein that is only visible to the eukaryotic cell during the bacteria life-cycle. Asmat et al. suggested that engagement of the eukaryotic pIgR via virulence factor Choline-binding Protein A (CbpA, PspC) might induce a similar calcium increase (136) as that which was observed during our calcium assays. During intracellular measurement assays, we observed a reduction in calcium signaling during ΔCbpA infections as compared to wild-type *S. pneumoniae*. ΔCbpA bacteria also produced almost twice as much hydrogen peroxide, with equal numbers of bacteria, creating a situation in which hydrogen peroxide concentrations in the ΔCbpA mutant bacteria might introduce confounding factors if we examined it more in the context of transepithelial PMN migration (Figure 4.4A and B). We cannot discount the possibility that CbpA or another, related, virulence factor might be engaging the pIgR and signaling in a similar manner.

Another common virulence factor that might be influencing the epithelium is the biofilm that forms during bacterial niche development. PLY has been shown to assist in formation (154) of the biofilm. We tested whether reductions in PLY or hydrogen peroxide might disrupt biofilm formation during experimental infection steps. Whether incubating with the PLY-deficient ΔPLY mutant or disrupting hydrogen peroxide with catalase, we saw slightly less biofilm formation as compared to wild-type cells (Figure 4.4C). It remains to be seen, however, how the biofilm might influence calcium influx in the epithelium.

One last theory is that the epithelial cells, themselves have a catalase that neutralizes the hydrogen peroxide production from the bacteria and to combat this, the bacteria have an unidentified virulence factor that neutralizes the catalase. Eukaryotic catalase activity might also explain why in co-cultures with *Haemophilus influenzae*, it is *Streptococcus* and not *Haemophilus* that wins out during bacterial growth. As there is no such identified virulence factor, this is complete conjecture but would explain why viable *S. pneumoniae* are necessary for induction of PMN migration during purified PLY supplement experiments. Without the catalase-inhibitor, PLY may act but hydrogen peroxide that we add exogenously is neutralized and cannot signal, thus curtailing HXA_3/MRP2 signaling.

On the eukaryotic front, we have demonstrated that MRP2 is critical for the robust pulmonary HXA_3-dependent transepithelial PMN migration that occurs during *S. pneumoniae* infection. It has recently been communicated that the pulmonary HXA_3 process also relies on the intracellular activity of PLA_2 (17). It remains to be seen how

PLA_2 activity might modulate MRP2 localization to the plasma membrane of the lung epithelium.

Although it was posed in other areas of this thesis, one particular topic of interest is the identity of the efflux payload(s) mediated by MRP1. We have demonstrated that MRP1 is associated with anti-inflammatory activity (through L-AMEND, Figure 2.11) during basal state, but the components of L-AMEND remain unidentified. PMN activation/inhibition is classically accomplished by extracellular engagement of G-Protein Coupled Receptors (GPCRs). It has recently been reported that P-gp mediates efflux of endocannabinoids in the intestine to reduce and resolve inflammatory events through GPCR signaling, but it remains to be seen whether MRP1 might interact with inflammatory cells in a similar manner (159). Identification of L-AMEND can be completed through combinations of mass spectrometry, analytical chemistry, functional PMN migration assays, and GPCR activity assays.

Figure 4.3

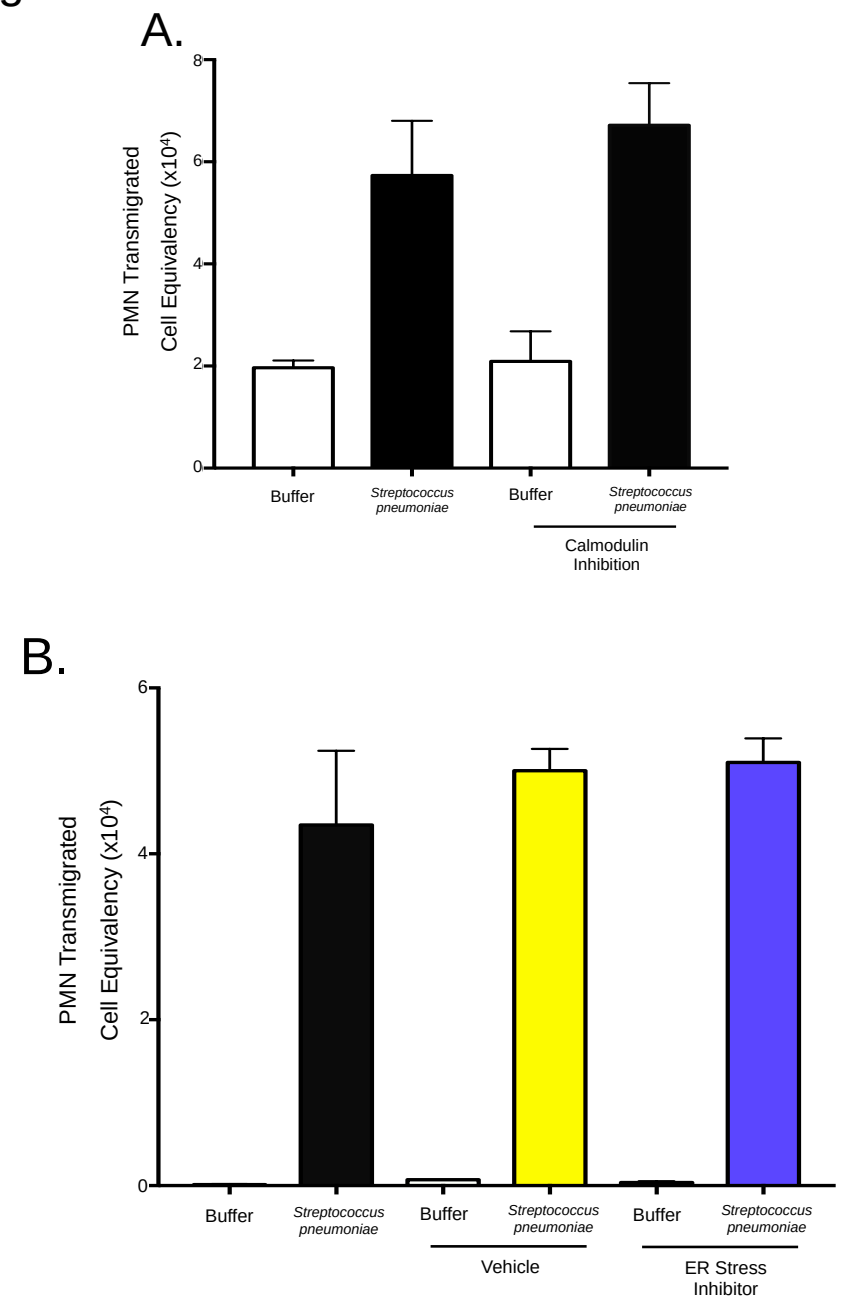
A.
PMN Transmigrated
Cell Equivalency (x10⁴)
8
6
4
2
0
Buffer
Streptococcus pneumoniae
Buffer
Streptococcus pneumoniae
Calmodulin Inhibition
B.
PMN Transmigrated
Cell Equivalency (x10⁴)
6
4
2
0
Buffer
Streptococcus pneumoniae
Buffer
Streptococcus pneumoniae
Buffer
Streptococcus pneumoniae
Vehicle
ER Stress Inhibitor

Figure 4.3 PMN transepithelial migration during *S. pneumoniae* infection does not rely on ER stress signaling or calmodulin

When examining how calcium might be signaling to induce PMN migration, we sought to determine if calmodulin might be necessary. The calmodulin inhibitor W-13 was purchased and cells were treated for one hour pre-infection with W-13 then underwent infection and subsequent PMN migration. Calmodulin inhibition did not result in any reduction in PMN migration. Similarly, we utilized the ER stress inhibitor Salubrinal to inhibit the ER stress unfolded-protein signaling process and performed a PMN migration assay. This treatment did not impact PMN migration either, pointing to other possible calcium signaling being important during infection.

When comparing the epithelial response to bacteria in both the pulmonary and intestinal tract, one area of interest is the conserved nature of the HXA_3/MRP2 axis. Previous reports have demonstrated a convergence in HXA_3 production at PLA_2 release of arachidonic acid, which occurs in both the pulmonary and intestinal tissue (11, 12, 16, 17). At this juncture of HXA_3 synthesis, from arachidonic release to 12/15-Lipoxygenase activity and production of HXA_3, the players are all the same in the pulmonary and intestine epithelium. Upstream, however, there are unique virulence factors that initiate PLA_2. We have identified two possible candidates: hydrogen peroxide and PLY. It is already known PLY is able to activate PLA_2 in endothelial cells (155) but no evidence exists for its induction in epithelial cells. In a more general sense, once a virulence factor is identified, identifying other virulence factors from other bacterial infections and comparing mechanisms of PLA_2 activation would be very informative.

Finally, there is a pertinent question about the convergence of MP2 translocation and 12/15 Lipoxygenase activation. In this study, we consistently observed MRP2 apical enrichment only in conditions where transepithelial PMN migration also occurred. There appears to be an obvious commonality between these two events that almost necessitates further investigation.

Figure 4.4

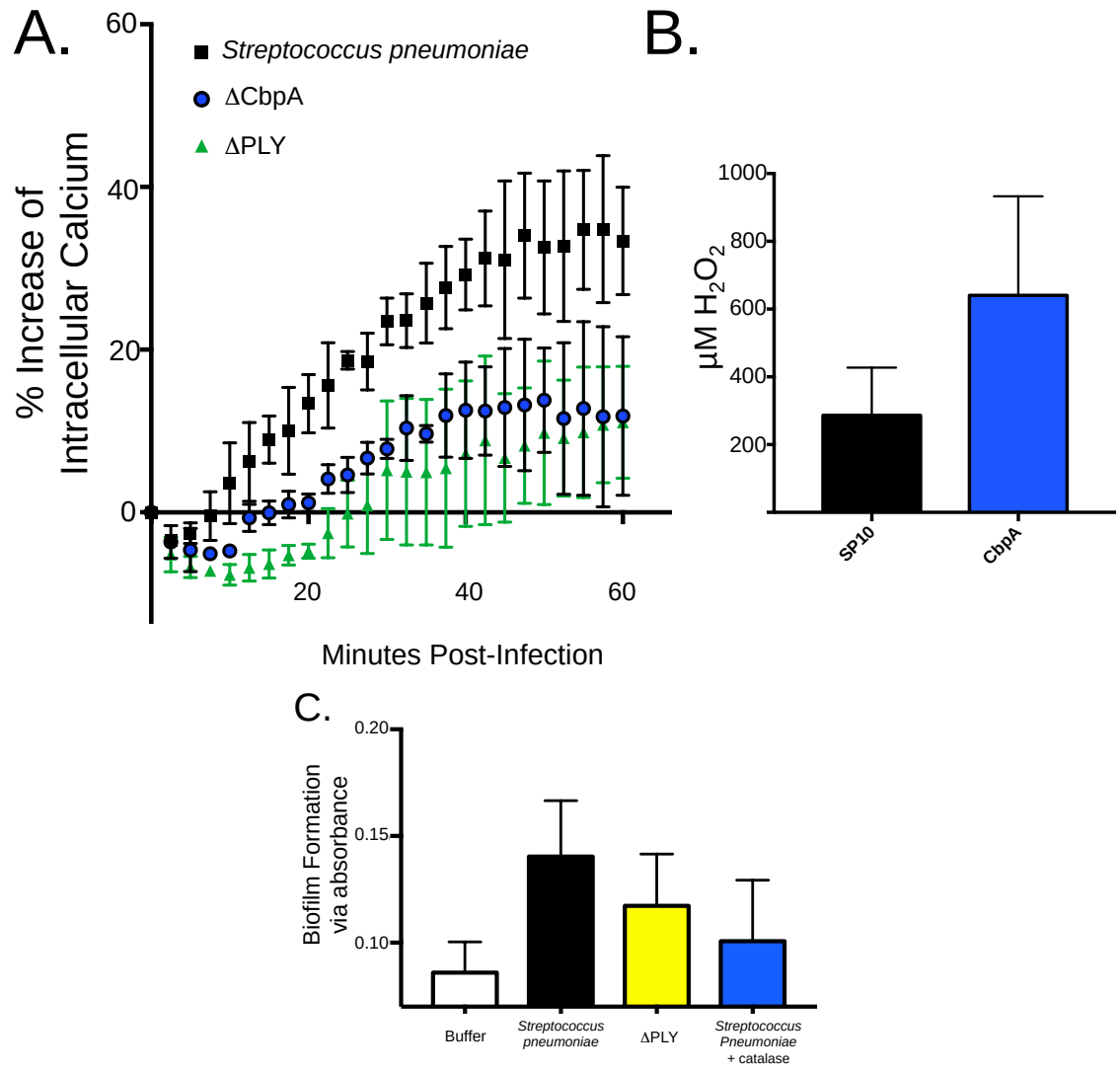
A.
B.
C.
Streptococcus pneumoniae
ΔCbpA
ΔPLY
% Increase of Intracellular Calcium
Minutes Post-Infection
μM H2O2
SP10
CbpA
Biofilm Formation via absorbance
Buffer
Streptococcus pneumoniae
ΔPLY
Streptococcus Pneumoniae + catalase

Figure 4.4 Possible third signals for *S. pneumoniae* PMN migration

Hydrogen peroxide and PLY are insufficient to generate PMN migration by themselves at the concentrations that are associated with our 10 MOI infectious dose. (A) In seeking a third signal from *S. pneumoniae*, we chose to examine the protein CbpA which has been reported to be critical for intracellular calcium build-up through its association with the poly-Ig Receptor (pIgR). While CbpA-deficient mutants were unable to generate wild-type amounts of intracellular calcium during infection, ΔCbpA bacteria also generated almost twice as much hydrogen peroxide as wild-type counter parts, leading to possibly confounding results. (B) Biofilm formation as measured in crystal violet stain after culture with the indicated bacteria. Both catalase and ΔPLY mutants exhibited slightly less biofilm formation as wild-type bacteria, though it was not statistically significant. This points to the possibility that CbpA and biofilm activity might be involved but must be examined in other ways to conclude whether they are critical for PMN migration.

4.14 Concluding remarks

While many questions still exist as to how the pulmonary epithelium fully coordinates PMN infiltration during *S. pneumoniae* infection, this work has clarified some crucial players and processes. At basal state, MRP1 remains high on the epithelial surface and effluxes an anti-inflammatory molecule to reduce the risk of non-specific PMN infiltration. This mirrors activity of the ABC-transporter P-gp in the intestinal tract. *S. pneumoniae*, upon infiltrating the lower respiratory system, comes in contact with the apical surface of the epithelium and initializes a proinflammatory state. *S. pneumoniae* releases PLY, hydrogen peroxide, and at least one additional unidentified but critical virulence factor. These virulence factors work together to activate the $HXA_{3/}$MRP2 axis. Infection and interaction with the aforementioned virulence factors coincides with a reduction of MRP1, allowing for pro-inflammatory processes to begin. Arachidonic acid is released from the plasma membrane by PLA_2 and converted to HXA_3 by 12/15-Lipoxygenase. HXA_3 is transported to the infected apical surface and forms a chemoattractant gradient that draws PMNs from the basolateral surface of the epithelium. HXA_3 production and release occurs in a similar manner during bacterial infection of the intestine, leading to the expectation that HXA_3 efflux is consistent across other mucosal surfaces with a common instigating event, such as plasma membrane disruption or calcium signaling. One other critical step during *S. pneumoniae*-elicited transepithelial PMN migration is that intracellular calcium increases through the combined activity of hydrogen peroxide, pneumolysin, and the unidentified third virulence factor. Intracellular calcium increase sets in motion MRP2 increase on the plasma membrane. MRP2 effluxes

HXA_3 to the apical lumen to draw PMNs from the basolateral to apical surface of the epithelium. In the case of *Streptococcus pneumoniae* infection, there is a tradeoff by allowing PMNs to infiltrate: while PMNs are necessary to control the bacterial infection, they also open paracellular junctions to allow for bacteria to invade the blood stream. By limiting the transepithelial travel of PMNs, we can effectively reduce the incidence of experimental bacteremia, which might have implications for other inflammatory and autoimmune diseases.

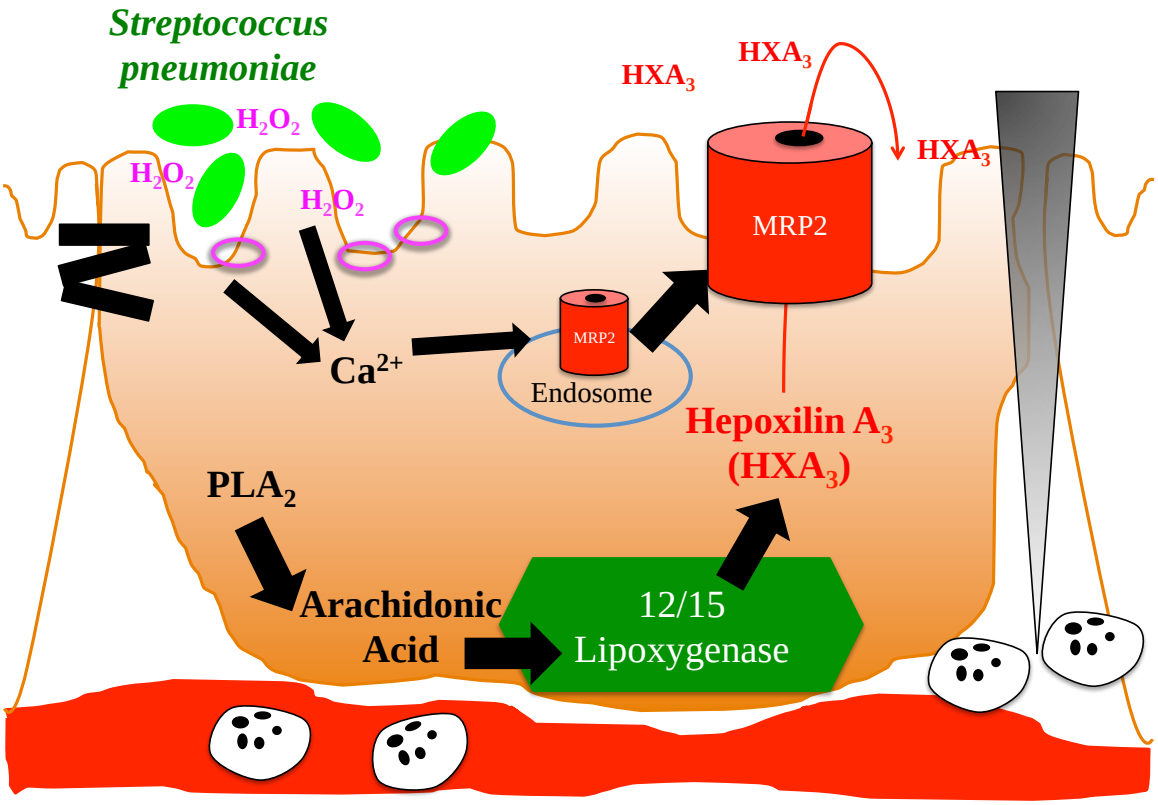

Figure 4.3 Revised model of Pulmonary HXA_3-directed PMN transepithelial migration by MRP2

As detailed by this work, *Streptococcus pneumoniae* infect the lower respiratory system and produce a number of virulence factors including pneumolysin and hydrogen peroxide. During this inflammatory, MRP1 reduces on the apical surface of the epithelium. Intracellular calcium increases in a manner dependent on pneumolysin, hydrogen peroxide, and a third, unidentified, virulence factor. This initializes production of HXA_3 and increase of MRP2 on the apical surface of the plasma membrane, likely through endosomal fusion. MRP2 effluxes the pro-inflammatory HXA_3 to draw PMNs to the site of infection, an action that both promotes clearance of the bacteria but also correlates with development of bacteria during experimental infection.

Appendix A

Possible mechanism by which Annexin A2 modulates MRP2 localization via hydrogen peroxide and pneumolysin

As stated in the future works section of this thesis, Annexin A2 is an interesting molecule to examine during pneumococcal infection of epithelial cells. We observe increases in Annexin A2 in wild-type infections examining whole-cell lysate probed by western blot but not during catalase treatment or pneumolysin-deficient contexts. We also observe a perturbation in the normal localization of Annexin A2 examining immunofluorescence whereas ΔPLY infections and catalase treatments cause infections to reflect an uninfected morphology (Figure A.1). Annexin A2 is currently thought to be important in, among other things, microvesicle shedding and membrane repair (150-152). It is already known that hydrogen peroxide and pneumolysin activate Annexin A2 in some contexts and that Annexin A2 requires calcium increases to function. It remains to be seen, however, how specifically Annexin A2 is involved in HXA_3 production and MRP2 localization.

Our current theory is that hydrogen peroxide, together with pneumolysin, allow for external calcium influx and mobilization of Annexin A2. Separately, $cPLA_2$ is activated by dissociation with a small subunit protein S100A10 (p11) (156). This p11 forms a heterotetramer with 2 p11 monomers and 2 separate Annexin A2 monomers in a calcium dependent manner and mediates microvesicle shedding of plasma membrane damaged by pneumolysin. We also speculate that Annexin A2 might be involved in

plasma membrane fusion of MRP2-containing vesicles, increasing the MRP2 at the site of infection, the apical surface. Annexin A2 is also a protein with links to *Salmonella* infection (157) and pedestal formation during *E. coli* infection (158), making it a tantalizing target to examine as a common thread between intestinal and pulmonary induction of local MRP2 increases.

These current theories take into account hydrogen peroxide and pneumolysin activity but do not explain the necessity of a third virulence factor that assists in inducing PMN transmigration and MRP2 apical enrichment. Annexin signaling is very sensitive to specific local calcium concentrations and might require a certain threshold of calcium to be reached before being activated. Might that calcium threshold be crossed only when the third signal is incorporated with the other two? This theory also doesn't take into account the *Salmonella* virulence factor SipA, for if SipA is able to cause PMN migration by itself, how might it signal through Annexin A2?

Figure A.1

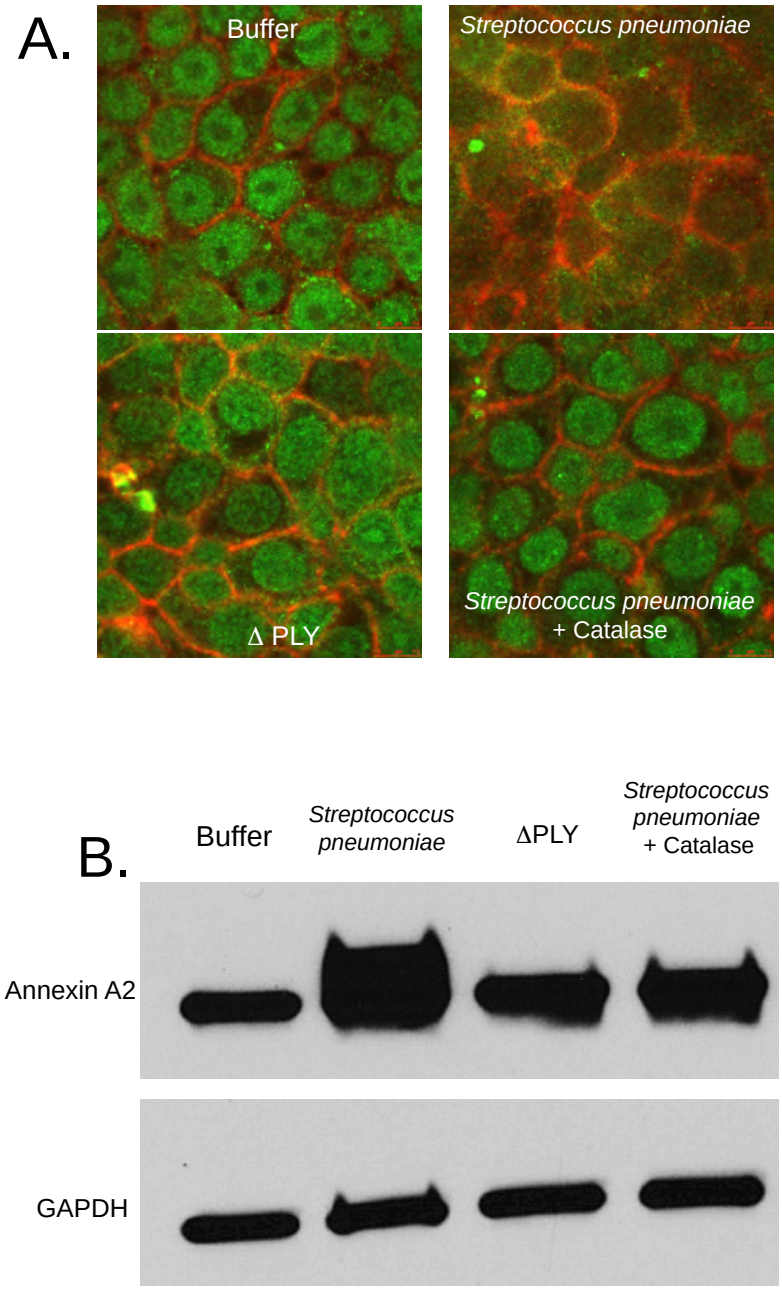
A.
Buffer
Streptococcus pneumoniae
Δ PLY
Streptococcus pneumoniae
+ Catalase
B.
Buffer
Streptococcus pneumoniae
ΔPLY
Streptococcus pneumoniae
+ Catalase
Annexin A2
GAPDH

Figure A.1 Annexin A2 signaling differs between wild-type *S. pneumoniae* and ΔPLY and catalase-treated bacteria

(A) H292 cells were cultured on semipermeable membranes to confluency and treated with either HBSS (Buffer), infected with *S. pneumoniae*, infected with ΔPLY bacteria, or infected with *S. pneumoniae* together with catalase. Annexin A2 immunofluorescence staining appears very clear and throughout the cytoplasm in uninfected cells. Catalase treatment and ΔPLY mutants exhibit similar staining post-infection. Wild-type *S. pneumoniae*, however, exhibits a more diffuse staining which may reflect a progression towards the membrane. (B) Western blot of whole cell lysate probing for Annexin A2. Annexin A2 appears to increase with wild-type bacterial infection whereas the uninfected sample (Buffer), ΔPLY mutant infection, and catalase treatment seem to stay lower.

Additional Materials and Methods

All PMN transepithelial migrations, calcium measurements, immunofluorescence, and western blots performed as described in Chapters II (pages 62-66) and III.

Specific reagents:

Epoxide hydrolase purchased from Cayman Chemical (Cat#10011669). Lipid solution was resuspended and incubated with 100 µg/mL for 1 hour as previously described (108).

Thromboxane A_2 inhibitor (Cox-1 inhibitor) Indomethacin was purchased from Santa Cruz Biotechnology (Cat#sc-200503) and used at 200 nM for 1 hour, washed away, and PMN migration conducted as previously described.

TLR4 (invivogen cat#PAb-hTLR4) and TLR2 (ebioscience cat# TL2.1) blocking antibody were incubated with H292 cells (10 µg/mL) prior to infection and PMN migration conducted as previously described.

Calmodulin inhibitor (Sigma Aldrich SML0717-5MG) was diluted at 300 µM for 1 hour and PMN migration conducted as previously described.

ER Stress inhibitor Salubrinal (Sigma Aldrich Cat#SML0951-5MG) was used to treat H292 cells at 50 µM for one hour and PMN migration conducted as described.

Biofilm assay conducted as follows: Bacteria were cultured to the desired OD, placed in a microtiter 96-well plate and incubated for 1 hour. Post-incubation, bacteria were removed and plates were washed, stained with 1% crystal violet for 30 mins, washed, and solubilized with 30% glacial acetic acid. Absorbance was read at 595nm. Samples were run in triplicate.

Annexin A2 antibody purchased from Abcam (Cat#41803).

References:

1. **Read MA, Whitley MZ, Williams AJ, Collins T.** 1994. NF-kappa B and I kappa B alpha: an inducible regulatory system in endothelial activation. Journal of Experimental Medicine **179:**503-512.

2. **Choi EY, Santoso S, Chavakis T.** 2010. Mechanisms of neutrophil transendothelial migration. Journal of Frontiers in Bioscience **14:**1596–1605.

3. **McCormick BA, Hofman PM, Kim J, Carnes DK, Miller SI, Madara JL.** 1995. Surface Attachment of *Salmonella* Typhimurium to Intestinal Epithelia Imprints the Subepithelial Matrix with Gradients Chemotactic for Neutrophils. The Journal of Cell Biology **131:**1599-1608.

4. **Mrsny RJ, Gewirtz AT, Siccardi D, Savidge T, Hurley BP, Madara JL, McCormick BA.** 2004. Identification of hepoxilin A3 in inflammatory events: A required role in neutrophil migration across intestinal epithelia. PNAS **101:**7421–7426.

5. **Zemans RL, Colgan SP, Downey GP.** 2009. Transepithelial migration of neutrophils: mechanisms and implications for acute lung injury. Am J Respir Cell Mol Biol **40:**519-535.

6. **Korkmaz B, Horwitz MS, Jenne DE, Gauthier F.** 2010. Neutrophil Elastase, Proteinase 3, and Cathepsin G as Therapeutic Targets in Human Diseases. Pharmacological Reviews **62:**726-759.

7. **Pace-Asciak CR, Klein J, Speilberg SP.** 1986. Epoxide hydratase assay in human platelets using hepoxilin A, as a lipid substrate. Biochimica et Biophysica Acta **875:**406-409.

8. **Pace-Asciak CR, Lee W-S.** 1989. Purification of Hepoxilin Epoxide Hydrolase from Rat Liver. The Journal of Biological Chemistry **264:**9310-9313.

9. **Pace-Asciak CR.** 1988. Formation and metabolism of hepoxilin A3 by the rat brain. Biochemical and Biophysical Research Communications **151:**493-498.

10. **McCormick BA, Parkos CA, Colgan SP, Carnes DK, Madara JL.** 1998. Apical Secretion of a Pathogen-Elicited Epithelial Chemoattractant Activity in Response to Surface Colonization of Intestinal Epithelia by *Salmonella* Typhimurium. The Journal of Immunology **160:**455-466.

11. **Mumy KL, Bien JD, Pazos MA, Gronert K, Hurley BP, McCormick BA.** 2008. Distinct isoforms of phospholipase A2 mediate the ability of *Salmonella enterica* serotype Typhimurium and *Shigella flexneri* to induce the transepithelial migration of neutrophils. Infection and Immunity **76:**3614-3627.

12. **Boll EJ, Struve C, Sander A, Demma Z, Krogfelt KA, McCormick BA.** 2012. Enteroaggregative *Escherichia coli* promotes transepithelial migration of neutrophils through a conserved 12-lipoxygenase pathway. Cellular Microbiology **14:**120-132.

13. **Pazos M, Siccardi D, Mumy KL, Bien JD, Louie S, Shi HN, Gronert K, Mrsny RJ, McCormick BA.** 2008. Multidrug Resistance-Associated Transporter 2 Regulates Mucosal Inflammation by Facilitating the Synthesis of Hepoxilin A3. Journal of Immunology **181:**8044-8052.

14. **Wittekindt OH.** 2017. Tight junctions in pulmonary epithelia during lung inflammation. Pflugers Arch **469:**135-147.

15. **Silva M, Song C, Nadeau WJ, Matthews JB, McCormick BA.** 2004. *Salmonella* Typhimurium SipA-induced neutrophil transepithelial migration: involvement of a PKC-alpha-dependent signal transduction pathway. Am J Physiol Gastrointest Liver Physiol **286:**G1024-1031.

16. **Hurley BP, Williams NL, McCormick BA.** 2006. Involvement of phospholipase A2 in *Pseudomonas aeruginosa*-mediated PMN transepithelial migration. Am J Physiol Lung Cell Mol Physiol **290:**L703-L709.

17. **Bhowmick R, Clark S, Bonventre JV, Leong JM, McCormick BA.** 2017. Cytosolic Phospholipase A2 Promotes Pulmonary Inflammation and Systemic Disease during *Streptococcus pneumoniae* Infection. Infection and Immunity **85:**e00280-00217.

18. **Hurley BP, Siccardi D, Mrsny RJ, McCormick BA.** 2004. Polymorphonuclear Cell Transmigration Induced by *Pseudomonas aeruginosa* Requires the Eicosanoid Hepoxilin A 3. Journal of Immunology **173:**5712-5720.

19. **Bhowmick R, Tin Maung NH, Hurley BP, Ghanem EB, Gronert K, McCormick BA, Leong JM.** 2013. Systemic disease during *Streptococcus pneumoniae* acute lung infection requires 12-lipoxygenase-dependent inflammation. Journal of Immunology **191:**5115-5123.

20. **Lee CA, Silva M, Siber AM, Kelly AJ, Galyov E, McCormick BA.** 2000. A secreted *Salmonella* protein induces a proinflammatory response in epithelial cells, which promotes neutrophil migration. PNAS **97:**12283–12288.

21. **Slot AJ, Molinski SV, Cole SP.** 2011. Mammalian multidrug-resistance proteins (MRPs). Essays Biochem **50:**179-207.

22. **Tarling EJ, de Aguiar Vallim TQ, Edwards PA.** 2013. Role of ABC transporters in lipid transport and human disease. Trends Endocrinol Metab **24:**342-350.

23. **Borst P, Evers R, Kool M, Wijnholds J.** 2000. A Family of Drug Transporters: the Multidrug Resistance-Associated Proteins. Journal of the National Cancer Institute **92:**1295-1302.

24. **Bakos E, Hegedu T, Hollo Z, Welker E, Tusnady GE, Zaman GJR, Flens MJ, Varadi A, Sarkadi B.** 1996. Membrane Topology and Glycosylation of the Human Multidrug Resistance-associated Protein. Journal of Biological Chemistry **271:**12322–12326.

25. **Minami S, Ito K, Honma M, Ikebuchi Y, Anzai N, Kanai Y, Nishida T, Tsukita S, Sekine S, Horie T, Suzuki H.** 2009. Posttranslational regulation of Abcc2 expression by SUMOylation system. Am J Physiol Gastrointest Liver Physiol **296:**G406-413.

26. **Stolarczyk EI, Reiling CJ, Paumi CM.** 2011. Regulation of ABC Transporter Function Via Phosphorylation by Protein Kinases. Current Pharmaceutical Biotechnology **12:**621–635.

27. **van der Deen M, de Vries EG, Timens W, Scheper RJ, Timmer-Bosscha H, Postma DS.** 2005. ATP-binding cassette (ABC) transporters in normal and pathological lung. Respiratory Research **6:**59.

28. **Rivera E, Gomez H.** 2010. Chemotherapy resistance in metastatic breast cancer: the evolving role of ixabepilone. Breast Cancer Research **12**.

29. **Wijnholds J, Mol CAAM, Deemter Lv, Haas Md, Scheffer GL, Baas F, Beijnen JH, Scheper RJ, Hatse S, Clercq ED, Balzarini J, Borst P.** 2000. Multidrug-resistance protein 5 is a multispecific organic anion transporter able to transport nucleotide analogs. PNAS **97:**7476–7481.

30. **Wilk JN, Bilsborough J, Viney JL.** 2005. The *mdr1a*–/– Mouse Model of Spontaneous Colitis. Immunologic Research **31:**151–159.

31. **Yacyshy B, Maksymowych W, Bowen-Yacyshyn MB.** 1999. Differences in P-Glycoprotein-170 Expression and Activity Between Crohn's Disease and Ulcerative Colitis. Human Immunology **60:**677–687.

32. **Onnie CM, Fisher SA, Pattni R, Sanderson J, Forbes A, Lewis CM, Mathew CG.** 2006. Associations of Allelic Variants of the Multidrug Resistance Gene (*ABCB1* or *MDR1*) and Inflammatory Bowel Disease and Their Effects on Disease Behavior: A Case-control and Meta-analysis Study. Inflammatory Bowel Diseases **12:**263–271.

33. **Brinar M, Cukovic-Cavka S, Bozina N, Ravic KG, Markos P, Ladic A, Cota M, Krznaric Z, Vucelic B.** 2013. *MDR1* polymorphisms are associated with inflammatory bowel disease in a cohort of Croatian IBD patients. BMC Gastroenterology **13**.

34. **Siccardi D, Mumy KL, Wall DM, Bien JD, McCormick BA.** 2008. *Salmonella enterica* serovar Typhimurium modulates P-glycoprotein in the intestinal epithelium. Am J Physiol Gastrointest Liver Physiol **294:**G1392-1400.

35. **Blokzijl H, van Steenpaal A, Vander Borght S, Bok LI, Libbrecht L, Tamminga M, Geuken M, Roskams TA, Dijkstra G, Moshage H, Jansen PL, Faber KN.** 2008. Up-regulation and cytoprotective role of epithelial multidrug resistance-associated protein 1 in inflammatory bowel disease. Journal of Biological Chemistry **283:**35630-35637.

36. **Hove TT, Drillenburg P, Wijnholds J, Velde AAt, Deventer SJHv.** 2002. Differential Susceptibility of Multidrug Resistance Protein-1 Deficient Mice to DSS and TNBS-Induced Colitis. Digestive Diseases and Sciences **47:**2056–2063.

37. **Ronaldson PT, Ashraf T, Bendayan R.** 2010. Regulation of multidrug resistance protein 1 by tumor necrosis factor alpha in cultured glial cells: involvement of nuclear factor-kappaB and c-Jun N-terminal kinase signaling pathways. Mol Pharmacol **77:**644-659.

38. **Cole SP, Deeley RG.** 2006. Transport of glutathione and glutathione conjugates by MRP1. Trends Pharmacol Sci **27:**438-446.

39. **Silverstein PS, Audus KL, Qureshi N, Kumar A.** 2010. Lipopolysaccharide increases the expression of multidrug resistance-associated protein 1 (MRP1) in RAW 264.7 macrophages. J Neuroimmune Pharmacol **5:**516-520.

40. **van de Ven R, de Jong MC, Reurs AW, Schoonderwoerd AJN, Jansen G, Hooijberg JH, Scheffer GL, de Gruijl TD, Scheper RJ.** 2006. Dendritic Cells Require Multidrug Resistance Protein 1 (ABCC1) Transporter Activity for Differentiation. The Journal of Immunology **176:**5191-5198.

41. **Mottino AD, Hoffman T, Jennes L, Vore M.** 2000. Expression and Localization of Multidrug Resistant Protein mrp2 in Rat Small Intestine. The Journal of Pharmacology and Experimental Therapeutics **293:**717–723.

42. **Hidemura K, Zhao YL, Ito K, Nakao A, Tatsumi Y, Kanazawa H, Takagi K, Ohta M, Hasegawa T.** 2003. Shiga-Like Toxin II Impairs Hepatobiliary Transport of Doxorubicin in Rats by Down-Regulation of Hepatic P Glycoprotein and Multidrug Resistance-Associated Protein Mrp2. Antimicrobial Agents and Chemotherapy **47:**1636-1642.

43. **Elferink MG, Olinga P, Draaisma AL, Merema MT, Faber KN, Slooff MJ, Meijer DK, Groothuis GM.** 2004. LPS-induced downregulation of MRP2 and BSEP in human liver is due to a posttranscriptional process. Am J Physiol Gastrointest Liver Physiol **287:**G1008-1016.

44. **Krishnamurthy P, Schwab M, Takenaka K, Nachagari D, Morgan J, Leslie M, Du W, Boyd K, Cheok M, Nakauchi H, Marzolini C, Kim RB, Poonkuzhali B, Schuetz E, Evans W, Relling M, Schuetz JD.** 2008. Transporter-mediated protection against thiopurine-induced hematopoietic toxicity. Cancer Res **68:**4983-4989.

45. **Jahnel J, Fickert P, Hauer AC, Hogenauer C, Avian A, Trauner M.** 2014. Inflammatory bowel disease alters intestinal bile acid transporter expression. Drug Metab Dispos **42:**1423-1431.

46. **Rius M, Hummel-Eisenbeiss J, Keppler D.** 2008. ATP-dependent transport of leukotrienes B4 and C4 by the multidrug resistance protein ABCC4 (MRP4). J Pharmacol Exp Ther **324:**86-94.

47. **van der Deen M, Marks H, Willemse BW, Postma DS, Muller M, Smit EF, Scheffer GL, Scheper RJ, de Vries EG, Timens W.** 2006. Diminished expression of multidrug resistance-associated protein 1 (MRP1) in bronchial epithelium of COPD patients. Virchows Arch **449:**682-688.

48. **Verbon A, Leemans JC, Weijer S, Forquini S, Poll Tvd.** 2002. Mice lacking the multidrug resistance protein 1 have a transiently impaired immune response during tuberculosis. Clinical Experimental Immunology **130:**32-36.

49. **Schultz MJ, Wijnholds J, Peppelenbosch MP, Vervoordeldonk MJBM, Speelman P, van Deventer SJH, Borst P, van der Poll T.** 2001. Mice Lacking the Multidrug Resistance Protein 1 Are Resistant to *Streptococcus pneumoniae*-Induced Pneumonia. Journal of Immunology **166:**4059-4064.

50. **Rangasamy T, Cho CY, Thimmulappa RK, Zhen L, Srisuma SS, Kensler TW, Yamamoto M, Petrache I, Tuder RM, Biswal S.** 2004. Genetic ablation of *Nrf2* enhances susceptibility to cigarette smoke-induced emphysema in mice. J Clin Invest **114:**1248-1259.

51. **Torky AR, Stehfest E, Viehweger K, Taege C, Foth H.** 2005. Immuno-histochemical detection of MRPs in human lung cells in culture. Toxicology **207:**437-450.

52. **Lin ZP, Zhu YL, Johnson DR, Rice KP, Nottoli T, Hains BC, McGrath J, Waxman SG, Sartorelli AC.** 2008. Disruption of cAMP and prostaglandin E2

transport by multidrug resistance protein 4 deficiency alters cAMP-mediated signaling and nociceptive response. Molecular Pharmacology **73:**243-251.

53. **Schymeinsky J, Mayer H, Tomsic C, Tilp C, Schuetz JD, Cui Y, Wollin L, Gantner F, Erb KJ.** 2013. The absence of mrp4 has no effect on the recruitment of neutrophils and eosinophils into the lung after LPS, cigarette smoke or allergen challenge. PLoS One **8:**e61193.

54. **Yother J.** 2011. Capsules of *Streptococcus pneumoniae* and other bacteria: paradigms for polysaccharide biosynthesis and regulation. Annu Rev Microbiol **65:**563-581.

55. **Gierke R, McGee L, Beall B, Pilishivili T.** 2017. Manual for the surveillance of vaccine-preventable diseases. Centers for Disease Control and Prevention, Centers for Disease Control and Prevention, Atlanta, GA.

56. **Hamborsky J, Kroger A, Wolfe CS.** 2015. Epidemiology and Prevention of Vaccine-Preventable Diseases. Centers for Disease Control and Prevention, Washington D.C. Public Health Foundation, Washington D.C.

57. **Kadioglu A, Weiser JN, Paton JC, Andrew PW.** 2008. The role of *Streptococcus pneumoniae* virulence factors in host respiratory colonization and disease. Nat Rev Microbiol **6:**288-301.

58. **Mook-Kanamori BB, Geldhoff M, van der Poll T, van de Beek D.** 2011. Pathogenesis and pathophysiology of pneumococcal meningitis. Clin Microbiol Rev **24:**557-591.

59. **Cundell DR, Gerard NP, Gerard C, Idanpaan-Helkkila I, Tuomanen EI.** 1995. *Streptococcus pneumoniae* anchorto activated human cells by the receptor for platelet-activating factor. Nature **377:**435-438.

60. **Rosenow C, Ryan P, Weiser JN, Johnson S, Fontan P, Ortqvist A, Masure HR.** 1997. Contribution of novel choline-binding proteins to adherence, colonization and immunogenicity of *Streptococcus pneumoniae*. Molecular Microbiology **25:**819-829.

61. **Brock SC, McGraw PA, Wright PF, Crowe JE.** 2002. The Human Polymeric Immunoglobulin Receptor Facilitates Invasion of Epithelial Cells by *Streptococcus pneumoniae* in a Strain-Specific and Cell Type-Specific Manner. Infection and Immunity **70:**5091-5095.

62. **Jedrzejas MJ, Mello LV, de Groot BL, Li S.** 2002. Mechanism of hyaluronan degradation by *Streptococcus pneumoniae* hyaluronate lyase. Structures of complexes with the substrate. J Biol Chem **277:**28287-28297.

63. **Holmes AR, McNab R, Millsap KW, Rohde M, Hammerschmidt S, Mawdsley JL, Jenkinson HF.** 2001. The pavA gene of *Streptococcus*

pneumoniae encodes a fibronectin-binding protein that is essential for virulence. Molecular Microbiology **41:**1395-1408.

64. **Bergmann S, Rohde M, Chhatwal GS, Hammerschmidt S.** 2001. α-Enolase of *Streptococcus pneumoniae* is a plasminogen-binding protein displayed on the bacterial cell surface. Molecular Microbiology **40:**1273-1287.

65. **Lux T, Nuhn M, Hakenbeck R, Reichmann P.** 2007. Diversity of bacteriocins and activity spectrum in *Streptococcus pneumoniae*. J Bacteriol **189:**7741-7751.

66. **Pericone CD, Overweg K, Hermans PWM, Weiser JN.** 2000. Inhibitory and Bactericidal Effects of Hydrogen Peroxide Production by *Streptococcus pneumoniae* on Other Inhabitants of the Upper Respiratory Tract. Infection and Immunity **68:**3990-3997.

67. **Balachandran P, Hollingshead SK, Paton JC, Briles DE.** 2001. The autolytic enzyme LytA of *Streptococcus pneumoniae* is not responsible for releasing pneumolysin. J Bacteriol **183:**3108-3116.

68. **Hyams C, Camberlein E, Cohen JM, Bax K, Brown JS.** 2010. The *Streptococcus pneumoniae* capsule inhibits complement activity and neutrophil phagocytosis by multiple mechanisms. Infect Immun **78:**704-715.

69. **Standish AJ, Weiser JN.** 2009. Human neutrophils kill *Streptococcus pneumoniae* via serine proteases. J Immunol **183:**2602-2609.

70. **van der Windt D, Bootsma HJ, Burghout P, van der Gaast-de Jongh CE, Hermans PW, van der Flier M.** 2012. Nonencapsulated *Streptococcus pneumoniae* resists extracellular human neutrophil elastase- and cathepsin G-mediated killing. FEMS Immunol Med Microbiol **66:**445-448.

71. **Beiter K, Wartha F, Albiger B, Normark S, Zychlinsky A, Henriques-Normark B.** 2006. An endonuclease allows *Streptococcus pneumoniae* to escape from neutrophil extracellular traps. Curr Biol **16:**401-407.

72. **Marks M, Burns T, Abadi M, Seyoum B, Thornton J, Tuomanen E, Pirofski LA.** 2007. Influence of neutropenia on the course of serotype 8 pneumococcal pneumonia in mice. Infection and Immunity **75:**1586-1597.

73. **Bou Ghanem EN, Clark S, Roggensack SE, McIver SR, Alcaide P, Haydon PG, Leong JM.** 2015. Extracellular Adenosine Protects against *Streptococcus pneumoniae* Lung Infection by Regulating Pulmonary Neutrophil Recruitment. PLoS Pathog **11:**e1005126.

74. **Pilishvili T, Noggle B, Moore MR.** 2012. Manual for the Surveillance of Vaccine-Preventable Diseases. Centers for Disease Control and Prevention, Washinton D.C.

75. **Baird BR, Cheronis JC, Sandhaus RA, Berger EM, White CW, Repine JE.** 1986. O2 metabolites and neutrophil elastase synergistically cause edematous injury in isolated rat lungs. Journal of Applied Physiology **61:**2224-2229.

76. **Flick MR, Perel A, Staub NC.** 1981. Leukocytes are Required for Increased Lung Microvascular Permeability after Microembolization in Sheep. Circulation Research **48:**344-351.

77. **Menendez R, Cavalcanti M, Reyes S, Mensa J, Martinez R, Marcos MA, Filella X, Niederman M, Torres A.** 2008. Markers of treatment failure in hospitalised community acquired pneumonia. Thorax **63:**447-452.

78. **Clarke TB, Francella N, Huegel A, Weiser JN.** 2011. Invasive bacterial pathogens exploit TLR-mediated downregulation of tight junction components to facilitate translocation across the epithelium. Cell Host and Microbe **9:**404-414.

79. **Attali C, Durmort C, Vernet T, Di Guilmi AM.** 2008. The interaction of *Streptococcus pneumoniae* with plasmin mediates transmigration across endothelial and epithelial monolayers by intercellular junction cleavage. Infection and Immunity **76:**5350-5356.

80. **McCormick BA.** 2007. Bacterial-induced hepoxilin A3 secretion as a pro-inflammatory mediator. FEBS J **274:**3513-3518.

81. **Furugen A, Yamaguchi H, Tanaka N, Shiida N, Ogura J, Kobayashi M, Iseki K.** 2013. Contribution of multidrug resistance-associated proteins (MRPs) to the release of prostanoids from A549 cells. Prostaglandins Other Lipid Mediators **106:**37-44.

82. **Englund G, Jacobson A, Rorsman F, Artursson P, Kindmark A, Ronnblom A.** 2007. Efflux transporters in ulcerative colitis: decreased expression of BCRP (ABCG2) and Pgp (ABCB1). Inflammatory Bowel Diseases **13:**291-297.

83. **Panwala CM, Jones JC, Viney JL.** 1998. A Novel Model of Inflammatory Bowel Disease: Mice Deficient for the Multiple Drug Resistance Gene, *mdr1a*, Spontaneously Develop Colitis. Journal of Immunology **161:**5733-5744.

84. **van Schilfgaarde M, van Alphen L, Eijk P, Everts V, Dankert J.** 1995. Paracytosis of *Haemophilus influenzae* through Cell Layers of NCI-H292 Lung Epithelial Cells. Infection and Immunity **63:**4729–4737.

85. **Galka F, Wai SN, Kusch H, Engelmann S, Hecker M, Schmeck B, Hippenstiel S, Uhlin BE, Steinert M.** 2008. Proteomic characterization of the whole secretome of *Legionella pneumophila* and functional analysis of outer membrane vesicles. Infection and Immunolgy **76:**1825-1836.

86. **Clark RT, Hope A, Lopez-Fraga M, Schiller N, Lo DD.** 2009. Bacterial particle endocytosis by epithelial cells is selective and enhanced by tumor necrosis factor receptor ligands. Clinical and Vaccine Immunology **16:**397-407.

87. **Westlake CJ, Cole SPC, Deeley RG.** 2005. Role of the NH2-terminal Membrane Spanning Domain of Multidrug Resistance Protein 1/ABCC1 in Protein Processing and Trafficking. Molecular Biology of the Cell **16:**2483–2492.

88. **Akao T, Hanada M, Sakashita Y, Sato K, Morita M, Imanaka T.** 2007. Efflux of baicalin, a flavone glucuronide of Scutellariae Radix, on Caco-2 cells through multidrug resistance-associated protein 2. J Pharm Pharmacol **59:**87-93.

89. **Horikawa M, Kato Y, Tyson CA, Sugiyama Y.** 2002. The Potential for an Interaction between MRP2 (ABCC2) and Various Therapeutic Agents: Probenecid as a Candidate Inhibitor of the Biliary Excretion of Irinotecan Matabolites. Drug Metabolism and Pharmacokinetics **17:**23-33.

90. **Potschka H, Fedrowitz M, Loscher W.** 2003. Multidrug resistance protein MRP2 contributes to blood-brain barrier function and restricts antiepileptic drug activity. J Pharmacol Exp Ther **306:**124-131.

91. **U.S. Department of Health and Human Services.** 1991. Toxicology and Carcinogenesis Studies of Probenecid in F344/N rats and B6C3F1 mice. U.S. Department of Health and Human Services, National Toxicology Program P.O. Box 12233 Research Triangle Park, NC 27709.

92. **Copsel S, Bruzzone A, May M, Beyrath J, Wargon V, Cany J, Russel FGM, Shayo C, Davio C.** 2014. Multidrug resistance protein 4/ ATP binding cassette transporter 4: a new potential therapeutic target for acute myeloid leukemia. Oncotarget **5:**9308-9321.

93. **Tollner K, Brandt C, Romermann K, Loscher W.** 2015. The organic anion transport inhibitor probenecid increases brain concentrations of the NKCC1 inhibitor bumetanide. Eur J Pharmacol **746:**167-173.

94. **Hollo Z, Homolya L, Hegedus T, Sarkadi B.** 1996. Transport properties of the multidrug resistance-associated protein (MRP) in human tumour cells. FEBS**:**99-104.

95. **Laneuville O, Reynaud D, Nigam S, Pace-Asciak CR.** 1993. Hepoxilin A3 inhibits the rise in free intracellular calcium evoked by formyl- methionyl-leucyl-phenylalanine, platelet-activating factor and leukotriene B4. Biochemical Journal **295:**393-397.

96. **Andrews PC, Babior BM.** 1983. Endogenous Protein Phosphorylation by Resting and Activated Human Neutrophils. Blood **61:**333-340.

97. **Schmeck B, Gross R, N'Guessan PD, Hocke AC, Hammerschmidt S, Mitchell TJ, Rosseau S, Suttorp N, Hippenstiel S.** 2004. *Streptococcus pneumoniae*-induced caspase 6-dependent apoptosis in lung epithelium. Infect Immun **72:**4940-4947.

98. **Chiavolini D, Pozzi G, Ricci S.** 2008. Animal models of *Streptococcus pneumoniae* disease. Clinical Microbiology Reviews **21:**666-685.

99. **Penaloza HF, Nieto PA, Munoz-Durango N, Salazar-Echegarai FJ, Torres J, Parga MJ, Alvarez-Lobos M, Riedel CA, Kalergis AM, Bueno SM.** 2015.

Interleukin-10 plays a key role in the modulation of neutrophils recruitment and lung inflammation during infection by *Streptococcus pneumoniae*. Immunology **146:**100-112.

100. **Knapp S, Wieland CW, van 't Veer C, Takeuchi O, Akira S, Florquin S, van der Poll T.** 2004. Toll-Like Receptor 2 Plays a Role in the Early Inflammatory Response to Murine Pneumococcal Pneumonia but Does Not Contribute to Antibacterial Defense. The Journal of Immunology **172:**3132-3138.

101. **Branger J, Knapp S, Weijer S, Leemans JC, Pater JM, Speelman P, Florquin S, van der Poll T.** 2004. Role of Toll-Like Receptor 4 in Gram-Positive and Gram-Negative Pneumonia in Mice. Infection and Immunity **72:**788-794.

102. **Mizgerd JP, Meek BB, Kutkoski GJ, Bullard DC, Beaudet AU, Doerschuk CM.** 1996. Selectins and Neutrophil Traffic: Margination and *Streptococcus Pneumoniae*-induced Emigration in Murine Lungs. Journal of Experimental Medicine **184:**639–645.

103. **Tasaka S, Richer SE, Mizgerd JP, Doerschuk CM.** 2002. Very late antigen-4 in CD18-independent neutrophil emigration during acute bacterial pneumonia in mice. American Journal of Respiratory and Critical Care Medicine **166:**53-60.

104. **Doyle NA, Bhagwan SD, Meek BB, Kutkoski GJ, Steeber DA, Tedder TF, Doerschuk CM.** 1997. Neutrophil margination, sequestration, and emigration in

the lungs of L-selectin-deficient mice. Journal of Clinical Investigation **99:**526-533.

105. **Tasaka S, Qin L, Saijo A, Albelda SM, DeLisser HM, Doerschuk CM.** 2003. Platelet endothelial cell adhesion molecule-1 in neutrophil emigration during acute bacterial pneumonia in mice and rats. American Journal of Respiratory and Critical Care Medicine **167:**164-170.

106. **Mizgerd JP, Horwitz BH, Quillen HC, Scott ML, Doerschuk CM.** 1999. Effects of CD18 Deficiency on the Emigration of Murine Neutrophils During Pneumonia. Journal of Immunology **163:**995-999.

107. **Mizgerd JP, Quinlan WM, LeBlanc BW, Kutkoski GJ, Bullard DC, Beaudet AL, Doerschuk CM.** 1998. Combinatorial requirements for adhesion molecules in mediating neutrophil emigration during bacterial peritonitis in mice. Journal of Leukocyte Biology **64:**291–297.

108. **Pazos MA, Pirzai W, Yonker LM, Morisseau C, Gronert K, Hurley BP.** 2015. Distinct cellular sources of hepoxilin A3 and leukotriene B4 are used to coordinate bacterial-induced neutrophil transepithelial migration. J Immunol **194:**1304-1315.

109. **Agbor TA, Demma ZC, Mumy KL, Bien JD, McCormick BA.** 2011. The ERM protein, ezrin, regulates neutrophil transmigration by modulating the apical

localization of MRP2 in response to the SipA effector protein during *Salmonella* Typhimurium infection. Cellular Microbiology **13:**2007-2021.

110. **Strohmeier GR, Lencer WI, Patapoff TW, Thompson LF, Carlson SL, Moe SJ, Carnes DK, Mrsny RJ, Madara JL.** 1997. Surface expression, polarization, and functional significance of CD73 in human intestinal epithelia. Journal of Clinical Investigation **99:**2588-2601.

111. **Han H, Headley MB, Xu W, Comeau MR, Zhou B, Ziegler SF.** 2013. Thymic stromal lymphopoietin amplifies the differentiation of alternatively activated macrophages. J Immunol **190:**904-912.

112. **Kaper JB, Nataro JP, Mobley HL.** 2004. Pathogenic *Escherichia coli*. Nat Rev Microbiol **2:**123-140.

113. **Hallstrom KN, Srikanth CV, Agbor TA, Dumont CM, Peters KN, Paraoan L, Casanova JE, Boll EJ, McCormick BA.** 2015. PERP, a host tetraspanning membrane protein, is required for *Salmonella*-induced inflammation. Cell Microbiol **17:**843-859.

114. **Srikanth CV, Wall DM, Maldonado-Contreras A, Shi H, Zhou D, Demma Z, Mumy KL, McCormick BA.** 2010. *Salmonella* pathogenesis and processing of secreted effectors by caspase-3. Science **330:**390-393.

115. **Bryant JC, Dabbs RC, Oswalt KL, Brown LR, Rosch JW, Seo KS, Donaldson JR, McDaniel LS, Thornton JA.** 2016. Pyruvate oxidase of

Streptococcus pneumoniae contributes to pneumolysin release. BMC Microbiol **16:**271.

116. **Tilley SJ, Orlova EV, Gilbert RJ, Andrew PW, Saibil HR.** 2005. Structural basis of pore formation by the bacterial toxin pneumolysin. Cell **121:**247-256.

117. **Malley R, Henneke P, Morse SC, Cieslewicz MJ, Lipsitch M, Thompson CM, Kurt-Jones E, Paton JC, Wessels MR, Golenbock DT.** 2003. Recognition of pneumolysin by Toll-like receptor 4 confers resistance to pneumococcal infection. PNAS **100:**6.

118. **McCormick BA, Hofman PM, Kim J, Carnes DK, Miller SI, Madara JL.** 1993. *Salmonella* Typhimurium attachment to human intestinal epithelial monolayers: transcellular signalling to subepithelial neutrophils. The Journal of Cell Biology **123:**895-907.

119. **Hirst RA, Kadioglu A, O'Callaghan C, Andrew PW.** 2004. The role of pneumolysin in pneumococcal pneumonia and meningitis. Clin Exp Immunol **138:**195-201.

120. **JB R, D C, JC P, TJ M, PW A, EN J.** 1995. Dual function of pneumolysin in the early pathogenesis of murine pneumococcal pneumonia. Journal of Clinical Investigation. Journal of Clinical Investigation **95(**142-150.

121. **Pericone CD, Park S, Imlay JA, Weiser JN.** 2003. Factors Contributing to Hydrogen Peroxide Resistance in *Streptococcus pneumoniae* Include Pyruvate

Oxidase (SpxB) and Avoidance of the Toxic Effects of the Fenton Reaction. Journal of Bacteriology **185:**6815-6825.

122. **Potter AJ, Trappetti C, Paton JC.** 2012. *Streptococcus pneumoniae* uses glutathione to defend against oxidative stress and metal ion toxicity. J Bacteriol **194:**6248-6254.

123. **Rai P, Parrish M, Tay IJ, Li N, Ackerman S, He F, Kwang J, Chow VT, Engelward BP.** 2015. *Streptococcus pneumoniae* secretes hydrogen peroxide leading to DNA damage and apoptosis in lung cells. Proc Natl Acad Sci U S A **112:**E3421-3430.

124. **Garcia-Suarez Mdel M, Florez N, Astudillo A, Vazquez F, Villaverde R, Fabrizio K, Pirofski LA, Mendez FJ.** 2007. The role of pneumolysin in mediating lung damage in a lethal pneumococcal pneumonia murine model. Respir Res **8:**3.

125. **Moreland JG, Bailey G.** 2006. Neutrophil transendothelial migration in vitro to *Streptococcus pneumoniae* is pneumolysin dependent. Am J Physiol Lung Cell Mol Physiol **290:**L833-840.

126. **Maus UA, Srivastava M, Paton JC, Mack M, Everhart MB, Blackwell TS, Christman JW, Schlondorff D, Seeger W, Lohmeyer J.** 2004. Pneumolysin-Induced Lung Injury Is Independent of Leukocyte Trafficking into the Alveolar Space. The Journal of Immunology **173:**1307-1312.

127. **Travassos LH, Girardin SE, Philpott DJ, Blanot D, Nahori MA, Werts C, Boneca IG.** 2004. Toll-like receptor 2-dependent bacterial sensing does not occur via peptidoglycan recognition. EMBO Rep **5:**1000-1006.

128. **Soltani CE, Hotze EM, Johnson AE, Tweten RK.** 2007. Specific protein-membrane contacts are required for prepore and pore assembly by a cholesterol-dependent cytolysin. J Biol Chem **282:**15709-15716.

129. **Lawrence SL, Feil SC, Morton CJ, Farrand AJ, Mulhern TD, Gorman MA, Wade KR, Tweten RK, Parker MW.** 2015. Crystal structure of *Streptococcus pneumoniae* pneumolysin provides key insights into early steps of pore formation. Sci Rep **5:**14352.

130. **Lisher JP, Tsui H-CT, Ramos-Montañez S, Hentchel KL, Martin JE, Trinidad JC, Winkler ME, Giedroca DP.** 2017. Biological and Chemical Adaptation to Endogenous Hydrogen Peroxide Production in *Streptococcus pneumoniae* D39. mSphere **2:**e00291-00216.

131. **Braun JS, Sublett JE, Freyer D, Mitchell TJ, Cleveland JL, Tuomanen EI, Weber JR.** 2002. Pneumococcal pneumolysin and H2O2 mediate brain cell apoptosis during meningitis. Journal of Clinical Investigation **109:**19-27.

132. **Feldman C, Anderson R, Cockeran R, Mitchell T, Cole P, Wilson R.** 2002. The effects of pneumolysin and hydrogen peroxide, alone and in combination, on human ciliated epithelium in vitro. Respiratory Medicine **96:**580-585.

133. **Seki M, Iida Ki, Saito M, Nakayama H, Yoshida Si.** 2004. Hydrogen Peroxide Production in *Streptococcus pyogenes*: Involvement of Lactate Oxidase and Coupling with Aerobic Utilization of Lactate. Journal of Bacteriology **186:**2046-2051.

134. **Yesilkaya H, Andisi VF, Andrew PW, Bijlsma JJ.** 2013. *Streptococcus pneumoniae* and reactive oxygen species: an unusual approach to living with radicals. Trends Microbiol **21:**187-195.

135. **Castro J, Bittner C, Humeres A, Montecinos V, Vera J, Barros L.** 2004. A cytosolic source of calcium unveiled by hydrogen peroxide with relevance for epithelial cell death. Cell Death and Differentiation **11:**468–478.

136. **Asmat TM, Agarwal V, Rath S, Hildebrandt JP, Hammerschmidt S.** 2011. *Streptococcus pneumoniae* infection of host epithelial cells via polymeric immunoglobulin receptor transiently induces calcium release from intracellular stores. J Biol Chem **286:**17861-17869.

137. **Marie-ClaudeTrombe.** 1999. Calcium Signaling in *Streptococcus pneumoniae*: Implication of the Kinetics of Calcium Transport. Microbial Drug Resistance **5:**247-252.

138. **Faria RX, Reis RAM, Casabulho CM, Alberto AVP, de Farias FP, Henriques-Pons A, Alves LA.** 2009. Pharmacological properties of a pore

induced by raising intracellular Ca^{2+}. American Journal of Physiology-Cell Physiology **297:**C28-C42.

139. **Tweten RK.** 1988. Nucleotide Sequence of the Gene for Perfringolysin 0 (Theta-Toxin) from *Clostridium perfringens*: Significant Homology with the Genes for Streptolysin 0 and Pneumolysin. Infection and Immunity **56:**3235-3240.

140. **Hotze EM, Le HM, Sieber JR, Bruxvoort C, McInerney MJ, Tweten RK.** 2013. Identification and characterization of the first cholesterol-dependent cytolysins from Gram-negative bacteria. Infect Immun **81:**216-225.

141. **Sunil K, Narayana B.** 2008. Spectrophotometric determination of hydrogen peroxide in water and cream samples. Bull Environ Contam Toxicol **81:**422-426.

142. **Schreiber T, Swanson PE, Chang KC, Davis CC, Dunne WM, Karl IE, Reinhart K, Hotchkiss RS.** 2006. Both Gram-negative and Gram-positive experimental pneumonia induce profound lymphocyte but not respiratory epithelial cell apoptosis. Shock **26:**271-276.

143. **Mercado-Lubo R, Zhang Y, Zhao L, Rossi K, Wu X, Zou Y, Castillo A, Leonard J, Bortell R, Greiner DL, Shultz LD, Han G, McCormick BA.** 2016. A *Salmonella* nanoparticle mimic overcomes multidrug resistance in tumours. Nat Commun **7:**12225.

144. **Yang Q, Onuki R, Nakai C, Sugiyama Y.** 2007. Ezrin and radixin both regulate the apical membrane localization of ABCC2 (MRP2) in human intestinal epithelial Caco-2 cells. Exp Cell Res **313:**3517-3525.

145. **Chu XY, Strauss JR, Mariano MA, Li J, Newton DJ, Cai X, Wang RW, Yabut J, Hartley DP, Evans DC, Evers R.** 2006. Characterization of mice lacking the multidrug resistance protein MRP2 (ABCC2). J Pharmacol Exp Ther **317:**579-589.

146. **Dessing MC, Hirst RA, de Vos AF, van der Poll T.** 2009. Role of Toll-like receptors 2 and 4 in pulmonary inflammation and injury induced by pneumolysin in mice. PLoS One **4:**e7993.

147. **Loose M, Hudel M, Zimmer KP, Garcia E, Hammerschmidt S, Lucas R, Chakraborty T, Pillich H.** 2015. Pneumococcal hydrogen peroxide-induced stress signaling regulates inflammatory genes. J Infect Dis **211:**306-316.

148. **Battig P, Muhlemann K.** 2008. Influence of the *spxB* gene on competence in *Streptococcus pneumoniae*. J Bacteriol **190:**1184-1189.

149. **Babiychuk EB, Draeger A.** 2015. Defying death: Cellular survival strategies following plasmalemmal injury by bacterial toxins. Semin Cell Dev Biol **45:**39-47.

150. **Wolfmeier H, Schoenauer R, Atanassoff AP, Neill DR, Kadioglu A, Draeger A, Babiychuk EB.** 2015. Ca^{2+}-dependent repair of pneumolysin pores: A new

paradigm for host cellular defense against bacterial pore-forming toxins. Biochim Biophys Acta **1853:**2045-2054.

151. **Andrews NW, Almeida PE, Corrotte M.** 2014. Damage control: cellular mechanisms of plasma membrane repair. Trends Cell Biol **24:**734-742.

152. **Wolfmeier H, Radecke J, Schoenauer R, Koeffel R, Babiychuk VS, Drucker P, Hathaway LJ, Mitchell TJ, Zuber B, Draeger A, Babiychuk EB.** 2016. Active release of pneumolysin prepores and pores by mammalian cells undergoing a *Streptococcus pneumoniae* attack. Biochim Biophys Acta **1860:**2498-2509.

153. **Grindheim AK, Hollas H, Raddum AM, Saraste J, Vedeler A.** 2016. Reactive oxygen species exert opposite effects on Tyr23 phosphorylation of the nuclear and cortical pools of annexin A2. J Cell Sci **129:**314-328.

154. **Shak JR, Ludewick HP, Howery KE, Sakai F, Yi H, Harvey RM, Paton JC, Klugman KP, Vidal JE.** 2013. Novel role for the *Streptococcus pneumoniae* toxin pneumolysin in the assembly of biofilms. MBio **4:**e00655-00613.

155. **Rubins JB, Mitchell TJ, Andrew PW, Niewoehner DE.** 1994. Pneumolysin Activates Phospholipase A in Pulmonary Artery Endothelial Cells. Infection and Immunity **62:**3829-3836.

156. **Wu T, Angus CW, Yao X-L, Logun C, Shelhamer JH.** 1997. p11, a Unique Member of the S100 Family of Calcium-binding Proteins, Interacts with and

Inhibits the Activity of the 85-kDa Cytosolic Phospholipase A2. The Journal of Biological Chemistry **272:**17145–17153.

157. **Jolly C, Winfree S, Hansen B, Steele-Mortimer O.** 2014. The Annexin A2/p11 complex is required for efficient invasion of *Salmonella* Typhimurium in epithelial cells. Cell Microbiol **16:**64-77.

158. **Munera D, Martinez E, Varyukhina S, Mahajan A, Ayala-Sanmartin J, Frankel G.** 2012. Recruitment and membrane interactions of host cell proteins during attachment of enteropathogenic and enterohaemorrhagic *Escherichia coli*. Biochem J **445:**383-392.

159. **Szabady RL, Louissaint C, Lubben A, Xie B, Reeksting S, Tuohy C, Demma Z, Foley SE, Faherty CS, Llanos-Chea A, Olive A, Mrsny RJ, McCormick BA.** Intestinal P-glycoprotein exports endocannabinoids to prevent inflammation and maintain homeostasis. In Press